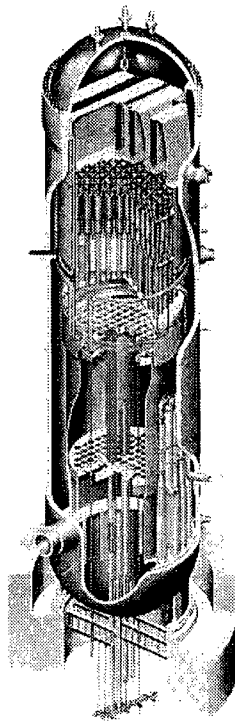


BWVRVIP-1 4NP-A: BWR Vessel and Internals Project

Evaluation of Crack Growth in BWR Stainless Steel RPV Internals



NON-PROPRIETARY INFORMATION

NOTICE: This report contains the non-proprietary information that is included in the proprietary version of this report. The proprietary version of this report contains proprietary information that is the intellectual property of BWVRVIP utility members and EPRI. Accordingly, the proprietary report is available only under license from EPRI and may not be reproduced or disclosed, wholly or in part, by any licensee to any other person or organization.

BWRVIP-14NP-A: BWR Vessel and Internals Project

Evaluation of Crack Growth in BWR Stainless Steel RPV Internals

1016569NP

Final Report, January 2009

EPRI Project Manager
R. Pathania

DISCLAIMER OF WARRANTIES AND LIMITATION OF LIABILITIES

THIS DOCUMENT WAS PREPARED BY THE ORGANIZATION(S) NAMED BELOW AS AN ACCOUNT OF WORK SPONSORED OR COSPONSORED BY THE BWR VESSEL AND INTERNALS PROJECT (BWRVIP) AND ELECTRIC POWER RESEARCH INSTITUTE, INC. (EPRI). NEITHER BWRVIP, EPRI, ANY MEMBER OF EPRI, ANY COSPONSOR, THE ORGANIZATION(S) BELOW, NOR ANY PERSON ACTING ON BEHALF OF ANY OF THEM:

(A) MAKES ANY WARRANTY OR REPRESENTATION WHATSOEVER, EXPRESS OR IMPLIED, (I) WITH RESPECT TO THE USE OF ANY INFORMATION, APPARATUS, METHOD, PROCESS, OR SIMILAR ITEM DISCLOSED IN THIS DOCUMENT, INCLUDING MERCHANTABILITY AND FITNESS FOR A PARTICULAR PURPOSE, OR (II) THAT SUCH USE DOES NOT INFRINGE ON OR INTERFERE WITH PRIVATELY OWNED RIGHTS, INCLUDING ANY PARTY'S INTELLECTUAL PROPERTY, OR (III) THAT THIS DOCUMENT IS SUITABLE TO ANY PARTICULAR USER'S CIRCUMSTANCE; OR

(B) ASSUMES RESPONSIBILITY FOR ANY DAMAGES OR OTHER LIABILITY WHATSOEVER (INCLUDING ANY CONSEQUENTIAL DAMAGES, EVEN IF BWRVIP, EPRI OR ANY EPRI REPRESENTATIVE HAS BEEN ADVISED OF THE POSSIBILITY OF SUCH DAMAGES) RESULTING FROM YOUR SELECTION OR USE OF THIS DOCUMENT OR ANY INFORMATION, APPARATUS, METHOD, PROCESS, OR SIMILAR ITEM DISCLOSED IN THIS DOCUMENT.

ORGANIZATION(S) THAT PREPARED THIS DOCUMENT

Structural Integrity Associates

NON-PROPRIETARY INFORMATION

NOTICE: This report contains the non-proprietty information that is included in the proprietary version of this report. The proprietary version of this report contains proprietary information that is the intellectual property of BWRVIP utility members and EPRI. Accordingly, the proprietary report is available only under license from EPRI and may not be reproduced or disclosed, wholly or in part, by any Licensee to any other person or organization.

NOTE

For further information about EPRI, call the EPRI Customer Assistance Center at 800.313.3774 or e-mail askepri@epri.com.

Electric Power Research Institute, EPRI, and TOGETHER...SHAPING THE FUTURE OF ELECTRICITY are registered service marks of the Electric Power Research Institute, Inc.

Copyright © 2008 Electric Power Research Institute, Inc. All rights reserved.

CITATIONS

This report was prepared by

Structural Integrity Associates
3315 Almaden Expressway
Suite 24
San Jose, CA 95118-1557

Principal Investigators

N. Cofie
A. Giannuzzi
B. Gordon

This report describes research sponsored by the Electric Power Research Institute (EPRI) and its BWRVIP participating members.

The report is a corporate document that should be cited in the literature in the following manner:

BWRVIP-14NP-A: BWR Vessel and Internals Project, Evaluation of Crack Growth in BWR Stainless Steel RPV Internals. EPRI, Palo Alto, CA: 2008. 1016569NP.

This report is based on the following previously published report:

BWR Vessel and Internals Project, Evaluation of Crack Growth in BWR Stainless Steel RPV Internals (BWRVIP-14). EPRI, Palo Alto, CA: 1996. TR-105873.

Principal Investigators:

Structural Integrity Associates
General Electric Nuclear Energy
Modeling and Computing Services
Entergy Operations, Inc.
EPRI Repair and Replacement Center
University of California, Berkeley
Sandia National Laboratories
Dominion Engineering, Inc.

REPORT SUMMARY

The Boiling Water Reactor Vessel and Internals Project (BWRVIP), formed in June 1994, is an association of utilities focused exclusively on BWR vessel and internals issues. This report provides a method for assessment of crack growth in BWR stainless steel shrouds and other stainless steel internal components. A previous version was published as BWRVIP-14 (EPRI report TR-105873). This report (BWRVIP-14-A) incorporates changes proposed by the BWRVIP in response to U.S. Nuclear Regulatory Commission (NRC) Requests for Additional Information, recommendations in the NRC Safety Evaluation (SE), and other necessary revisions identified since the previous publication of the report. All changes are marked with margin bars. In accordance with an NRC request, the Safety Evaluations are included here as appendices and the report number includes an "A" indicating the version of the report accepted by the NRC staff.

Background

Events in 1993 and 1994 confirmed that intergranular stress corrosion cracking (IGSCC) is a significant issue for BWR internals. U.S. BWR executives formed the BWRVIP in June 1994, to address integrity issues arising from service-related degradation of these key components, beginning with core shroud cracking.

One major issue facing the nuclear industry is the issue of core shroud re-inspection and premature repair, which can impose unnecessary economic hardship on utilities. The re-inspection interval depends upon the extent of cracking observed during the baseline examination and prediction of crack growth as a function of future operating time. The current method for determining re-inspection interval is based on characterizing all observed cracks as through-wall cracks and propagating these cracks around the circumference of the shroud, assuming a conservative crack growth rate of 5×10^{-5} in/hr (11.1 mm/y). It is believed that a more realistic re-inspection interval can be established if a crack growth model is developed that can account for the growth of cracks in both the through-thickness and length directions.

Objective

- To develop a generalized crack growth correlation for stainless steel.
- To formalize the method for determination of through-thickness stainless steel crack growth rates in horizontal weld heat affected zones (HAZs) in stainless steel, based on empirical data that account for parameters known to affect crack propagation.

Approach

The project team compiled an extensive database that included both experimental data points and in-plant crack arrest verification system (CAVS) data. The team used the database to derive an empirical, best-fit, stress intensity factor (K) dependent, crack growth correlation that also accounts for environmental conditions such as conductivity, electrochemical potential (ECP), and temperature. The team then developed a conservative 95th percentile model for through-thickness crack growth, which was a factor of 10.3 greater than the best-fit correlation. The model was then tested against field data and found to provide a realistic bound to the data. The report was submitted to the NRC for their review and approval. Comments from that review, as appropriate, have been incorporated into this revision of the report.

Results

Based on extensive crack growth data collected from several sources, an empirical through-wall crack growth correlation has been developed for use in the evaluation of BWR stainless steel internals for fluences $<5 \times 10^{20}$ n/cm². The correlation is applicable for weld-sensitized components and is bounding for non-sensitized components. The report provides analysis and measurements of residual stresses in core shroud welds and discusses fracture mechanics methods employed in determining stress intensity factors. The report provides three alternative methods for crack growth evaluation. Using conservative ECP and conductivity estimates, results confirm that American Society of Mechanical Engineers (ASME) Section XI safety margins are not compromised by extended operation of core shrouds with IGSCC indications.

EPRI Perspective

The empirical correlation developed in this study can be used to conservatively predict the through-thickness crack growth rate for austenitic stainless steels at various ECPs corresponding to different locations in the core shroud. The model is applicable over the specific ranges of stress intensity, water conductivity, and ECP for which the correlation was developed. Application of this method provides assurance that stainless steel components in BWRs with IGSCC indications can continue to operate safely, while reducing utility costs by supporting reasonable intervals for re-inspection and avoiding the costs of unnecessary repair.

Keywords

Boiling Water Reactor
Core Shroud
Crack Growth Rate
Residual Stresses
Stress Corrosion Cracking
Vessel and Internals

RECORD OF REVISIONS

Revision Number	Revisions
BWRVIP-14	Original Report (TR-105873)
BWRVIP-14-A	<p>TR-105873 was revised to incorporate changes proposed by the BWRVIP in responses to NRC Requests for Additional Information, recommendations in the NRC Safety Evaluation (SE), and other necessary revisions identified since the last issuance of the report. All changes except corrections to typographical errors are marked with margin bars. In accordance with a NRC request, the NRC SE is included here as an appendix and the report number includes an "A" indicating the version of the report accepted by the NRC staff. Non-essential format changes were made to comply with the current EPRI publication guidelines.</p> <p>Appendix J deleted: Plant Specific Crack Extension Calculations</p> <p>Appendix J added: NRC Final Safety Evaluation</p> <p>Appendix K added: BWRVIP Response to Final Safety Evaluation</p> <p>Appendix L added: NRC Position on BWRVIP Response to Final SE</p> <p>Appendix M added: NRC Clarification to Position on BWRVIP Response to Final SE</p> <p>Appendix N added: NRC Technical Evaluation Report</p> <p>Appendix O added: BWRVIP Response to NRC Technical Evaluation Report</p> <p>Appendix P added: NRC Staff Evaluation of BWRVIP Response to NRC Safety Evaluation</p> <p>Appendix Q added: U.S. BWR Plants with Shroud Cracking</p> <p>Details of the revisions can be found in Appendix R.</p>

EXECUTIVE SUMMARY

The objectives of this report are to develop a generalized crack growth correlation for unirradiated stainless steel and to formalize a methodology for determination of through-thickness crack growth rates in horizontal weld heat affected zones (HAZs) based on empirical data that account for parameters that are known to affect crack propagation. The assessment was limited to the circumferential welds of the shroud where most of the reported intergranular cracking has occurred to date. The methodology can however be easily extended to the vertical welds of the shroud and other BWR internals components with only minor modifications. This methodology has been developed specifically for crack growth in the depth (through-thickness) direction. Residual and applied stresses and stress intensity factors have been developed for crack propagation in this orientation.

The methodology involves development of an empirical model that can account for the variability of important intergranular stress corrosion cracking (IGSCC) parameters in providing a conservative, yet realistic assessment of the crack growth rate (CGR) in BWR stainless steel components. The first step in the development of the evaluation methodology involved the determination of a crack growth model for stainless steel. Although a correlation has been previously provided by the U.S. Nuclear Regulatory Commission (U.S. NRC), in their technical report NUREG-0313, Revision 2, it is believed by the BWR industry that this correlation does not adequately account for the varying degree of material and environmental conditions experienced by the entire fleet of operating BWRs. It is also believed that since the publication of this document in 1988, additional in-plant and laboratory crack growth data have become available and improved inspection and analytical tools are in hand which can be used to develop an alternative crack growth model; a model which can take into account variables which were not specifically addressed, but rather were bounded collectively, in the earlier NUREG correlation.

In Section 2 of this report, an extensive database consisting of stainless steel crack growth rates is described. This data came from several sources including General Electric Nuclear Energy (GE), ABB-Atom (ABB), and Argonne National Laboratories (ANL). The data included both experimental data points and in-plant crack arrest verification system (CAVS) data. Most of the data in the database have adequate definition of environmental conditions and other important crack growth parameters thus permitting a more realistic generic crack growth model to be developed.

The database was used in Section 3 of this report to derive an empirical, stress intensity factor (K) dependent crack growth law that also accounts for environmental conditions such as conductivity, electrochemical potential (ECP) and temperature. The development of the model was based on pattern recognition and multivariate modeling techniques that have been used quite successfully in previous similar projects. A best-fit model was derived based on the data and a

crack growth curve based upon the 95th percentile on this best-fit model was recommended for crack growth evaluation of the shroud and other stainless steel internals. The 95th percentile is a factor of 10.3 higher than the best-fit correlation. It should be noted that this model is an empirical correlation based upon available data and engineering judgment. This empirical crack growth model, because of the limited nature of the data available, was based predominantly on test data for sensitized material tests, and a limited number of tests on non-sensitized material. Other crack growth correlations are available that address sensitization and radiation effects. The empirical correlation is applicable, therefore, for weld-sensitized components and is bounding for non-sensitized components. The model is applicable over the specific ranges of variables examined and is recommended for use solely within these ranges. It should be noted that the range of variables addressed by this empirical correlation represents the water chemistry, material, and stress conditions expected in BWR service.

**Content Deleted -
EPRI Proprietary Information**

In Section 5 of this report, fracture mechanics models were used to determine the through-wall stress intensity factor (K) distributions for the recommended residual stress profiles. A single distribution was determined for both inside and outside surface initiated flaws of the shroud. Because of the shape of the through-wall residual stress profile, higher K values were obtained near the wall surfaces indicating high crack growth rates at these locations. K diminishes as the crack propagates into the wall and leads to significantly lower crack growth rates.

The evaluation methodology for determination of crack growth rate for BWR shrouds is provided in Section 6. Three alternate approaches are presented: a K-independent approach; a conservative 95th percentile K-dependent approach using the empirical correlation developed in this report along with conservative ECP and water chemistry; and a plant-specific approach using actual plant ECP and water chemistries with the empirical correlation. An example problem representing actual BWR shroud conditions is presented in Section 6 to demonstrate how the current crack growth correlation, the weld residual stress, and the stress intensity factor

recommendations can be used to perform a plant-specific evaluation of flawed shrouds. The results of this example demonstrated that significant operating periods are likely for most flawed conditions in BWR core shroud welds before ASME Code Section XI core shroud safety margins are challenged.

The empirical crack growth correlation was tested against recent operating plant reinspection ultrasonic (UT) data performed at three plants which previously exhibited core shroud cracking in their circumferential welds. The empirical model was used to predict the 95th percentile for the crack growth observed at these plants, using the environmental conditions at the cracked locations. The 95th percentile model provided an upper bound for 9 of the 11 data points, with the other points falling just above the curve. In this example, no inspection error was estimated for the UT and a conservative crack depth change estimate was used for evaluating the UT data. The model clearly accounted for the growth of these flaws. The current stress intensity independent, flat 5×10^{-5} in/hr crack growth rate proposed by the U.S. NRC would have been conservative by a factor of 5 compared to the current empirical model estimate, and by more than a factor of two compared to the most conservative (most rapid growth) field data points, at that stress intensity. The model predicts a lower crack growth rate as the crack grows deeper and K decreases. This is consistent with inspection data from the field.

It is proposed that the BWRVIP crack growth correlation and methodology presented in this report should be used to evaluate crack growth in core shroud welds and other stainless steel internals. It is believed that application of this methodology provides assurance that BWRs with cracks in the core shroud can continue to operate safely while reducing utility costs by supporting reasonable intervals for reinspection and avoiding the costs of unnecessary or premature repairs.

ACKNOWLEDGMENTS

The members of the BWRVIP Crack Growth Working Group, listed below, are gratefully acknowledged for their efforts which led to the successful completion of the original version of this document.

ai ri ma e am airma
 i ye
 e r e c
 y ia u i
 E art i
 r
 Steve e
 ave r a
 arry e
 a at a ia r ect a a er
 at ee am
 i
 au a er
 a ema

Entergy Operations
 Southern Nuclear Company
 Niagara Mohawk Power Corp.
 Structural Integrity Associates
 Tennessee Valley Authority
 GE Nuclear Energy
 GPU Nuclear
 Pennsylvania Power & Light
 Electric Power Research Institute
 Electric Power Research Institute
 Electric Power Research Institute
 Public Service Electric & Gas
 Carolina Power & Light
 Carolina Power & Light

Principal Investigators:

ie
 ia u i
 yte
 E e ic e
 r
 r
 E Ea
 ert
 eter
 e
 i ie
 S ie
 S e
 ami
 rei er
 r
 E S u t
 ri ma e am

Structural Integrity Associates, Inc.
 Structural Integrity Associates, Inc.
 Structural Integrity Associates, Inc.
 General Electric Nuclear Energy
 General Electric Nuclear Energy
 General Electric Nuclear Energy
 Modeling and Computing Services
 Modeling and Computing Services
 EPRI Repair and Replacement Center
 University of California, Berkeley
 University of California, Berkeley
 Sandia National Laboratories
 Sandia National Laboratories
 Sandia National Laboratories
 Dominion Engineering, Inc
 Dominion Engineering, Inc.
 Dominion Engineering, Inc.
 Entergy Operations

CONTENTS

1 INTRODUCTION	1-1
1.1 Background on Cracking of Stainless Steel Internals	1-1
1.2 Objective and Scope	1-8
1.3 Implementation Requirements	1-9
2 COMPILATION OF CRACK GROWTH DATA.....	2-1
2.1 Structural Integrity Associates Database	2-1
2.2 GE Nuclear Energy Database	2-2
3 EMPIRICAL CRACK GROWTH CORRELATION STUDIES	3-1
3.1 Evaluation of the Database for Model Development	3-1
3.2 Development of Empirically-Based Stainless Steel Crack Growth Rate Correlation	3-2
3.3 Correlation Models	3-7
3.4 Comparison of Model Predictions With Experimental Data.....	3-9
3.5 Comparison of Model Predictions With Field Data.....	3-13
4 OPERATING AND RESIDUAL STRESS EVALUATION.....	4-1
4.1 Operating Stresses Experienced by Core Shroud	4-1
4.2 Background on Weld Residual Stresses	4-1
4.3 Residual Stress Measurements of Core Shroud Welds	4-3
4.3.1 Near-Surface Residual Stress Measurements	4-3
4.3.2 Through-Thickness Residual Stress Measurements at River Bend Nuclear Station	4-7
4.4 Analytical Determination of Residual Stresses in Core Shroud Welds	4-11
4.5 Comparison Between Experimental and Analytical Results.....	4-13
4.6 Weld Residual Stress Distribution for Analysis of Core Shroud Welds	4-17
4.7 Methodology for Addressing Localized Stresses	4-24
4.8 Stress Relaxation Effects	4-28

5 FRACTURE MECHANICS CONSIDERATIONS	5-1
5.1 Stress Intensity Factors Due to Applied Stresses	5-1
5.2 Stress Intensity Factors Due to Weld Residual Stresses	5-2
5.3 Effect of Localized Stresses on Stress Intensity Factor Distribution	5-9
5.4 Allowable Flaw Size for BWR Shroud	5-10
6 EVALUATION METHODOLOGY FOR CORE SHROUD CRACK GROWTH	6-1
6.1 Evaluation Procedure	6-1
6.1.1 Stress Intensity Factor (K) Independent Approach.....	6-2
6.1.2 Stress Intensity Factor (K) Dependent Approach	6-2
6.1.3 Stress Intensity Factor (K) and Environment Dependent Approach.....	6-3
6.2 Example of Application of K and Environment Dependent Approach	6-4
6.3 Comparison of Analytical Crack Growth Prediction With Field Data	6-7
7 SUMMARY AND CONCLUSIONS	7-1
8 REFERENCES	8-1
A CRACK GROWTH RATE DATA: ABB ATOM AND ARGONNE NATIONAL LABORATORIES	A-1
B CRACK GROWTH RATE DATA: GE NUCLEAR ENERGY	B-1
C CRACK GROWTH RATE CORRELATION	C-1
D RIVER BEND SHROUD MATERIAL PROPERTIES	D-1
E NEAR SURFACE RESIDUAL STRESS MEASUREMENTS AT RIVER BEND NUCLEAR STATION.....	E-1
F THROUGH-THICKNESS RESIDUAL STRESS MEASUREMENT ON RIVER BEND CORE SHROUD	F-1
G NEAR SURFACE RESIDUAL STRESS MEASUREMENTS AT GRAND GULF NUCLEAR STATION.....	G-1
H ANALYTICAL PREDICTION OF RESIDUAL STRESSES IN BWR SHROUD WELDS	H-1
I IN-PLANT CRACK EXTENSION DETERMINATION FROM SUCCESSIVE UT EXAMINATIONS	I-1

J	USNRC FINAL SAFETY EVALUATION OF BWRVIP-14	J-1
K	BWRVIP RESPONSE TO NRC FINAL SAFETY EVALUATION OF BWRVIP-14.....	K-1
L	USNRC POSITION ON BWRVIP RESPONSE TO NRC FINAL SAFETY EVALUATION OF BWRVIP-14	L-1
M	USNRC CLARIFICATION TO POSITION ON BWRVIP RESPONSE TO NRC FINAL SAFETY EVALUATION OF BWRVIP-14.....	M-1
N	USNRC TECHNICAL EVALUATION REPORT ON BWRVIP-14-A DATED JULY 30, 2004	N-1
O	BWRVIP RESPONSE TO NRC TECHNICAL EVALUATION REPORT DATED SEPTEMBER 12, 2005.....	O-1
P	NRC STAFF EVALUATION OF BWRVIP RESPONSE TO NRC SAFETY EVALUATION DATED AUGUST 22, 2007	P-1
Q	PLANTS WITH SHROUD CRACKING.....	Q-1
R	RECORD OF REVISIONS	R-1

LIST OF FIGURES

Figure 1-1 Typical BWR Core Shroud	1-4
Figure 1-2 Location of BWR Core Shroud Circumferential Welds (BWR 3/4)	1-5
Figure 1-3 Location of BWR Core Shroud Circumferential Welds (BWR 6)	1-6
Figure 1-4 Typical Weld Details of Core Shroud Circumferential Welds.....	1-7
Figure 3-1 Effect of Conductivity	3-3
Figure 3-2 Effect of K on Crack Growth of Type 304 Stainless Steel	3-4
Figure 3-3 Effect of Temperature on Crack Growth of Type 304 Stainless Steel	3-5
Figure 3-4 Effect of ECP on Crack Growth of Type 304 Stainless	3-6
Figure 3-5 Model Prediction for Best-Fit and 95 th Percentile for Conductivity of 0.3 $\mu\text{S}/\text{cm}$	3-9
Figure 3-6 Comparison of Stainless Steel Crack Growth Model Predictions (95 th Percentile) With Experimental Data (Conductivity of 0.1 $\mu\text{S}/\text{cm}$ Temperature of 288°C and Varying ECP)	3-10
Figure 3-7 Comparison of Stainless Steel Crack Growth Model Predictions (95 th Percentile) With Experimental Data (Conductivity of 0.2 $\mu\text{S}/\text{cm}$ Temperature of 288°C and Varying ECP)	3-11
Figure 3-8 Comparison of Stainless Steel Crack Growth Model Predictions (95 th Percentile) With Experimental Data (Conductivity of 0.3 $\mu\text{S}/\text{cm}$ Temperature of 288°C and Varying ECP)	3-12
Figure 3-9 Comparison of Model Prediction With Field Data.....	3-14
Figure 4-1 NRC Accepted Axial Weld Residual Stress Distribution for Large Diameter Piping [3]	4-2
Figure 4-2 Test Specimens for Through-Wall Residual Stress Measurements at River Bend Nuclear Station	4-9
Figure 4-3 Weld Profiles and Planes for Through-Wall Weld Residual Stress Measurements at River Bend Nuclear Station	4-10
Figure 4-4 Comparison of Experimental and Analytical Through-Wall Residual Stress Distribution for Weld H5	4-14
Figure 4-5 Comparison of Experimental and Analytical Through-Wall Residual Stress Distribution for Weld H6a	4-15
Figure 4-6 Comparison of Experimental and Analytical Through-Wall Residual Stress Distribution for Weld H6b	4-16
Figure 4-7 Through-Wall Axial Residual Stress Distributions in HAZ for Shell-to-Shell Weld of Core Shroud (H4/H5) and Comparison With the Standard Curve	4-18
Figure 4-8 Through-Wall Axial Residual Stress Distributions in HAZ for Core Shroud Shell-to-Ring Welds (H2/H3) and Comparison With Standard Curve	4-20

Figure 4-9 Through-Wall Axial Residual Stress Distributions in Weld for Core Shroud H6a Shell-to-Ring Welds and Comparison With Standard Curve	4-21
Figure 4-10 Through-Wall Axial Residual Stress Distributions in Core Shroud H6b Shell-to-Ring Welds and Comparison With Standard Curve	4-22
Figure 4-11 Comparison of Experimental Measurements (Surface and Through-Wall) With Standard Curve	4-23
Figure 4-12 Through-Wall Stress Distributions for Weld Residual Stress, Maximum Membrane Stress and Surface Residual Stress	4-25
Figure 4-13 Combined Through-Wall Stress Distribution.....	4-26
Figure 4-14 The Three Types of Localized Repairs Used in the Weld Repair Study [12].....	4-27
Figure 4-15 Stress Relaxation Due to Neutron Irradiation [13]	4-29
Figure 5-1 Parameter F_1 to Describe Stress Intensity Factor K_1 for the Part-Through-Wall, Part Circumference Flaws [15].....	5-2
Figure 5-2 Normalized Stress Intensity Factor Magnification Factors for Circumferential Crack in Cylinder ($t/R = 0.1$) [16] K_1 for BWR Shroud Axial Weld Residual Stress Distribution (R/t Varying Between 10 and 500) [23]	5-4
Figure 5-3 Generic K_1 Distribution for BWR Shroud Axial Residual Stress (Based on $R/t = 60$)	5-5
Figure 5-4 Flaw Reduction Factors for Determination of K_1 for Weld Residual Stresses in BWR Shrouds with Part-Circumference Flaws.....	5-8
Figure 5-5 K Distribution for a Combination of Weld Residual Stress, Surface Residual Stress and 3.2 ksi Membrane Stress [26]	5-9
Figure 6-1 Crack Growth Results for Normal and Hydrogen Water Chemistry Based on Combined K Distribution Shown in Figure 5-5 and Table 5-1	6-6
Figure 6-2 Comparison of Through-Thickness Crack Growth Calculated With BWRVIP-14 K and Environment Dependent Model with Measured Crack Growth for Several Plants	6-8

LIST OF TABLES

Table 3-1 Variables and Range of Calibration Data Considered in Crack Growth Correlation Studies.....	3-2
Table 4-1 Summary of Near Surface Residual Stress Measurements at Grand Gulf Nuclear Station.....	4-5
Table 4-2 Summary of Near Surface Residual Stress Measurements at River Bend Nuclear Station.....	4-7
Table 4-3 Through-Wall Axial Stress Distributions for BWR Shroud Welds	4-19
Table 5-1 Normalized Through-Wall Stress Intensity Factor Distribution for BWR Shroud Welds	5-6
Table 6-1 BWR Plants Core Shroud Crack Growth Data	6-9
Table 6-2 BWR Plant-Specific Core Shroud Crack Growth Results	6-10
Table R-1 Revision Details	R-3

1

INTRODUCTION

1.1 Background on Cracking of Stainless Steel Internals

The problem of intergranular stress corrosion cracking (IGSCC) in austenitic stainless steels and in nickel-based austenitic materials has presented a serious concern to plant availability for boiling water reactor (BWR) owners during the past 20 years. Initial observations of IGSCC in BWRs were associated with severely sensitized wrought Type 304 stainless steel piping that resulted from post weld heat treatment or high heat input welding. Additional service history revealed that these severe thermal treatments of materials prior to service were not necessary to cause IGSCC; that cracking could occur in weld-sensitized components, welded with moderate heat input and with no subsequent thermal treatment. The utility industry through EPRI (formerly the Electric Power Research Institute), the vendors, and contractors, led by GE Nuclear Energy (GE), research groups, and the Nuclear Regulatory Commission (NRC), expended significant time and financial resources to address the IGSCC issue and to provide remedial measures to the cracking. The NRC issued several documents including Inspection and Enforcement (I&E) notices, bulletins, regulatory guides, and generic letters on the issue.

EPRI sponsored research resulted in technical reports guidelines and workshops on the issue. GE performed research and prepared service information letters (SILs) addressing the IGSCC issue and advising the utility industry on actions appropriate to address the problem. Although the cracking in austenitic materials was widespread, until recently it was generally confined to components outside of reactor pressure vessel.

During the past decade, IGSCC of austenitic stainless steels and nickel-based alloys has begun to be observed within the reactor pressure vessel. Components such as jet pump beams, riser braces, access hole covers, core spray piping, feedwater spargers, shroud hold-down bolts, reactor pressure vessel cladding and the core shroud are among the vessel internals components which have recently exhibited cracking.

Cracking of vessel internals has involved both austenitic stainless steels and nickel-based alloys. Until the recent core shroud cracking, the IGSCC observed was readily manageable with existing means and did not significantly impact design safety margins of the plant. The core shroud cracking has been sufficiently significant in some plants to warrant repairs to the cracked weld heat affected zones or to require more frequent core shroud inspections.

The following paragraphs in this section describe the factors that contribute to the IGSCC observed in the core shroud, as limited to austenitic stainless steels, the industry experience with shroud cracking and the real and potential impact on the BWR Owners.

Cause of Cracking

Based upon prior work sponsored by EPRI, industry research groups and the NRC, the generally accepted factors responsible for IGSCC in austenitic stainless steels and nickel-based austenitic materials in the normal BWR environment are sufficient tensile stress, thermal sensitization and a sufficiently oxidizing environment. An additional factor that may contribute to intergranular cracking after long operating times at high neutron fluences is the effect of irradiation on the stress corrosion cracking susceptibility of the material.

The total stress state of a material includes applied and residual stresses. The applied stresses are the operating stresses to which the material is subjected in service and can be readily bounded by engineering stress analyses. The residual stresses include fabrication stresses such as machining, grinding and welding stresses and fit-up stresses associated with the component installation. It is generally accepted that these combined stresses must be near the material yield strength at temperature for IGSCC to occur.

Thermal sensitization of these alloys involves chromium depletion at the grain boundaries due to chromium carbide precipitation. The chromium depleted zone is no longer a "stainless" material but rather an alloy steel anode galvanically coupled to a large stainless steel cathode. If sufficient tensile stress is present at a sufficient temperature and in an oxidizing environment, then IGSCC can occur if the environment can support the corrosion reaction.

The environment influences the IGSCC of austenitic materials in the BWR environment in two ways. The normal water chemistry (NWC) BWR core environment is a very oxidizing environment that contains dissolved oxygen and hydrogen peroxide due to the radiolytic decomposition of water in the core region. This environment has been demonstrated to be sufficiently aggressive to provide the electrochemical driving force for IGSCC in weld-sensitized austenitic stainless steels. The thermodynamic tendency of a metal to be oxidized in an aqueous environment can be measured and quantified by its electrochemical corrosion potential (ECP). Hydrogen gas can be injected to reactor water to suppress radiolysis in the core and to react with these two oxidizing species and, thus, lower the ECP. IGSCC initiation is essentially mitigated when the ECP of stainless steel in the coolant is below -230 mV(SHE). This is the basis for hydrogen water chemistry (HWC). The efficiency of HWC can be significantly increased by the injection of catalytic noble metals via a process called noble metal chemical application (NMCA).

Effective mitigation can be obtained by implementing HWC solely or in combination with NMCA, hereafter referred to as HWC/NMCA. Furthermore, for the purposes of crack growth evaluation approaches discussed in Sections 6.1.1 and 6.1.2, NWC and HWC/NMCA environments are defined as follows:

NWC: ECP of stainless steel > -230 to $+200$ mV(SHE), average coolant conductivity < 0.15 $\mu\text{S/cm}$.

HWC/NMCA: ECP of stainless steel ≤ -230 mV(SHE), average coolant conductivity < 0.15 $\mu\text{S/cm}$ with at least 80% HWC availability.

Note that the $<0.15 \mu\text{S}/\text{cm}$ conductivity limit used to derive the crack growth rates for the K-independent (Section 6.1.1) and K-dependent (Section 6.1.2) approaches was chosen to bound the mean fleet conductivity of $0.10 \mu\text{S}/\text{cm}$ as described in the BWR Water Chemistry Guidelines 2004 Revision (BWRVIP-130 [38]).

The second environmental factor influencing IGSCC of austenitic materials is the concentration of aggressive anions such as chloride and sulfate that accelerate IGSCC initiation and propagation. Other ionic species such as chromates and nitrates, sodium and zinc are much less aggressive. In fact some species, such as zinc, appear to be beneficial to the IGSCC resistance of these materials. The concentration of ionic species is reflected in the electrical conductivity of reactor water. The relationship between conductivity and the concentration of aggressive anions will be plant specific. However, conductivity measurements provide a bounding indication of the concentration of these impurities.

Aside from increasing the ECP via radiolytic decomposition of the water within the core, the core shroud is also affected by neutron and gamma radiation damage to the material itself. High levels of neutron exposure cause vacancies and voids to form in these alloys enhancing the rates of segregation of impurities to grain boundaries and also enhancing chromium depletion at these grain boundaries. This “non-thermal” irradiation induced sensitization is generally observed in these austenitic materials in the range of fluences of $\sim 5 \times 10^{19}$ to $5 \times 10^{20} \text{ n}/\text{cm}^2$ ($E > 1.0 \text{ MeV}$) and above. A fluence of $5 \times 10^{19} \text{ n}/\text{cm}^2$ ($E > 1.0 \text{ MeV}$) can be achieved in as little as approximately one to two full power years in a high flux location of a typical BWR core shroud. The effect of neutron irradiation on the stress corrosion susceptibility of these austenitic materials is known as irradiation assisted stress corrosion cracking (IASCC). It is noteworthy that a review of the entire database revealed that the crack growth rates of thermally sensitized specimens were higher than that for irradiation-sensitized specimens, over the ranges evaluated. However, the amount of data available on irradiated specimens was too limited to allow any definitive conclusions to be drawn.

Industry Core Shroud IGSCC Experience

During the past five years, cracking has begun to be observed within the core shroud of BWRs. First observed in 1990 in a European plant, cracking (or crack like indications) have been reported in several overseas plants and a large number of plants in the United States. Appendix Q provides summary of circumferential cracking at U.S. plants to date. In all, circumferential cracking has been identified in at least 29 plants. None of this cracking has gone through-wall. The cracking has generally been confined to the weld heat affected zone (HAZ) in circumferential welds in the core shroud. Figures 1-1 through 1-3 illustrate the circumferential weld locations in a typical BWR 3/4 and BWR 6 core shroud. As can be seen from the weld details in Figure 1-4, all those welds are welded from both sides, with the exception of the dissimilar metal weld, H7. The cracking has generally occurred in Type 304 stainless steel weld HAZs although some cracking has also been observed in Type 304L stainless steel weld HAZs. Some limited cracking has also been reported in vertical welds in one or two plants, and the weld metal may have been involved in cracking of one U.S. plant.

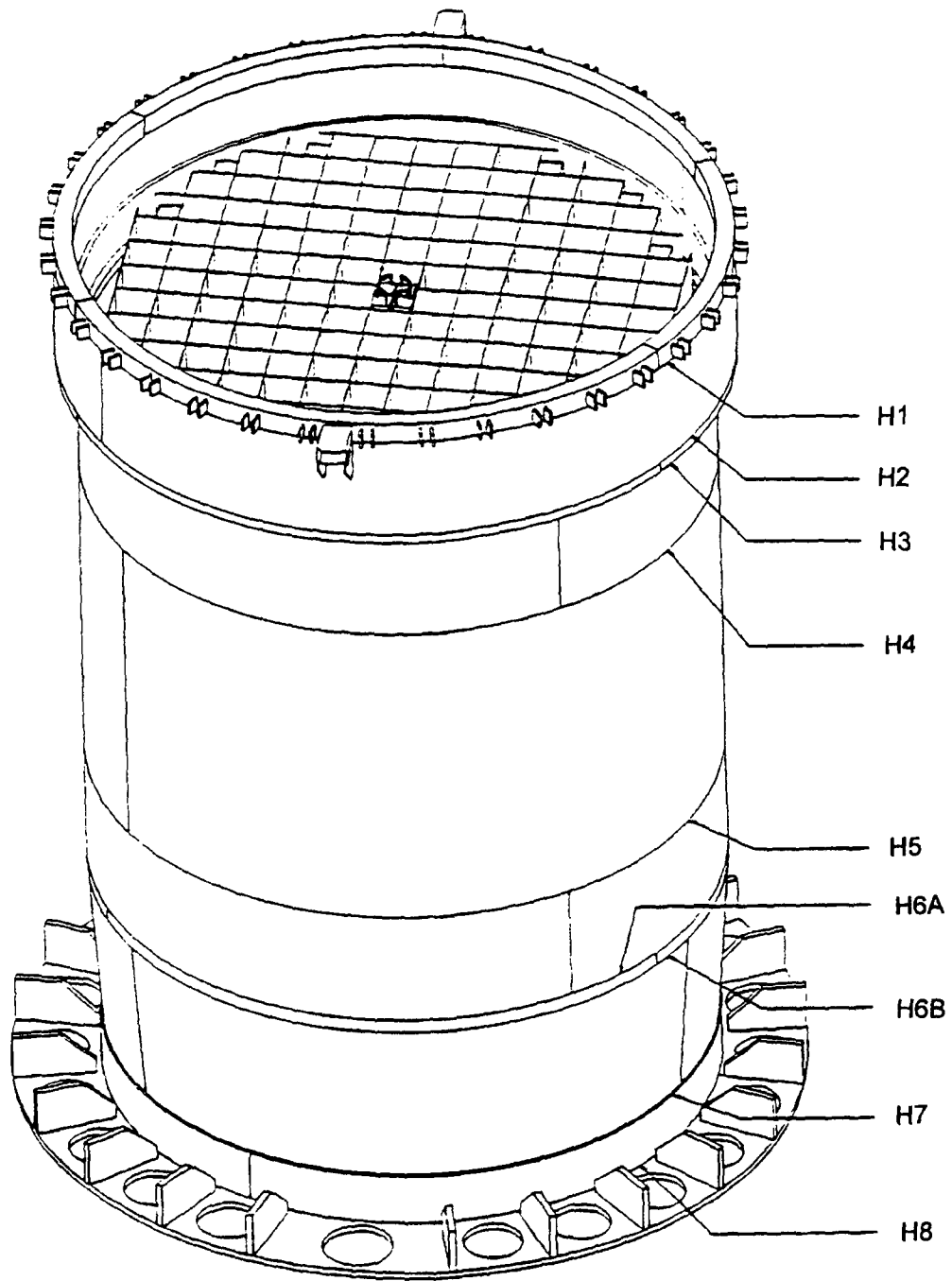


Figure 1-1
Typical BWR Core Shroud

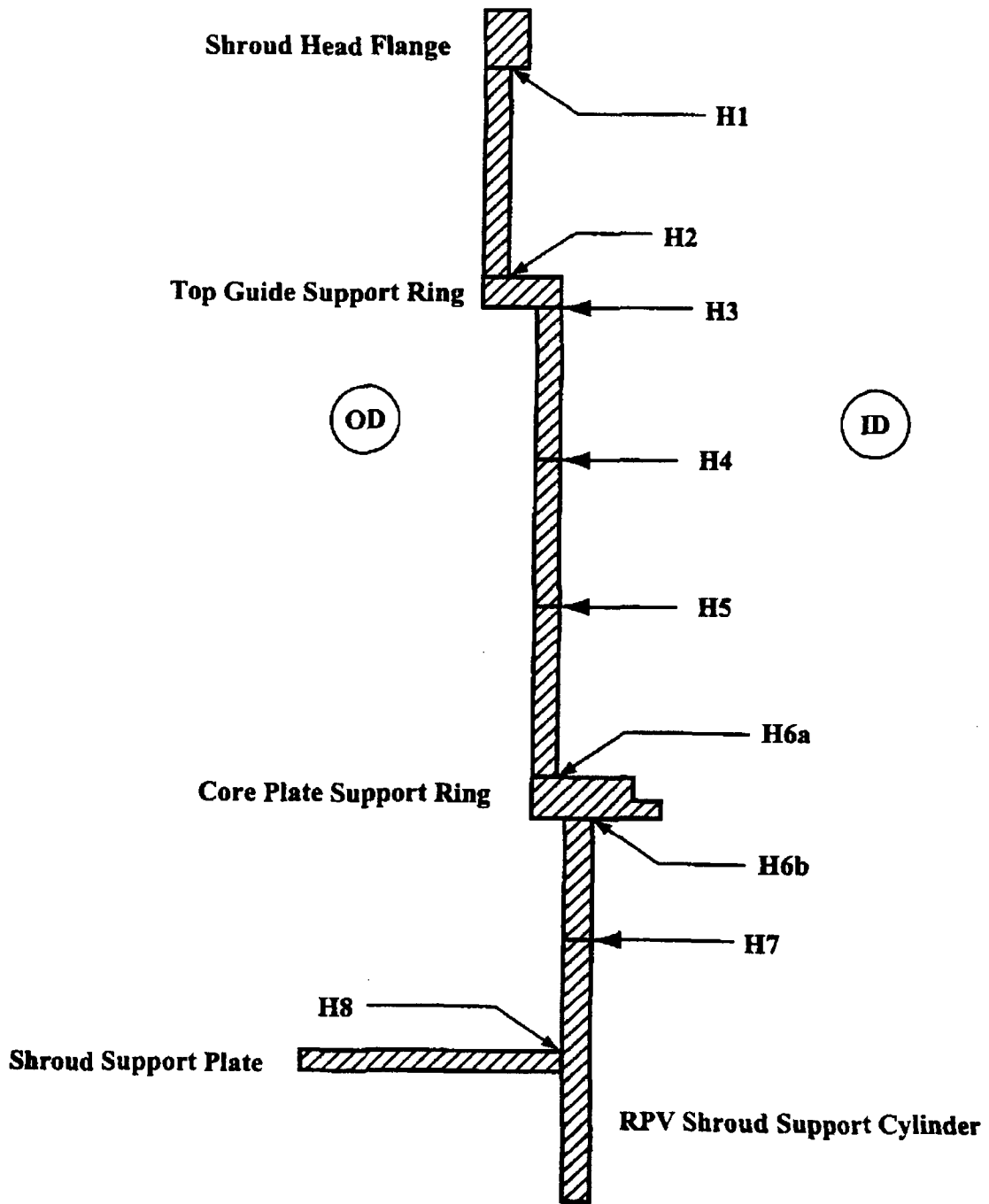


Figure 1-2
Location of BWR Core Shroud Circumferential Welds (BWR 3/4)

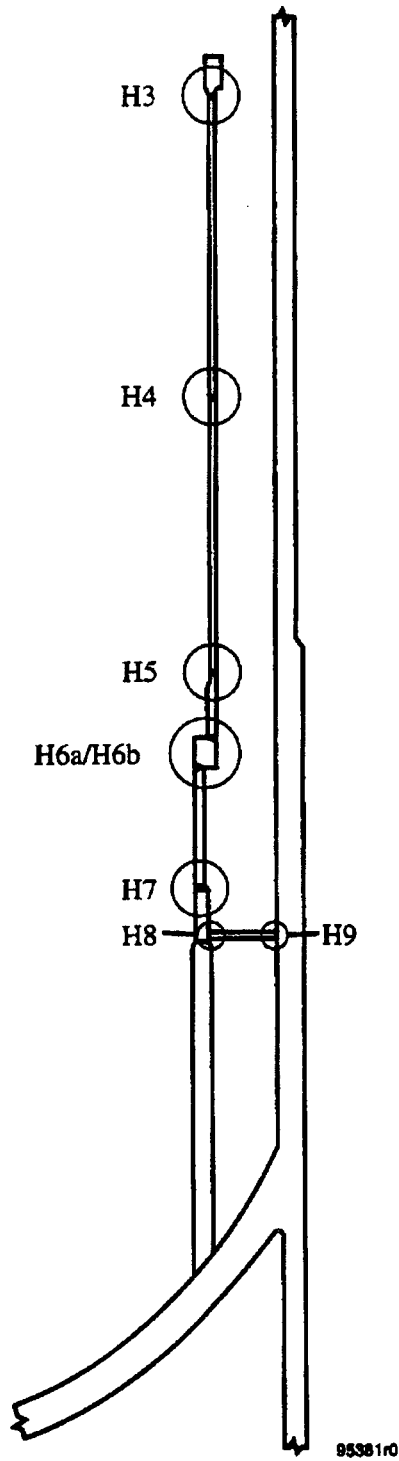


Figure 1-3
Location of BWR Core Shroud Circumferential Welds (BWR 6)

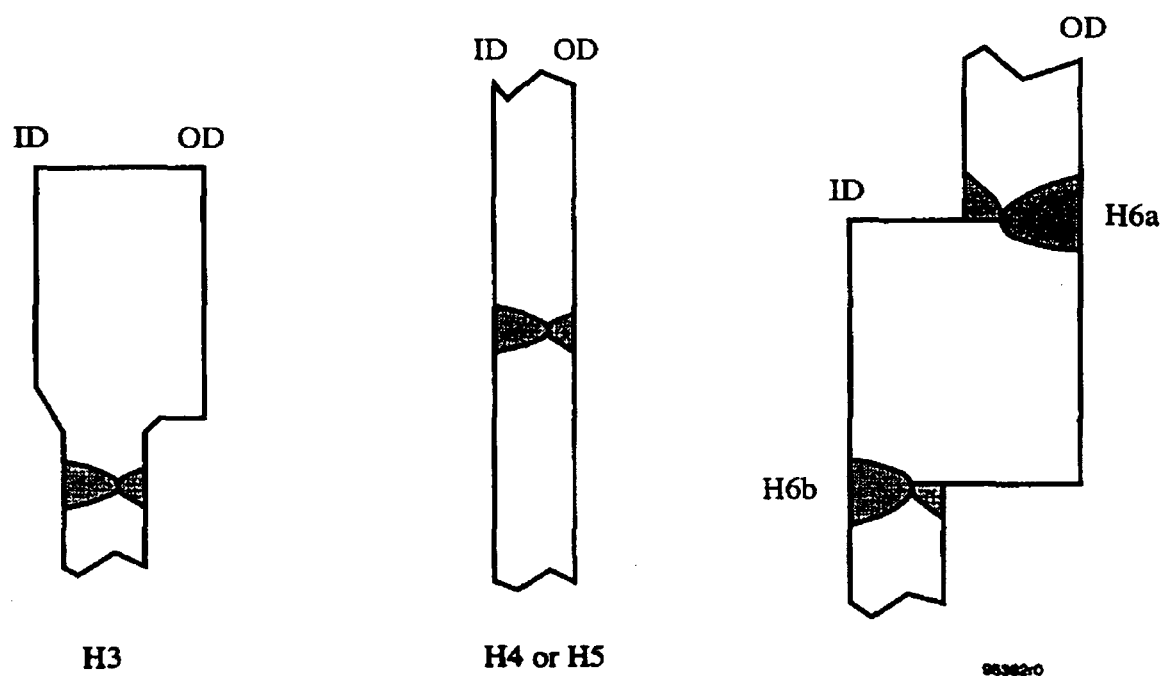


Figure 1-4
Typical Weld Details of Core Shroud Circumferential Welds

The circumferential cracking in the austenitic stainless steel weld HAZs has been modest for some plants, severe in others, and non-existent in other plants. Some correlation with shroud fabrication or prior water chemistry history has been observed since it appears that the newer plants or those operating with good water quality appear to have had less cracking than those operating with poorer initial water quality. Fabrication process may play an important role in crack initiation as plate-exposed “end grain” and severe machining or grinding appear to be contributors to early crack initiation. Total neutron fluence may be playing a role on crack initiation in some high fluence plants and the effect of irradiation on oxidizing potential may be assisting in crack growth in some of the beltline core shroud welds in high fluence plants.

Real and Potential Impact on Utilities

The IGSCC of core shrouds in BWRs has produced a new, significant operational and financial burden to the BWR utility owners. The cracking in the circumferential welds of some plants have raised issues as to the length of continued operation of the plant prior to reinspection or repair of a flawed core shroud. Although, the design safety margins for the core shroud have not been impacted to date, as a result of inspections or analyses performed on operating plants, concerns exist that these extremely conservative analyses justifying continued operation might impose additional inspection hardship or require unnecessary repair to the core shroud. This concern and the concern that at some future time the design safety margins might be affected has prompted the formation of a high level BWR Vessel and Internals Project (BWRVIP) by the BWR industry, with EPRI acting as project manager and coordinator. The objective of this project has been to understand the cracking phenomena within the vessel internals, provide

mitigating measures to limit any future cracking, develop advanced inspection and analytical tools to monitor and realistically bound the cracking and design and implement state-of-the-art repair measures to restore margin to the core shroud and other internals.

The utility industry has been burdened with the need to perform extensive inspections of their BWR core shrouds to assess the condition of the shroud. While the initial inspections were performed using enhanced visual techniques, access limitations have prompted most utilities to perform the most recent inspections using volumetric ultrasonic methods. These inspections have required development of new state-of-the-art equipment to inspect these welds and weld heat affected zones with precision and to accurately determine the IGSCC condition of these components. As the extent of cracking has become more widespread, inspections have been required at lower elevations in the core shroud involving welds H6, H7, and H8, where very limited access is available for positioning tracking equipment and transducers.

One of the major issues facing the utility industry with regard to the core shroud inspection is the issue of core shroud reinspection and premature repair that can impose an unnecessary economic hardship on the utility. The reinspection interval is dependent upon the extent of cracking observed during the baseline examination and prediction of the crack growth as a function of future operating time. The current methodology for determining reinspection interval is based on characterizing all observed cracks as through-wall cracks and propagating these cracks around the circumference of the shroud assuming a conservative crack growth rate of 5×10^{-5} in/hr. It is believed that a more realistic reinspection interval can be established if a crack growth model is developed which can account for both the through-thickness and the circumferential growth of the cracks. This crack growth model should include estimates of weld residual stresses in these circumferential welds as a function of crack depth and circumferential extent, degree of sensitization of the material, and the environments to which the core shroud is exposed. These environments vary within the shroud from very oxidizing at and above the core midplane, to moderately oxidizing below the core plate. In fact, under moderate HWC environment (1.0 to 1.6 ppm H₂), the ECP of stainless steel below core plate locations can be reduced to less than -230 mV(SHE) potential required for IGSCC protection of weld HAZs.

1.2 Objective and Scope

The objective of this report is to formalize the methodology for determination of stainless steel crack growth rates in the depth direction for horizontal weld HAZs with a fluence $\leq 5 \times 10^{20}$ n/cm² ($E > 1.0$ MeV) based on empirical data that account for parameters that are known to affect crack propagation. These through-wall crack growth rates (CGR) will then be available for use in the evaluation, inspection and repair criteria for BWR RPV internal components. The scope of CGR influencing factors will be tied to typical material susceptibility, water environment, and stress-state parameters associated with core shroud weld and weld HAZ. An empirical model will be developed that incorporates the effects of the important factors into a conservative, yet realistic, crack growth correlation for stainless steel in the BWR internals. The model developed in this report is an empirical correlation for through-thickness crack growth based upon available test data and engineering judgment. The correlation is developed using material, environment, and stress data that result from laboratory and in-plant test programs. It is then tested against field data and found to provide a realistic bound to the growth rates observed over the BWR operating regime.

The following sections of this report describe the work undertaken within this project to understand the state of stress, and material variability on the crack growth rates of austenitic stainless steels at ECPs and conductivities corresponding to those observed within the BWR core shroud under NWC conditions as well as under HWC conditions. Section 2 presents a compilation and assessment of crack growth data produced by laboratories and in field testing. This collection of data provides a compiled database for use in determining crack growth rates as a function of environment and stress intensity factor (K) in sensitized austenitic stainless steel. Section 3 provides an empirical crack growth rate correlation developed using material, environment and stress information provided in Section 2. This correlation is based upon sensitized material tests. The correlation is applicable, therefore, for weld-sensitized components and is bounding for non-sensitized components. The model is applicable over the specific ranges of stress intensity, water conductivity and ECP for which the correlation was developed. Section 4 provides the operating and residual stress data for the core shroud materials. Fracture mechanics methods employed in determining the stress intensity factors associated with the applied and residual stresses are presented in Section 5. Section 6 presents the evaluation methodology for estimation of crack growth rates in the through-thickness direction for BWR shrouds. Three alternate approaches are presented: a K-independent approach; a conservative 95th percentile K-dependent approach using the empirical correlation developed in this report along with conservative ECP and water chemistry; and a plant-specific approach using actual plant ECP and water chemistries with the empirical correlation. An example problem on crack growth evaluation of the shroud using the methodologies outlined in Sections 1 through 5 for a plant-specific analysis is also presented in Section 6. Section 7 presents the Summary and Conclusions from this study and provides the empirical correlation that can be used to conservatively predict the crack growth rate for austenitic stainless steels at various ECPs corresponding to different locations in the core shroud. Section 8 provides references used in the report. Detailed studies performed by several individual organizations to support the work presented in the main body of the report are presented in Appendices A through J.

1.3 Implementation Requirements

This report describes crack growth rates to be used in performing flaw evaluations on stainless steel internal components in BWRs. The requirements for crack growth rates delineated in Section 6 of the report shall be considered “needed” in accordance with Nuclear Energy Institute (NEI) 03-08, “Guideline for the Management of Materials Issues.” The remainder of the report is provided for information.

2

COMPILATION OF CRACK GROWTH DATA

Two separate databases were created to assist in the through-thickness crack growth correlation development for austenitic stainless steels with fluences $\leq 5 \times 10^{20}$ n/cm² (E > 1.0 MeV). The first database was created by Structural Integrity Associates (SI) based on available information obtained from several EPRI-sponsored research projects and also from work sponsored by the U.S. NRC. The second database was based on laboratory and crack arrest verification system (CAVS) data developed by GE.

2.1 Structural Integrity Associates Database

Details of this database are provided in Appendix A of this report. The data for this database was obtained from ABB-Atom through EPRI and from NRC-sponsored research at Argonne National Laboratories (ANL). The data from these two sources were chosen because, unlike other stainless steel crack growth data, they have all the identifiable testing parameters and testing conditions for all the test data. The data obtained from these sources were judged to be excellent in terms of completeness, relevance and traceability. All the parameters that are associated with each of the test data in this database are described below. References from which data was compiled are provided in Appendix A.

A total of 170 data points were obtained from ABB-Atom. The data included tests on corrosion fatigue and constant load tests. Most of these data were cyclic data. A total of 44 data points for Type 304 under constant load were used in the model formation. A summary of the range of data from this source is as follows:

Materials	Type 304, Type 316NG
Test Temperature (°C)	288
Conductivity (μS/cm)	0.1 to 1.2
Oxygen, Concentration (ppb)	5 to 200
Hydrogen Concentration (ppb)	10 to 125
ECP (mV[SHE])	-350 to 160
EPR (C/cm ²)	0 to 30
Load Ratio (R)	0.5 to 1.0
Frequency (Hz)	2×10^{-4} to 2×10^{-2}
Stress Intensity Factor (MPa√m)	11 to 60

A total of 272 data points were obtained from ANL. Similarly, this data also consisted of corrosion fatigue and constant load tests. From this population, a total of 7 Type 304 stainless steel constant load tests were used in developing the crack growth correlation. The following provides a summary of the range of key parameters contained in this database:

Materials	Type 304, 316NG, 347, CF-3M, CF-3, CF-8M, CF-8
Test Temperature (°C)	288
Conductivity (μS/cm)	0.2 to 3.7
O ₂ Concentration (ppm)	0.2 to 8
ECP (mV[SHE])	-560 to 258
EPR (C/cm ²)	0 to 30
Ferrite Level (%)	5.0 to 27.8 (for Cast Materials)
Load Ratio (R)	0.25 to 1.0
Frequency (Hz)	0.008 to 0.1
K (MPa√m)	17.6 to 72

2.2 GE Nuclear Energy Database

Details of this database are provided in Appendix B of this report. The data were derived from two different sources (see Appendix B for references to the source of data). The first source of data was the studies that were performed as part of the pipe cracking investigations and were used as the basis for the NRC disposition line [3]. The data were reassessed for the test conditions and the stated crack growth rate. The tests were performed largely by GE. The tests that were performed were conducted in one of two environments: 0.2 ppm oxygen and 6 ppm (referred to in the literature as 8 ppm due to the upper test specification limit) oxygen 288°C high purity BWR water. The tests were conducted at conductivity levels that are higher than the conductivity levels associated with the current typical operational levels at BWRs. The data were performed under well-controlled test conditions and are useful to expand the total range for the correlation development. The tests that were run did not include any ECP measurements. Therefore, the ECP were assigned based on the test environment. The ECP assigned was derived from a comparison of several ECP/water chemistry correlations. The ECP values that were assigned were 60 mV(SHE) and 120 mV(SHE) for the GE 0.2 ppm and 6 ppm tests, respectively. Because of the uncertainty about ECP, this data set was not used to develop the correlation but was used to test the correlation as illustrated in Appendix C.

The second, comprehensive data summary was developed by reviewing and assigning crack growth rates to the data from CAVS tests that were performed at actual operating plants. These tests were performed at Brunswick 1, Duane Arnold, FitzPatrick, Hatch 1, Limerick, Nine Mile Point 1, Pilgrim, Peach Bottom 2 and 3 and an overseas plant over the time period of 1988 through 1993. These test systems included ECP measurements and are fully documented tests. Data from these tests were used to develop the crack growth correlation.

3

EMPIRICAL CRACK GROWTH CORRELATION STUDIES

The database of laboratory data developed by SI and GE in Section 2 of this report are analyzed for the purpose of developing an empirical crack growth correlation for stainless steel. The objective is to analyze the data so as to derive a crack growth model of the form,

$$\frac{da}{dt} = CK^n \quad \text{Equation 3-1}$$

where K is the stress intensity factor. K is a parameter that describes the stress field near a crack. It is dependent on the applied stresses, the crack size and the geometry of the cracked body. The other parameters in Equation 3-1 are C , an environmental term, a , the crack depth, t , the time, and n , a power exponent. In this expression, C and possibly n may depend upon the electrochemical potential, the conductivity, and other variables as appropriate.

3.1 Evaluation of the Database for Model Development

The combined database was evaluated to ensure that only relevant data was used in the model correlation development. From this evaluation, it was observed that nearly half of the data were CAVS data provided by GE. These data are representative of plant water ionic species. The tests were conducted in autoclaves that were attached directly to various locations in the reactor coolant loop. Limited in-core crack growth data were also available from four reactors. These data were not used to develop the correlation but were instead used to test the final correlation (Appendix C). These data were excluded in developing the correlation since they are irradiated and the fluence was not available. There is presently considerable uncertainty as to the exact mechanism(s) that are responsible for IASCC, but it is also known that fluence is an important variable for correlating IASCC [1], and accurate values for that variable were not available within the in-core specimen database. In addition, they are wedge-loaded double cantilever beam (DCB) specimens whereas the specimens used to develop the correlation were thermally sensitized and were actively loaded compact tension (CT) specimens. One observation from this database was that the crack growth rate of thermally sensitized specimens was higher than irradiation-sensitized specimens. It should be noted that the correlation was developed with data from thermally sensitized specimens and is believed to be conservative for irradiation-sensitized materials.

Some CAVS specimens were listed with a comment in the database, such as start-up, beginning of hydrogen injection, hot standby, etc. These short-term transient conditions are not representative of the long duration, steady operating conditions. Consequently, data from these specimens were not used in the analysis.

A relatively large subset of laboratory data was excluded because the specimens were cyclically loaded. Even though some of the frequencies were relatively low, preliminary pattern recognition results showed higher crack growth rates for the cyclic data, increasing as the frequency increases. The purpose of the present work was to develop a correlation for stress corrosion cracking, i.e., static load, that was representative of the BWR internals. Consequently, only static load data were used in the calibration.

Having eliminated the above data from further considerations, the resulting database had 122 useable observations that were used to develop the crack growth correlation model for stainless steel. The adequacy of this resulting database for model development is discussed in Appendix C of this report.

3.2 Development of Empirically-Based Stainless Steel Crack Growth Rate Correlation

The empirically based stainless steel crack growth rate correlation was developed using the pattern recognition and multivariate modeling tools that have been used on several previous projects [1, 2]. Additional details of the model development are provided in Appendix C of this report and only a summary is provided in this section. The steps in the analysis included identifying correlations among the presumed independent variables, using pattern recognition techniques to identify the most sensitive variables and the form of functional dependence, performing multivariable modeling by nonlinear least square techniques, and analyzing the quality of fit by statistical methods and by plotting normalized and residual plots. The list of the variables that were considered in the pattern recognition and their range of values are shown in Table 3-1. The effect of these variables on the crack growth correlation is provided in the following pages. It is noteworthy that the test of the model is performed against a field data set using the least squares fit and a 95th percentile to encompass this data. This approach is used to illustrate the conservative nature of the model encompassing all but a few of the field data.

Table 3-1
Variables and Range of Calibration Data Considered in Crack Growth Correlation Studies

Model Variable	Minimum	Maximum
Conductivity, $\mu\text{S}/\text{cm}$	0.055	1.50
ECP, mV(SHE)	-575	250
Temperature, $^{\circ}\text{C}$	210	289
Stress Intensity, $\text{MPa}\sqrt{\text{m}}$	11	60

Conductivity. Conductivity strongly influences crack growth rate. The overall effect of conductivity is consistent in the smaller subsets of data, although its exponent varies over a factor of 2. The power law dependence given by Equation 3-1 agrees reasonably well with the data (considering the scatter) over the range 0.1 to 1 $\mu\text{S}/\text{cm}$ (Figure 3-1).

**Content Deleted -
EPRI Proprietary Information**

**Figure 3-1
Effect of Conductivity**

Conductivity is an easily measured indicator of the concentration of total ionic species present. Since some ionic species are more aggressive than others, the relationship between conductivity and SCC behavior varies depending on ionic species. There was insufficient data to calibrate models for specific anions. However, as shown in Appendix C (Figure C-8), the model is representative for sulfate, and conservative for chloride.

Stress Intensity Factor, K. The effect of stress intensity, K , on the normalized crack growth rate of Type 304 stainless steel is shown in Figure 3-2. The slope of the dependence of crack growth rate on K is not stable as smaller subsets of data are considered, as noted in Appendix C. In the small number of cases where the same heat was tested in the same environment at two or more K levels, the exponent varies from about -6 to +12. Most of this variation is undoubtedly due to scatter in very small samples over a narrow range in K . Over the 122 observations used for calibration, a best-fit exponent near the value in the NUREG-0313, Revision 2 [3] was found (2.181 vs. 2.161). The GE PLEDGE model [4], with strain rate proportional to K^4 and da/dt proportional to (strain rate)^{0.5} would agree with an exponent of 2. However, there is also some support for a near-zero exponent when K is above a threshold value, because "plateau behavior" has been observed in a number of studies of stress corrosion and corrosion fatigue cracking. In particular, the GE subset of data analyzed here shows such an effect, with a basically flat ($K^{-0.14}$) dependence on loading. No plateau behavior has been assumed in the empirical model. Alternatively, a power law has been used which is believed to be conservative over the range of K considered.

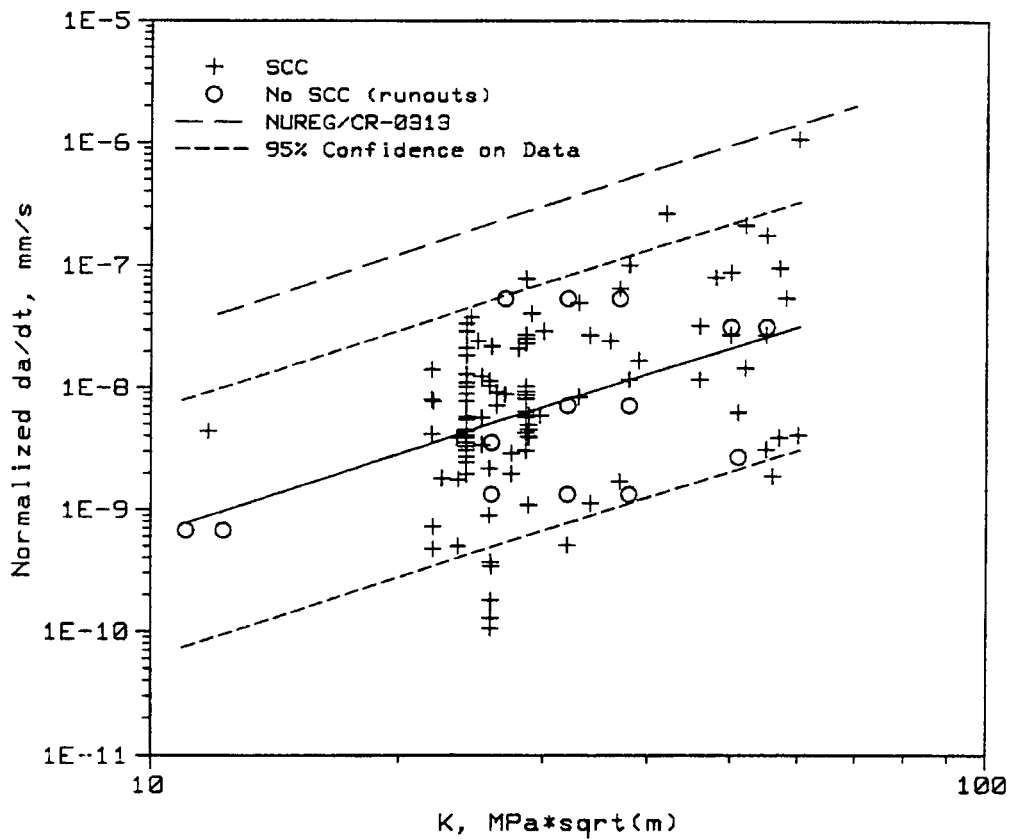


Figure 3-2
Effect of K on Crack Growth of Type 304 Stainless Steel

Temperature. A strong effect of temperature was noted in the data, with higher SCC susceptibility at lower temperatures (Figure 3-3). This is consistent with other testing that showed a maximum in SCC sensitivity near 200°C [5]. The range in temperature in the data comes from the CAVS specimens, which are in autoclaves attached to reactor water clean up (RWCU) system and recirculation loops that are somewhat cooler than the reactor core.

**Content Deleted -
EPRI Proprietary Information**

**Figure 3-3
Effect of Temperature on Crack Growth of Type 304 Stainless Steel**

Electrochemical Corrosion potential EC . The trends in C are similar in shape but somewhat weaker than expected (Figure 3-4). A linear form fits the data as well as other forms that were tried. The model has a saturating form of C dependence that suggests insensitivity to C above 200 mV and below -400 mV, but it is similarly near linear over the range of the data.

**Content Deleted -
EPRI Proprietary Information**

**Figure 3-4
Effect of ECP on Crack Growth of Type 304 Stainless**

Electrochemical potentiokinetic reactivation (EPR). Using the pattern recognition and multivariate analysis phases, it was determined that the degree of sensitization (R) was not a key variable for the 22 points included in the database. All trends with R were not significant and were contrary to the expected sign, i.e., da/dt decreased as R increased. The interpretation of R effects is clouded by the $R^2 = 0.1$ correlation with test temperature, which must arise from inadvertent patterns in the data, since it cannot be a physical relationship. In addition, many R values are estimated rather than measured, so it is the least well-known variable. Furthermore, the data available to develop the correlation was based predominantly on test data from thermally sensitized material. Only a limited number of tests on non-sensitized material were available. For all of these reasons, R is not included in the models developed here. Its absence is not critical because the calibration set included exclusively sensitized materials, so the model developed here is relevant to heavily weld-sensitized material ($R = 5 \text{ C cm}^2$) and should be conservative for non-sensitized or lightly-sensitized materials.

Only pre-cracked specimens were used in the present study to develop the crack growth rate correlation. In a previous study of a different database [1], the effect of sensitization as measured by the R test was evident in the probability of initiating cracks in constant extension rate tests (CERTs), but not in the pre-cracked specimen growth rates. This historical observation does not explain the current observation of a negative effect of R , but it does provide further evidence of the elusive nature of R effects in pre-cracked specimen data. The uncertainties with respect to this variable can only be resolved by obtaining more measured values for the current database and additional heats.

3.3 Correlation Models

The above observations were used to derive a crack growth correlation model for Type 304 stainless steel for application to the BWR shroud. For purposes of developing the correlation given here, only those observations with measured values of average conductivity and ECP were used for model calibration. This prevented the use of older data points that were used in the NUREG-0313, Revision 2 document, because average conductivity and ECP could only be estimated for those points.

The best-fit model (see Appendix C) for the Type 304 stainless steel data is:

$$\ln da/dt = 2.181 \ln(K) - 0.787 \text{Cond}^{-0.586} + 0.00362\text{ECP} + 6730/T_{\text{ABS}} - 35.567 \quad \text{Equation 3-2}$$

where the units are:

da/dt	=	crack growth rate (change in crack depth per unit time)	mm/s
K	=	stress intensity	MPa√m
$Cond$	=	average conductivity (determined at room temperature)	μS/cm
ECP	=	electrochemical corrosion potential	mV(SHE)
T_{ABS}	=	temperature	°K
SHE	=	Standard Hydrogen Electrode	
1mm/s	=	141.73 in/hr	

The range of data used to develop the model is shown in Table 3-1. It is recommended that the model should be applied only within these limits.

The above expression in Equation 3-2 represents the mean of the $\ln\left(\frac{da}{dt}\right)$ data. The agreement between the data and the model given by Equation 3-2 can be evaluated graphically by examining normalized plots, in which the data points are adjusted as well as possible to a set of common conditions (assuming that the model correctly reflects the effect of each variable). The equation for this adjustment is:

$$\ln(a/t)_{\text{norm}} = \ln(a/t)_{\text{data}} + \ln(a/t)_{\text{SC}} - \ln(a/t)_{\text{mod}} \quad \text{Equation 3-3}$$

here the meaning of each subscript is as follows:

$norm$	=	plotted values
$data$	=	actual observed value
SC	=	value calculated from the model at the standard conditions of all variables (except using the actual value of the x variable being plotted)
mod	=	value calculated from the model at the same conditions as the actual observed data

Referring to the normalized plots for the best-fit model, Figures 3-1 through 3-4, there is reasonable agreement between the data used for calibration and the model when all are adjusted as nearly as possible to common conditions. The common conditions were:

$$\begin{aligned} K &= 25.0 \text{ Mpa } \sqrt{\text{m}} \\ \text{Cond} &= 0.10 \text{ } \mu\text{S/cm} \\ \text{ECP} &= 0.0 \text{ mV(SHE)} \\ T &= 270^\circ\text{C} \end{aligned}$$

Figure 3-2 shows how the best-fit model (solid line) compares with the NUREG-0313, Revision 2 line (long dash) when plotted at the normalizing conditions given above. The short dashed line is the estimated 95th percentile of the residuals about the model, assuming they are log-normally distributed. The short dashed line is plotted at +1.645 standard deviation above the model (a factor of 10.3 on da/dt). The line will be referred to as the 95th percentile model or correlation in this report and has the form:

$$\ln da/dt = 2.181 \ln (K) - 0.787 \text{ Cond}^{-0.586} + 0.00362\text{ECP} + 6730/T_{\text{ABS}} - 33.235 \quad \text{Equation 3-4}$$

Plots of the best-fit model at conductivities of 0.3 $\mu\text{S/cm}$, 0.2 $\mu\text{S/cm}$ and 0.1 $\mu\text{S/cm}$ and below are presented in Figure 3-5. As can be seen from this plot, the best-fit model represents the mean of all the data. Also shown in Figure 3-5 are plots of the 95th percentile. The 95th percentile plots bound most of the data and will be recommended for use in the crack growth evaluation of the shroud, for the given water average conductivity and ECP selected. The evaluation methodology using the 95th percentile model is discussed in Section 6.

**Content Deleted -
EPRI Proprietary Information**

**Figure 3-5
Model Prediction for Best-Fit and 95th Percentile for Conductivity of 0.3 $\mu\text{S}/\text{cm}$**

3.4 Comparison of Model Predictions With Experimental Data

The predictions of the 95th percentile model [Equation (3-4)] at the BWR operating temperature of 288°C and three levels of conductivities (0.1, 0.2, and 0.3 $\mu\text{S}/\text{cm}$) at varying ECP values are shown in Figures 3-6 through 3-8. Also shown on these figures are the experimental data points used to derive the model and the NRC disposition curve in NUREG-0313, Revision 2 as well as a horizontal line representing a crack growth rate of 5×10^{-5} in/hr which is currently used in flaw evaluation of the shroud. As can be seen from these figures, for the same values of ECP, the

model predicts higher crack growth rates with increasing conductivity. It can also be observed from these figures that with the exception of a few points, the model predictions reasonably bounds the experimental data at the various conductivity levels and ECP values demonstrating the conservative nature of the model using the 95th percentile.

**Content Deleted -
EPRI Proprietary Information**

**Figure 3-6
Comparison of Stainless Steel Crack Growth Model Predictions (95th Percentile) With
Experimental Data (Conductivity of 0.1 μ S/cm Temperature of 288°C and Varying ECP)**

**Content Deleted -
EPRI Proprietary Information**

**Figure 3-7
Comparison of Stainless Steel Crack Growth Model Predictions (95th Percentile) With
Experimental Data (Conductivity of 0.2 μ S/cm Temperature of 288°C and Varying ECP)**

**Content Deleted -
EPRI Proprietary Information**

**Figure 3-8
Comparison of Stainless Steel Crack Growth Model Predictions (95th Percentile) With
Experimental Data (Conductivity of 0.3 μ S/cm Temperature of 288°C and Varying ECP)**

Figures 3-6 and 3-7 demonstrate that at average conductivity levels below 0.2 μ S/cm and ECP values below 200 mV(SHE), the crack growth rate of Type 304 stainless steel is significantly below the NRC disposition law. At an average conductivity of 0.3 μ S/cm and ECP of 200 mV(SHE), the model prediction is above the NRC disposition curve but not by a significant margin. At low conductivity (0.1 μ S/cm) and HWC conditions (ECP = -230) to -500 mV(SHE), the model predicts crack growth rates of more than an order of magnitude lower than the

NUREG curve. These figures also show the conservatism of the K-independent 5×10^{-5} in/hr value that is currently used to perform flaw evaluation of the shroud especially at K values below $30 \text{ ksi}\sqrt{\text{in}}$. The limited data of crack growth rates at high K values suggest that a strong case can be established for K-independence behavior in this regime. At high K values, none of the crack growth data exceeded 5×10^{-5} in/hr.

3.5 Comparison of Model Predictions With Field Data

The 95th percentile prediction and comparison with crack growth data from four plants (KKM, Chinshan, Browns Ferry and Brunswick) are shown in Figure 3-9. The plant inspection data used to determine the crack growth is presented in Section 6.3 with more details provided in Appendix I. The methodology for determining the stress intensity factor (K) as a function of crack depth is discussed in Section 5. Figure 3-9 illustrates the NUREG curve and the empirical model generated for NWC conditions with an ECP of 200 mV(SHE) and an average conductivity of $\leq 0.15 \mu\text{S}/\text{cm}$ (reference curve). Seven of the data points from Brunswick were obtained under HWC conditions and as expected, they all fall under the reference curve. The remaining points were all obtained under NWC conditions and all but one fall under the reference curve. The data also included some welds with fluence above $5 \times 10^{20} \text{ n}/\text{cm}^2$ from KKM. These data points also fall under the reference curve. In spite of the uncertainties in UT measurements, estimation of K and fluence effects, the 95th percentile model provides a reasonable bound for field data.

Additional information on shroud cracking to date in domestic BWRs in the U.S. is provided in Appendix Q. In all circumferential shroud cracking has been identified in at least 29 plants to date. None of the cracking in these shrouds is through-wall.

**Content Deleted -
EPRI Proprietary Information**

**Figure 3-9
Comparison of Model Prediction With Field Data**

4

OPERATING AND RESIDUAL STRESS EVALUATION

Stresses associated with BWR shrouds can be classified into two broad categories; operational stresses and fabrication-related stresses. Operational stresses are those associated with the normal operation of the plant and consist of stresses analyzed in the ASME Code stress reports. Fabrication stresses for the shroud consist mainly of weld residual stresses resulting from welding the various shroud plates and rings. Additional fabrication stresses include machining or grinding stresses and fit-up stresses.

4.1 Operating Stresses Experienced by Core Shroud

Operating stresses in the BWR shroud are relatively low. Through-wall membrane stresses are developed in the shroud as a result of deadweight, differential pressure and thermal expansion. A survey of stress reports for a representative number of BWR core shrouds indicate that the maximum operating membrane stress is on the order of 1.6 ksi.

4.2 Background on Weld Residual Stresses

During fabrication of the shroud, several plates and rings are welded together to form the cylindrical shape. As a result of the welding, residual stresses are developed. Key factors that determine the magnitude and distribution of the residual stresses are heat input during welding; weld sequence, weld starts and stops, and cooling time between passes; surrounding joint geometry; fit-up strains required to make pieces match up; base/weld metal mechanical properties; load weld repairs; post weld heat treatment; and any post weld mechanical processes such as grinding and machining. Even though it is believed that residual stresses play a significant role in any potential cracking of the shroud, the magnitude of these stresses and their distribution have not been studied extensively for the shroud configuration. A considerable amount of experimental and analytical work performed to determine the residual stress of butt welds in stainless steel piping [3, 7, 8, 9] have shown that, in general, near-yield level tensile residual stresses are developed on the inside surface. Small-diameter piping welds (thickness < 1.0 inch), exhibit through-wall linear bending residual stress distribution with tensile yield level stress on the inside surface [7]. The through-wall distribution for large-diameter piping is U-shaped, as shown in Figure 4-1, with tension on the inside and outside surface and compression in the middle half of the pipe wall. Also shown in Figure 4-1 is the through-wall axial residual stress distribution accepted by the NRC for IGSCC crack growth evaluation of large-diameter piping. Since the thickness of a typical BWR shroud is 1.5 inches, it can be expected that the through-wall residual stress distribution will be similar to that of the large-diameter piping shown in Figure 4-1. However, there are some significant differences between the two components such that the large-diameter piping residual stress distribution may not be directly applicable to the shroud. In the first place, most piping welds are fabricated one-sided

while a typical shroud is welded from both sides, as shown in Figure 1-3. Hence, the constraint during the welding process may be significantly different for the two components. Secondly, some of the weld locations of the shroud, especially at the welded rings for H3 and H6 are very stiff and the additional stiffness provided by the welded rings could influence the through-wall residual stress distribution. Thirdly, the heat input used in the fabrication of the shroud may be different from that used for the piping butt weld. The flexibility of the shroud measured in terms of the radius-to-thickness (R/t) ratio is also different than that of a typical piping weld which could also affect the residual stress distribution. Because of these differences, both experimental and analytical studies were performed to quantify the magnitude and distribution of the weld residual stresses in typical BWR shrouds. In performing these studies, it is recognized that one residual stress distribution may not be able to represent all the various weld locations of shroud. Consequently, specific studies were performed for the shell-to-shell welds, such as H4 and H5, as well as for the shell-to-ring welds, such as H3 and H6.

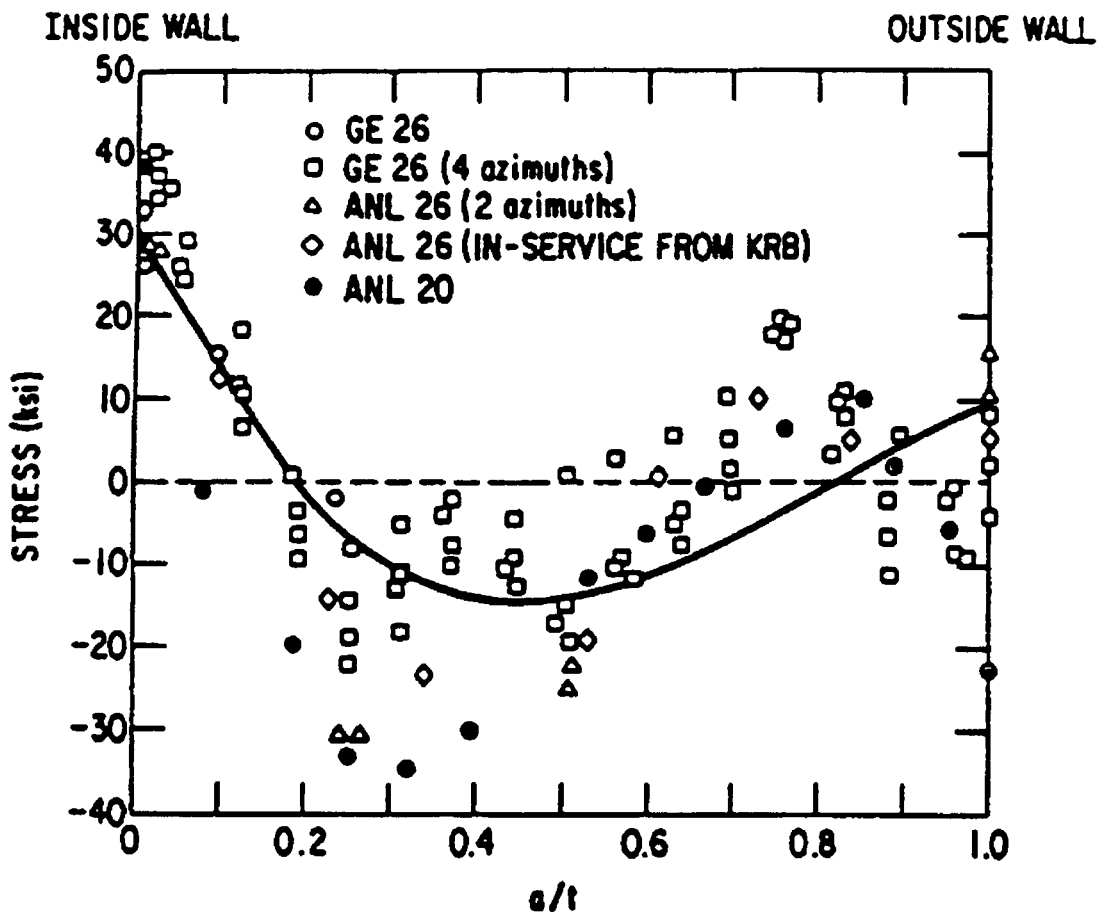


Figure 4-1
NRC Accepted Axial Weld Residual Stress Distribution for Large Diameter
Piping [3]

4.3 Residual Stress Measurements of Core Shroud Welds

The weld residual stress measurements of the shroud employed both surface residual stress measurements by using a blind hole drilling method and through-wall residual stress measurements utilizing the crack compliance method. The measurements were performed on spare BWR/6 shrouds for two plants that were never put in service as described in the following sections.

4.3.1 Near-Surface Residual Stress Measurements

The near-surface residual stress measurements were performed on spare BWR/6 reactor core shrouds at Grand Gulf Nuclear Station (GGNS) and River Bend Nuclear Station (RBNS). Details of these measurements are provided in Appendices E and G of this report. The following provides a summary of these measurements.

Measurements at Grand Gulf Nuclear Station (GGNS)

The spare shroud at GGNS was fabricated using Type 304L stainless steel and measured approximately 20 ft. high by 20 ft. in diameter with a wall thickness of approximately 2 inches. Residual stress measurements were made by Sandia National Laboratories, Albuquerque, New Mexico, at five weld locations on the outside (OD) surface and corresponding locations on the inside (ID) surface. These five locations corresponded to the H3, H4, H5, H6A, and H6B weld shown in Figure 1-1. At each location, measurements were made at the weld, the heat affected zone (HAZ) and outside the HAZ. The H3 OD, H6A ID, and H6B ID and OD weld crowns were not measured since they are fillet welds.

The residual stress measurements were made using the blind hole drilling method. This method is the standard technique used to determine surface residual stresses and described in ASTM Standard E837-94 [10]. The method involves bonding three strain gages in the form of a rosette at three angles, 0°, 45°, and 90° to form a circle. A hole is drilled in the middle of the rosette and as the hole is being drilled, the strain that is relieved is measured. The depth of the hole is limited to 40% of the gage diameter. Residual stresses can then be determined from the relieved strain using relationships provided in ASTM Standard E837-94. During the tests, a gage diameter of 0.202 inches and two hole diameters of 0.062 inches and 0.072 inches were utilized. The full depth of the drilled hole was 0.081 inches and the strain measurements made to a depth of 0.072 inches.

A total of 39 strain measurements were made on the shroud. Each measurement consisted of 10 strain readings recorded at 0.008 inch increments. The data was then reduced to calculate the hoop, longitudinal, and shear stresses. Because of the various surface treatments performed on the shroud surface (such as sand blasting and grinding) before the test, the first two to three data points were compressive and inconsistent compared with the other data points. As such, these data points were not considered in determining the surface residual stresses. Having eliminated these data points, the stresses as a function of depth were plotted to determine the uniformity of the stresses. As a result of this, three categories of measurements were established. Equivalent stresses that plotted out as a straight horizontal line showing uniformity were referred to as "good". Equivalent stresses that plotted as slightly curved line or was slightly angled were

referred to as “marginal”. The last category referred to as “non-uniform” was equivalent stresses that did not show any clear trend. Of the 39 measurements, 13 were good, 18 were marginal and 7 were non-uniform. The measurements that did exhibit non-uniform behavior were considered questionable and therefore eliminated from further considerations.

**Content Deleted –
EPRI Proprietary Information**

Measurements at River Bend Nuclear Station

The spare shroud at River Bend was also fabricated from Type 304L stainless steel with measured room temperature base metal yield stress of 35 ksi. Near surface residual stress measurements were made on both the inside surface and outside surface at welds H3, H4, H5, H6a, and H6b by the EPRI NDE Center staff. At each location, measurements were made, at 1/4 inch above the weld fusion line, the weld centerline and 1/4 inch below the weld fusion line.

The blind hole drilling method was also employed for the measurements consistent with the requirements of ASTM Standard E837-94 [10]. Strain readings were taken at consistent depth intervals and continued until the strain readings stabilized. This ensured that a direct correlation could be made among all rosettes and gages. The drilling continued to a consistent depth of 0.090 inches. The relief strain values stabilized at a drilled depth of about 0.060 to 0.075 inches. The strain measurements were then reduced to calculate the residual stresses.

The measured residual stresses are shown in Table 4-2. As can be seen from this table, most of the measured values are tensile and near or above yield level. Weld H6a showed somewhat less tensile residual stress above the fusion line and in one case it showed compressive residual stress. Similar to the measurements obtained from Grand Gulf, the conclusion to be drawn from the measurements at River Bend is that, in general, yield level tensile residual stresses are present at the surface of weld locations of the shroud. Details of the test procedure and measurements at River Bend are provided in Appendix E of this report.

Table 4-1
Summary of Near Surface Residual Stress Measurements at Grand Gulf Nuclear Station

**Content Deleted –
EPRI Proprietary Information**

Table 4-1
Summary of Near Surface Residual Stress Measurements at Grand Gulf Nuclear Station (Continued)

**Content Deleted -
EPRI Proprietary Information**

Table 4-2
Summary of Near Surface Residual Stress Measurements at River Bend Nuclear Station

**Content Deleted –
EPRI Proprietary Information**

4.3.2 Through-Thickness Residual Stress Measurements at River Bend Nuclear Station

Through-wall residual stress measurements of the shroud welds H5, H6A, and H6B at River Bend were performed by University of California, Berkeley using the crack compliance method. The theoretical background of this method and details of the methodology in application to the measurements of the shroud at River Bend are provided in Appendix F of this report. In summary, the method involves installing a strain gage at an optimal location of a specimen containing the weld. An electrical discharge wire machining (EDWM) is used to introduce a thin cut of increasing depth in the specimen. The strain distribution during the cutting process is measured. The relationship between the stress released and the measured strain is given by:

$$\varepsilon(a) = \sum_{i=0}^n \frac{\sigma_i}{E'} C_i(a)$$

Equation 4-1

The unknown residual stress distribution is represented by a series:

$$\sigma(x) = \sum_{i=0}^n \sigma_i P_i(x) \quad \text{Equation 4-2}$$

where:

$P_i(x)$ = the surface traction

σ_i = the amplitude factor for the i^{th} term $P_i(x)$

E' = an elastic constant

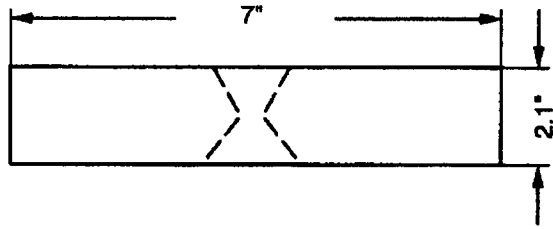
$C_i(n)$ = the crack compliance function for $P_i(x)$

The crack compliance functions were obtained by using fracture mechanics solutions in the literature or finite element analysis. When a number $m > n+1$ of strain measurements are made, a least square fit can be used to minimize the average errors involved in the measurement and estimation resulting in $n+1$ linearly independent equations given as:

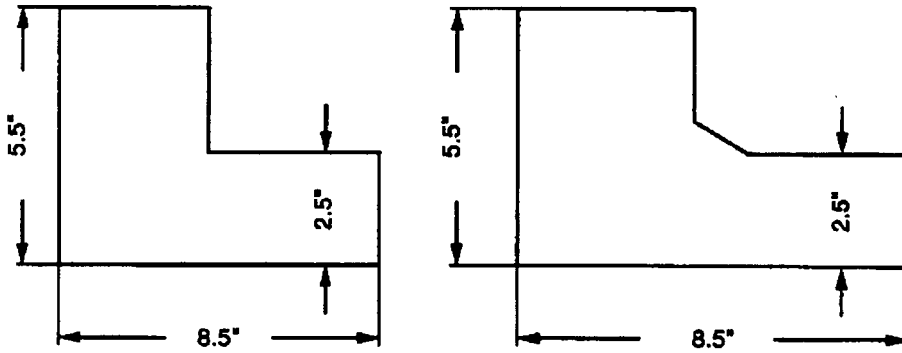
$$\frac{\partial}{\partial \sigma_i} \sum_{j=1}^m \left[\varepsilon(a_j) - \sum_{k=0}^n \sigma_k C_k(a_j) \right]^2 = 0 \quad i = 0, \dots, n \quad \text{Equation 4-3}$$

from which the unknown σ_i can be solved.

The above procedure was used to determine the through-wall residual stress distribution in the shroud for welds H5, H6a, and H6b. The geometry of the specimens that were used to obtain the measurements are shown in Figure 4-2, and the weld profiles as well as location of the measurements are shown in Figure 4-3. The strain and the through-wall residual stress distributions are presented in Appendix F (Figures F-4 through F-9).



(Weld H5)



(Weld H6A and H6B)

Figure 4-2
Test Specimens for Through-Wall Residual Stress Measurements at River Bend Nuclear Station

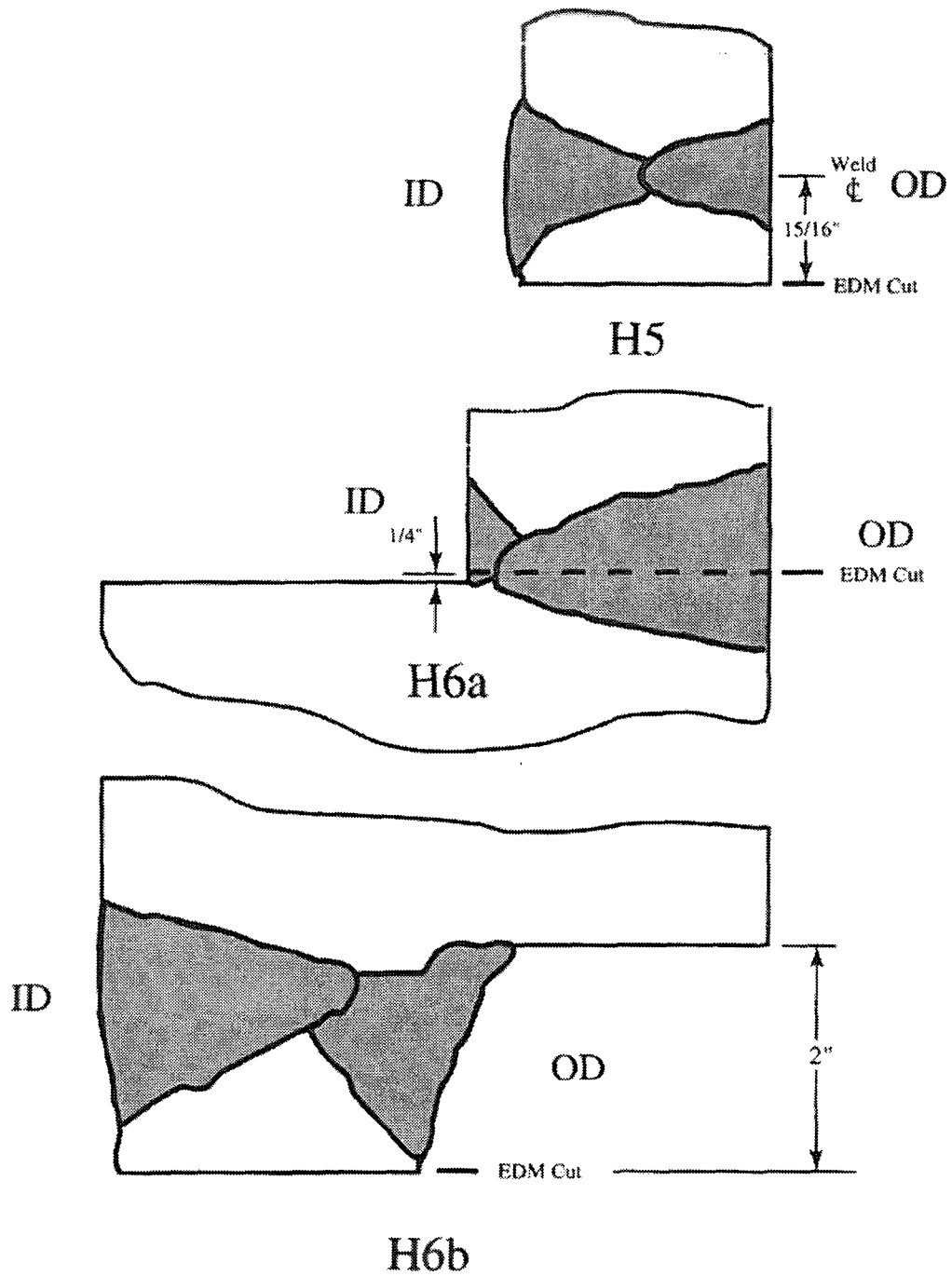


Figure 4-3
Weld Profiles and Planes for Through-Wall Weld Residual Stress Measurements at River Bend Nuclear Station

The use of this procedure required that the specimen be cut out of the shroud. Details of the parting out of the test specimen from the shroud for the through-wall residual stress measurements are provided in Appendix E. In summary, the severed piece was parted out of the remainder of the shroud using water jet cutting instead of the traditional plasma arc cutting. This resulted in a fairly smooth edge finish without inducing excessive heat build-up. Prior to the parting out of the specimen strain gages were mounted axially and circumferentially centered on the outside surface of weld H5. The cutting was made such that welds H5, H6a and H6b are included in the parted out specimen. The strain gages measured the relieved strain during the cutting process.

The original residual stress (σ_r) in the shroud consists of two parts:

$$\sigma_r = \sigma_1 + \sigma_2 \quad \text{Equation 4-4}$$

where:

σ_1 = stress measured in the specimen as described

σ_2 = change of stress when the specimen was cut out (parting out stress)

The distribution of σ_2 is determined by strain measurements obtained during the parting out process of the test specimen from the shroud. The through-wall measurements for σ_1 , σ_2 , and σ_r are presented in Appendix F. As described in Appendix F, the parting out stress (σ_2) is a through-wall bending stress with tension on the ID surface of the shroud. Hence, the final residual stress distribution (σ_r) is more tensile on the ID surface and less tensile on the OD surface of the shroud. The parting out stress was determined to be more significant for the shell-to-shell welds than the ring-to-shell welds.

4.4 Analytical Determination of Residual Stresses in Core Shroud Welds

In parallel with the experimental determination of weld residual stresses of the core shrouds at River Bend and Grand Gulf Nuclear Stations, finite element analyses were performed by Dominion Engineering Inc. to analytically determine the weld residual stresses. The objective of this activity was to develop an analytical technique to complement the experimental residual stress distribution. The analyses were performed using geometrical and weld procedure information for the spare core shroud at River Bend and a shroud mock-up fabricated by Tokyo Electric Power Company (TEPCO). The choice of the parameters of the River Bend shroud for analytical modeling is convenient because it offered the opportunity of comparing the results of the analytical evaluation with the experiment results discussed in the previous sections. For River Bend, the study focused on the circumferential welds H4, H5, H6a, and H6b, since the most significant cracking, in terms of extent and depth, has been reported to be in the HAZ of the circumferential welds. The circumferential H2 and H3 welds were analyzed for the TEPCO shroud mockup design.

The weld residual stress analyses were performed using the ANSYS finite element code [11]. The symmetrical nature of the shroud permitted an axisymmetric finite element model to be employed for the analysis. Because of the relatively high temperatures associated with the welding process and the resulting high strains, a thermo-elasto-plastic analyses was performed utilizing temperature-dependent material properties. For the analysis of the welds at River Bend, the yield strength of the weld metal was obtained from actual certified material test reports at River Bend that indicated a very high yield stress value of 67 ksi. The base material was assumed to be 40 ksi that is typical of values used for Type 304 stainless steel for this kind of analysis. Other than the yield stress, all material properties were assumed to be the same for the base and weld metals. It was assumed that both the base and weld metals behave as elastic-perfectly plastic materials. Eight to ten weld passes were assumed based on information obtained from the welding procedures used in the fabrication of the shroud at River Bend. In the analysis of the TEPCO shroud mockup, the same yield stress of 67 ksi was used for the base metal and the weld.

The simulation of the welding process consisted of three stages. In the first stage, a thermal analysis was performed. This involved application of appropriate thermal boundary conditions followed by simulation of each welding pass. Weld passes were simulated by successively activating the elements that make up each weld pass, applying a uniform heat generation rate to all the elements in the pass and then allowing the weld metal and shroud to cool to room temperature. Temperature distributions were calculated at a number of points in time during each weld pass and saved for use with the structural model. The second stage involved the structural analyses that were performed by the application of the temperature distribution to a structural model. Residual stresses were then determined by sequentially imposing the temperature distributions at each time step as loads on the structural model and then solving for the resultant stresses. In the final stage of the modeling process, the shroud was subjected to a post weld heat treatment for 24 to 48 hours at 750°F. This only involved welds H3, H4, H6a, and H6b.

To account for all the shroud welds under consideration, the analyses were performed on three separate finite models. One model was created for weld H3. One model was created for welds H4 and H5 since the weld preparations are essentially identical for these two welds. The third model included welds H6a and H6b since the effects of one of these welds on the other may not be negligible. A separate model was developed for welds H2 and H3 in the TEPCO shroud mock-up.

The results of the analyses for all the welds considered are shown in Appendix H (Figures H-13 through H-19). The results show the distribution of through-wall axial and hoop stresses at key locations of the weldments as well as contour plots. For the River Bend models (Figures H-14 through H-18), the plots reflect different yield strengths for the base metal and weld metal (40 and 67 ksi, respectively). For the TEPCO model (Figure H-13), the plots reflect identical yield strength of 67 ksi for both the base metal and the weld. The following observations are made for the shell-to-shell welds (H4 and H5) in Figures H-15 and H-16.

- The maximum hoop stress occurs on the side of the shroud where the last welding was performed (in this case, on the OD side).
- The axial stress is highest on the side of the shroud, opposite of where the last welding was performed (in this case, on the ID side).

- There is a zone of high compressive axial stress in the middle of the shroud wall.
- Stress relief performed on weld H4 causes the final residual stresses to be lower than on the similar weld H5 that is not stress relieved.

The analysis also demonstrated the residual stress distributions of the ring welds (H3, H6a, and H6b) are slightly different than that of the shell-to-shell welds shown in Figures H-13, H-14, and H-18. This suggests that the stresses at the ring welds are affected by the large mass of metal in close proximity of the weld that increases the stiffness of the shroud.

4.5 Comparison Between Experimental and Analytical Results

In this section, the surface and through-wall residual stress measurement reported earlier are compared with the analytical prediction, with the objective of establishing the basis for recommendation of appropriate residual stress distributions for use in the crack growth evaluation for the various welds of the shroud. The first comparison made with the analytical predictions examined the surface measurements. This comparison is considered to be of relatively less importance since only the analytically predicted stress at the surfaces is used. It should be realized that the measured surface stresses could be influenced by a number of factors, including the surface preparation such as grinding, and therefore may not provide very meaningful comparison from plant to plant. Figures H-13 through H-18 provide the comparison between the measured surface stresses and the analytical predictions. For the TEPCO shroud mock-up shown in Figure H-13, the calculated stresses provide an upper bound to the measured stresses. The scatter of the experimental data and the relatively few measurement locations made it difficult to draw any definitive conclusions regarding the comparison. Figures H-14 through H-18 provide comparison between the analytical prediction with the surface measurements at River Bend and Grand Gulf. Even though there is significant scatter in the experimental results, the measured and calculated stresses are both consistent with the presence of high surface stresses near the HAZ.

The comparison of the experimental and analytically predicted through-wall axial residual stress measurements is shown in Figures 4-4 through 4-6 for welds H5, H6a, and H6b, respectively. It can be seen from these figures that, in general, the analytical predictions have the same through-wall shape as the experimentally measured distribution; with tensile stresses on the inside and outside surfaces and compressive stresses in the middle half of the shroud wall.

**Content Deleted –
EPRI Proprietary Information**

**Figure 4-4
Comparison of Experimental and Analytical Through-Wall Residual Stress Distribution for Weld H5**

**Content Deleted –
EPRI Proprietary Information**

**Figure 4-5
Comparison of Experimental and Analytical Through-Wall Residual Stress Distribution for Weld H6a**

**Content Deleted –
EPRI Proprietary Information**

**Figure 4-6
Comparison of Experimental and Analytical Through-Wall Residual Stress Distribution for Weld H6b**

4.6 Weld Residual Stress Distribution for Analysis of Core Shroud Welds

For the purpose of providing generic guidance for residual stress distribution for analysis of core shroud welds, the welds were grouped into two categories. The first category includes the shell-to-shell welds. These are the H4 and H5 welds. The experimental (both surface and through-wall) and analytical through-wall residual stress distributions discussed earlier for these welds are shown in Figure 4-7. As can be seen from this figure, there is some variability in the residual stress distribution considering all the data. However, the trending of the residual stress distribution is very clear. Near the inner and outer walls of the shroud, the axial stresses are tensile and the middle half is compressive. The residual stress distribution curve shown in Figure 4-7 is made symmetric with respect to mid-wall of the shroud with the surface stresses at a conservative value of 50 ksi tensile. This value of stress is greater than the nominal yield stress of stainless steel that is typically 35-45 ksi. However, this conservative value was chosen to account for factors such as cold work and strain hardening of the material during fabrication and welding. The maximum compressive stress of 25 ksi at mid-wall was conservatively chosen as half of the maximum tensile stress.

The scatter of the experimental and analytical data points around the residual stress distribution in Figure 4-7 is similar to that of the NRC curve presented in NUREG-0313, Rev. 2 for thick diameter piping and shown in Figure 4-1. It can be seen, by comparing the residual stress curve for the shell-to-shell shroud welds in Figure 4-7 to the NRC recommended curve for large diameter piping in Figure 4-1, that the two curves exhibit similar through-wall behavior. One difference is that the curve from Figure 4-7 for the shroud conservatively assumes a maximum tensile stress of 50 ksi on both the inside and outside surfaces resulting in a symmetrical through-wall axial stress distribution. This is not unreasonable since piping butt welds are one-sided, welded from the inside out, while the shroud is welded from both sides and as such, a symmetrical distribution should be expected. The digitized values of the recommended curve are provided in Table 4-3.

The second category of welds includes the shell-to-ring welds similar to the H2, H3, H6a, and H6b welds. The experimental, analytical, and recommended through-wall distributions for welds in this category are shown in Figures 4-8 through 4-10 for H2/H3, H6a and H6b ring welds, respectively. The trend in the through-wall distribution for these welds is similar to the shell-to-shell welds. The residual stress distribution previously presented for the shell-to-shell welds in Figure 4-7 is also shown in Figures 4-8 through 4-10. As can be seen from this figure, this curve is also a reasonable curve for the shell-to-ring welds. Figure 4-11 also shows a comparison of only the experimentally determined stresses (both surface and through-wall) with the recommended curve. Once again, it can be seen that if only the experimental curves are considered, the residual stress distribution from Figure 4-7 appears to be reasonable representation of axial through-wall residual stress distribution for the shroud welds. Additional justification for the applicability of the generic residual through-wall stress distribution curve to both the shell-to-shell and shell-to-ring welds is provided in Appendix O.

**Content Deleted –
EPRI Proprietary Information**

Figure 4-7
Through-Wall Axial Residual Stress Distributions in HAZ for Shell-to-Shell Weld of Core Shroud (H4/H5) and Comparison With the Standard Curve

Table 4-3
Through-Wall Axial Stress Distributions for BWR Shroud Welds

**Content Deleted –
EPRI Proprietary Information**

**Content Deleted –
EPRI Proprietary Information**

**Figure 4-8
Through-Wall Axial Residual Stress Distributions in HAZ for Core Shroud Shell-to-Ring Welds (H2/H3) and Comparison With
Standard Curve**

**Content Deleted –
EPRI Proprietary Information**

**Figure 4-9
Through-Wall Axial Residual Stress Distributions in Weld for Core Shroud H6a Shell-to-Ring Welds and Comparison With
Standard Curve**

**Content Deleted –
EPRI Proprietary Information**

Figure 4-10
Through-Wall Axial Residual Stress Distributions in Core Shroud H6b Shell-to-Ring Welds and Comparison With Standard Curve

**Content Deleted -
EPRI Proprietary Information**

Figure 4-11
Comparison of Experimental Measurements (Surface and Through-Wall) With Standard |
Curve

It is acknowledged in the generic residual stress distribution provided herein, that the through-wall residual stress profiles at local regions of the shroud can be affected by several factors including fit-up stresses, weld joint geometries, welding parameters such as heat input, welding sequence, welding starts and stops, repairs, material properties and distortions of the shroud during installation. Indeed, the scatter in the data points in Figures 4-7 through 4-10 suggest that there may be, on occasion, residual stress profiles at local regions of the shroud that may be more conservative than the generic curve shown in Figure 4-7. While it may be difficult to give specific guidance as to how to address the various parameters for each individual BWR shroud, comfort should be taken from the fact that the effects of these factors are expected to be localized. In addition, other stresses, such as oxide wedging, may play a role in through-thickness crack growth. The magnitude of these stresses is not well defined and consequently they are not explicitly addressed in this report. However, in examining the field data, particularly for the Brunswick H3 and the KKM H4 cracking, the incremental crack growth appears to be reasonably well accommodated by the empirical correlation, absent consideration of the oxide wedging stresses. If oxide wedging stresses are significant, then they will shift the data points in Figure 3-9 to the right, thus making an even more favorable comparison of these data points with the 95th percentile curve. Thus, it is expected that while for some localized areas of the shroud welds, the generic curve may be non-conservative, this must be compensated by other localized regions with more favorable residual stress distributions. Hence, the possibility of having a deep growing crack around the entire circumference of the shroud is very small, consistent with field experience. It is, therefore, believed that the generic weld residual stress profile presented in Figure 4-7 provides a reasonable representation for the general global behavior of BWR shroud welds for safety evaluation purposes. Consideration of localized stresses in the evaluation is discussed in the following section.

4.7 Methodology for Addressing Localized Stresses

To fully address these localized stresses (both operating and secondary stresses) acting on the core shroud, two additional stress profiles are added to the above generic weld residual stress distributions as discussed in Reference [26].

1. A very conservative membrane stress to account for operating and local stresses on the shroud,
2. A surface residual stress distribution to account for local surface effects resulting from weld repairs and other local phenomena.

The approach taken is to determine an upper bound operating membrane stress on the shroud and then conservatively double this stress. This is then combined with the surface residual stress distribution and the generic weld residual stress distribution as presented in Figure 4-12. The resultant stress distribution is shown in Figure 4-13. The basis for these two additional stress distributions is provided in the following paragraphs.

**Content Deleted –
EPRI Proprietary Information**

**Figure 4-12
Through-Wall Stress Distributions for Weld Residual Stress, Maximum Membrane Stress
and Surface Residual Stress**

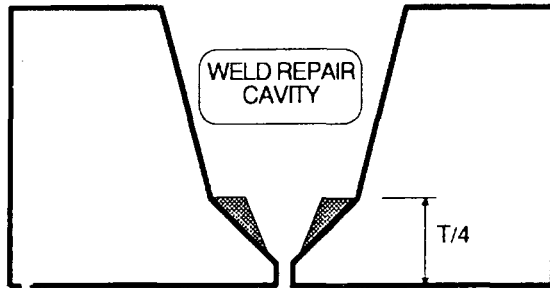
**Content Deleted –
EPRI Proprietary Information**

**Content Deleted –
EPRI Proprietary Information**

**Figure 4-13
Combined Through-Wall Stress Distribution**

Finite element analyses performed as part of this study confirmed that local residual stresses due to repair and fit-up can produce significant surface and through wall stresses in localized regions. It is recognized that fabrication-related repairs to the core shroud welds that involve deep excavations to remove defects (theoretically as deep as 1/2 wall since these are double V-groove welds) and rewelding to fill up the cavities may have generated high local stresses. In some cases, stresses at repairs may exceed the generic weld residual stress distributions recommended above. The highest stresses are likely to occur where an excavation was small in circumferential extent. Filling such an excavation is a very high constraint situation that leads to high weld shrinkage stresses. At the surface, where one of the principal stresses is by definition zero, the residual stress is limited by the yield strength of the material. The recommended stress distribution proposed in Figure 4-13 has a surface stress of approximately 60 ksi which is well in excess of the nominal yield strength of the base metal to allow for some strain hardening and should account for the actual surface stresses at repair locations. Deeper in the repair weld, where a hydrostatic tensile stress is possible, principal stresses may exceed the recommended distribution for repairs of small circumferential extent. For repairs of large circumferential extent that involve deep excavations (e.g. 1/2 T), the restraints on the repair welds are similar to those on the original fabrication welds and are expected to have residual stress distributions similar to those calculated for the final fabrication weld, i.e., the second side of the double V weld. Because both sides of the shroud were accessible during fabrication and welds were made from both sides, there should have been no weld defects that required excavations greater than 1/2 T for repair.

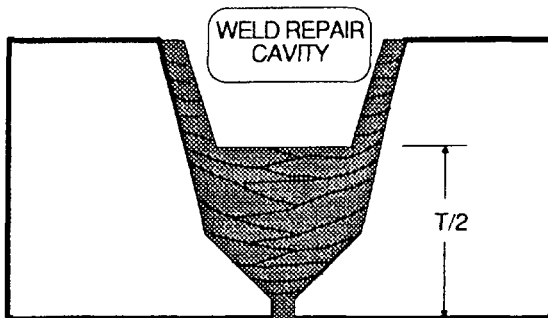
TYPES OF LOCALIZED WELD REPAIRS FOR THE WELD REPAIR
RESIDUAL STRESS EVALUATIONS



QUARTER THICKNESS WELD REPAIR

THROUGH WALL REPAIR MADE AFTER THE WELDING OF THE FIRST QUARTER OF THE WALL THICKNESS

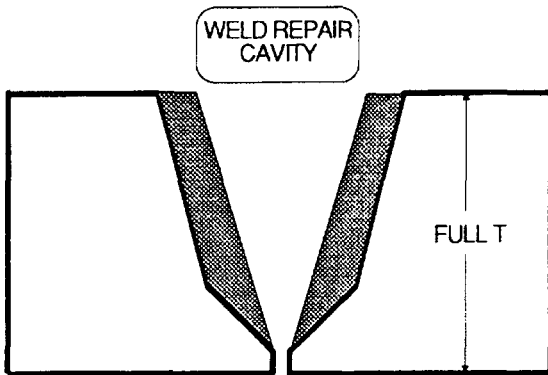
SIMULATES FINDING A ROOT BEAD DEFECT THROUGH IN-PROCESS RADIOGRAPHY, i.e., INSPECTING AFTER THE ROOT AND FIRST FOUR FILL LAYERS ARE COMPLETED



HALF THICKNESS WELD REPAIR

WELD REPAIR OF COMPLETED GROOVE WELD REQUIRING THE REMOVAL OF EXISTING WELD METAL TO A DEPTH OF T/2

SIMULATES FINDING A WELD DEFECT AT MIDWALL UPON FINAL RADIOGRAPHY OF THE COMPLETED WELD



FULL THICKNESS WELD REPAIR

MAJOR THROUGH WALL REPAIR OF A COMPLETED GROOVE WELD REQUIRING FULL REMOVAL OF THE EXISTING WELD METAL IN THE REPAIR AREA

SIMULATES FINDING A ROOT BEAD OR NEAR ROOT BEAD DEFECT UPON FINAL RADIOGRAPHY OF THE COMPLETED WELD

Figure 4-14
The Three Types of Localized Repairs Used in the Weld Repair Study [12]

Based upon standard principles of elastic stress analysis, it is estimated that the effect of the triaxial restraint present at the ends of a repair excavation should affect the residual stresses from the welding for a distance no greater than ten times the plate thickness. In the center of the repair weld, greater than ten thicknesses from either end, the geometry is essentially axisymmetric as was assumed in the weld residual stress simulation analysis presented in Section 4.4. Therefore, in the portions of long repairs that are away from the ends of the excavation, the generic weld residual stress distributions presented above should be applicable.

The high local stresses that may exist in the vicinity of repairs of small circumferential extent or near the ends of long repairs have little effect on the structural integrity of the shroud. Even if cracks grow rapidly in these regions of high stress, they should affect only a small percentage of the total shroud circumference. In addition, the residual stresses from high constraint local repairs will relax rapidly as cracks progress through or adjacent to the repair weld deposit. Since it is expected that essentially all in-process repairs were significantly less than or equal to half thickness, the local residual stresses from repairs should be relieved rapidly as cracks progress through the wall. In addition, where very deep repairs exist, cracks can grow rapidly to depths not predicted by the generic weld residual stress distribution. However, these short cracks have no significant effect on the structural reliability of the core shroud.

Through-wall membrane stresses are however, developed as a result of operating stresses acting on the shroud as discussed in Section 4.1. The maximum operating membrane stress distribution should be doubled to 3.2 ksi to conservatively account for the effects of fit-up and local repairs on the core shroud residual stresses.

Furthermore, due to the uncertainty associated with the local weld stresses, in addition to the weld residual stress profile and the conservative 3.2 ksi membrane stress described above, a stress profile shown in Figure 4-12 should be used to account for local surface effects resulting from weld repairs and other local phenomena should be added to determine the K distribution. This stress distribution is a curve fit of a distribution that has 10 ksi tensile stress on the outer 10% of the ID and OD of the shroud which is balanced by a compressive stress in the middle 80% of the shroud wall.

4.8 Stress Relaxation Effects

The residual stress distributions in the shroud welds do not take into account possible stress relaxation during service. There are two primary sources of residual stress relaxation. The first is attributable to neutron irradiation. This effect has been studied in Reference [13] for several stainless steels and nickel alloy materials. The results of this study, for stainless steel, are shown in Figure 4-15. It can be seen from this figure, for neutron fluence less than 10^{14} n/cm² (E >1.0 MeV), that the effect of fluence is negligible. Fluences above 10^{14} n/cm² (E >1.0 MeV) may have significant effect on relaxation of weld residual stress. It is expected that the midspan of the shroud exposed to the highest fast neutron flux will experience a fluence level up to 5.0×10^{20} n/cm² (E >1.0 MeV) over ten effective full power years (EFPY). This translates into a stress relaxation of 30%. The regions of the shroud outside the midspan region will experience levels of 1 to 20×10^{18} n/cm² (E >1.0 MeV) over 10 EFPY. This fluence level leads to stress relaxation of 10 to 15%. A conservative assumption was made to take no credit for stress relaxation due to irradiation in this study.

**Content Deleted –
EPRI Proprietary Information**

**Figure 4-15
Stress Relaxation Due to Neutron Irradiation [13]**

The second source of weld residual stress relaxation is due to temperature effects. At the BWR operating temperature of 550°F, there is a small relaxation of weld residual stresses as shown in studies performed in References [14] and [15]. This effect, however, is relatively small compared to irradiation-induced relaxation.

5

FRACTURE MECHANICS CONSIDERATIONS

A key parameter in the crack growth correlation developed in Section 3 for the core shroud horizontal welds is the stress intensity factor (K_I). In this section, the stress intensity factors for the operating stresses and the residual stresses discussed in Section 4 are developed to assist in the crack growth evaluation. Allowable flaw size determination for the shroud is also discussed. The crack growth evaluation and the allowable flaw size are used to determine the safe operating period of a flawed shroud.

5.1 Stress Intensity Factors Due to Applied Stresses

In general, the applied stresses consisting of dead weight, seismic and thermal loads are relatively small for the shroud as discussed in Section 4.1. As such, it will be conservatively assumed that these stresses are applied in pure tension. Several solutions for K_I have been provided in the literature for part-wall, part circumference flaws in cylinders. One solution that is particularly suited for a flawed shroud is that developed by Zahoor in the EPRI Ductile Fracture Handbook [16]. This expression is given by:

$$K_I = (\pi a)^{0.5} \sigma_t F_t \quad \text{Equation 5-1}$$

where:

$$\begin{aligned} \sigma_t &= \text{applied stress} \\ F_t &= 1.1 + x \cdot [0.15241 + 16.772 (x \cdot \theta/\pi)^{0.855} - 14.944 (x \cdot \theta/\pi)] \quad \text{Equation 5-2} \\ x &= a/t \\ \theta &= c/R_i \end{aligned}$$

R , R_i , and t are the pipe mean radius, inner radius, and wall thickness, respectively, θ is the flaw half-angle, and F_t is a geometric factor. The parameters a and $2c$ are the flaw depth and flaw length measured at the pipe inside surface, respectively. The through-wall variation of the parameter F_t for various flaw lengths around the circumference is shown in Figure 5-1. Another model that accounts for R_i/t ratios is discussed in Section 5.2. The model provided in Section 5.2 was used to determine K_I for the applied stresses. The model represented by Equations 5-1 and 5-2 was used to account for finite flaw length as explained in Section 5.2.

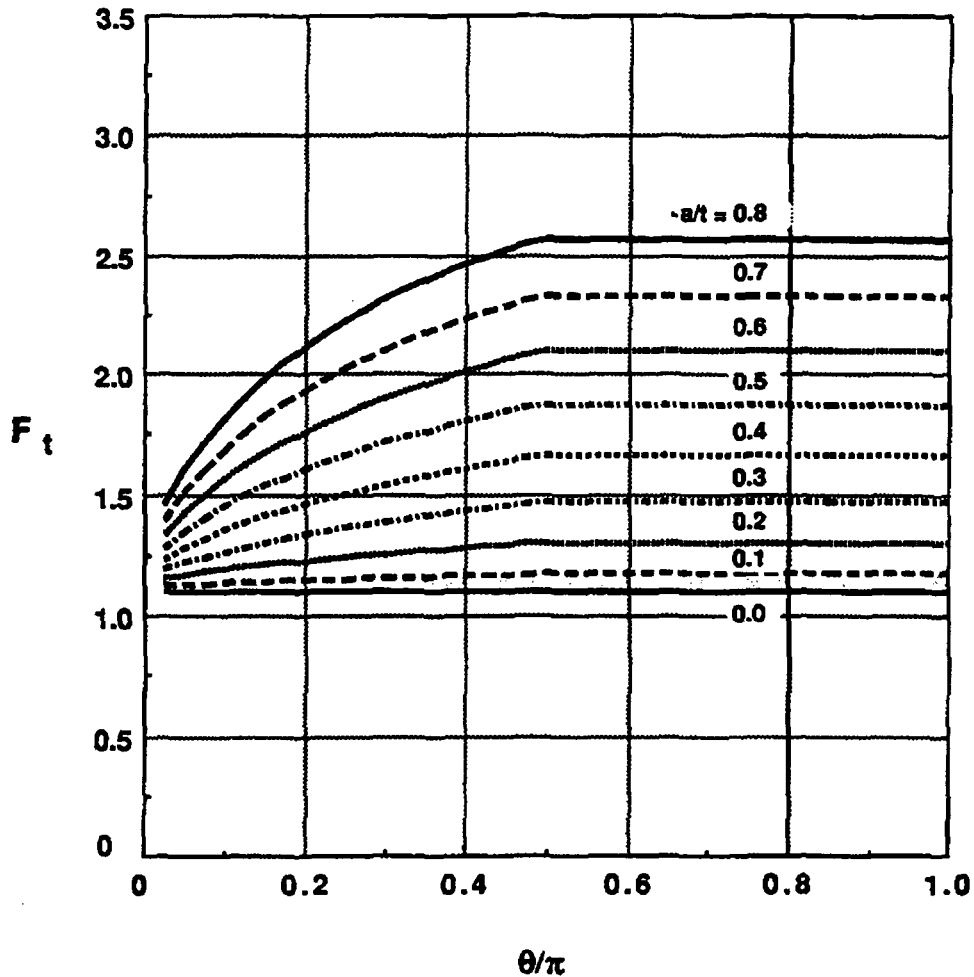


Figure 5-1
 Parameter F_t to Describe Stress Intensity Factor K_I for the Part-Through-Wall, Part Circumference Flaws [15]

5.2 Stress Intensity Factors Due to Weld Residual Stresses

Due to the non-uniform through-wall distribution of the weld residual stresses as shown in Section 4, a closed form solution for K_I is not available for this case. Hence, as presented in Reference [23], the methodology of Cheng and Finnie [17], is used to determine the K_I solution for the generic weld residual stress distribution discussed in Section 4. This methodology for calculating K is especially suitable because it applies to any arbitrary stress and R/t ratio. The expression for K_I is given as:

$$K_I = \sqrt{\pi a} \left\{ f^p(a/t) - \frac{F_\theta(a/t)}{s(a/t) + (\sqrt{R/t}/(3\pi\beta))} f^m(a/t) \right\} \quad \text{Equation 5-3}$$

where: a , t , and R are crack depth, thickness and mean radius, respectively, $\beta = [3(1-\mu^2)]^{1/4}$, $f^p(a/t)$ and $F_\theta(a/t)$ are functions obtained for an edge-cracked strip [18]. They may be expressed as:

$$f^p\left(\frac{a}{t}\right) = \left(\frac{2}{\pi}\right) f_0\left(\frac{a}{t}\right) \int_0^{a/t} [(1-z)(2+G-3Gz) \cos^{-1}\left(\frac{Fz}{1-z}\right) + \frac{F(1-Gz)}{\sqrt{1-\left(\frac{Fz}{1-z}\right)^2}}] \sigma(z) dz \quad \text{Equation 5-4}$$

where $z = x/t$

$$F = \frac{1-\frac{a}{t}}{\frac{a}{t}}; \quad G = \frac{\alpha(1-7\frac{a}{t})(1-\frac{a}{t})^5}{\frac{a}{t}} \quad \text{with } \alpha = \frac{3}{28} \quad \text{Equation 5-5}$$

and

$$F_\theta\left(\frac{a}{t}\right) = \int_0^{a/t} \left(\frac{a}{t}\right) f^p\left(\frac{a}{t}\right) f^m\left(\frac{a}{t}\right) d\left(\frac{a}{t}\right) \quad \text{Equation 5-6}$$

The other two functions $f^m(a/t)$ and $s(a/t)$ in Equation 5-3 can be obtained respectively by substituting a bending stress distribution in Equation 5-4 and by substituting $f^p(a/t)$ with $f^m(a/t)$ in Equation 5-6.

The K_1 distribution obtained with this model for the generic core shroud weld residual stress distribution is shown in Figure 5-2 for various R/t ratios. As can be seen from this figure, K_1 increases to a maximum positive value and then decreases to a point where K_1 crosses over from positive to negative. The crossover from positive to negative K shifts to the right as R/t increases. The above formulation has been compared with another formulation by Buchalet and Bamford [19] and compares very well for R/t ratio of 10 and for the edge-cracked plate ($R/t = \infty$). It should be noted that the K_1 formulation assumes a 360° circumferential flaw and, as such, the K_1 solution may be very conservative for cases where the actual flaw length in the shroud is relatively short.

For BWR core shrouds, the R/t ratio varies between 45 and 80. Most of the core shrouds have R/t ratios closer to 60. The K_1 distribution for R/t of 60 is therefore used on a generic basis. The generic K_1 distribution for both ID and OD initiated flaws is shown in Figure 5-3. As can be seen from this figure, K_1 increases on the inside and outside surfaces to a peak value at less than 15% through the wall. Thereafter, K_1 decreases and becomes compressive after about 60% of wall indicating crack arrest. This observation is significant because it shows that shallow cracks in the shroud may grow but the crack growth significantly decreases around mid-wall and could even arrest. This observation is supported by actual field data presented in Appendix I of this report that shows that shallow flaws grow relatively faster than deep flaws. Digitized values of the normalized K_1 distribution (K_1/\sqrt{t}) versus a/t are shown in Table 5-1 for the various stress distributions.

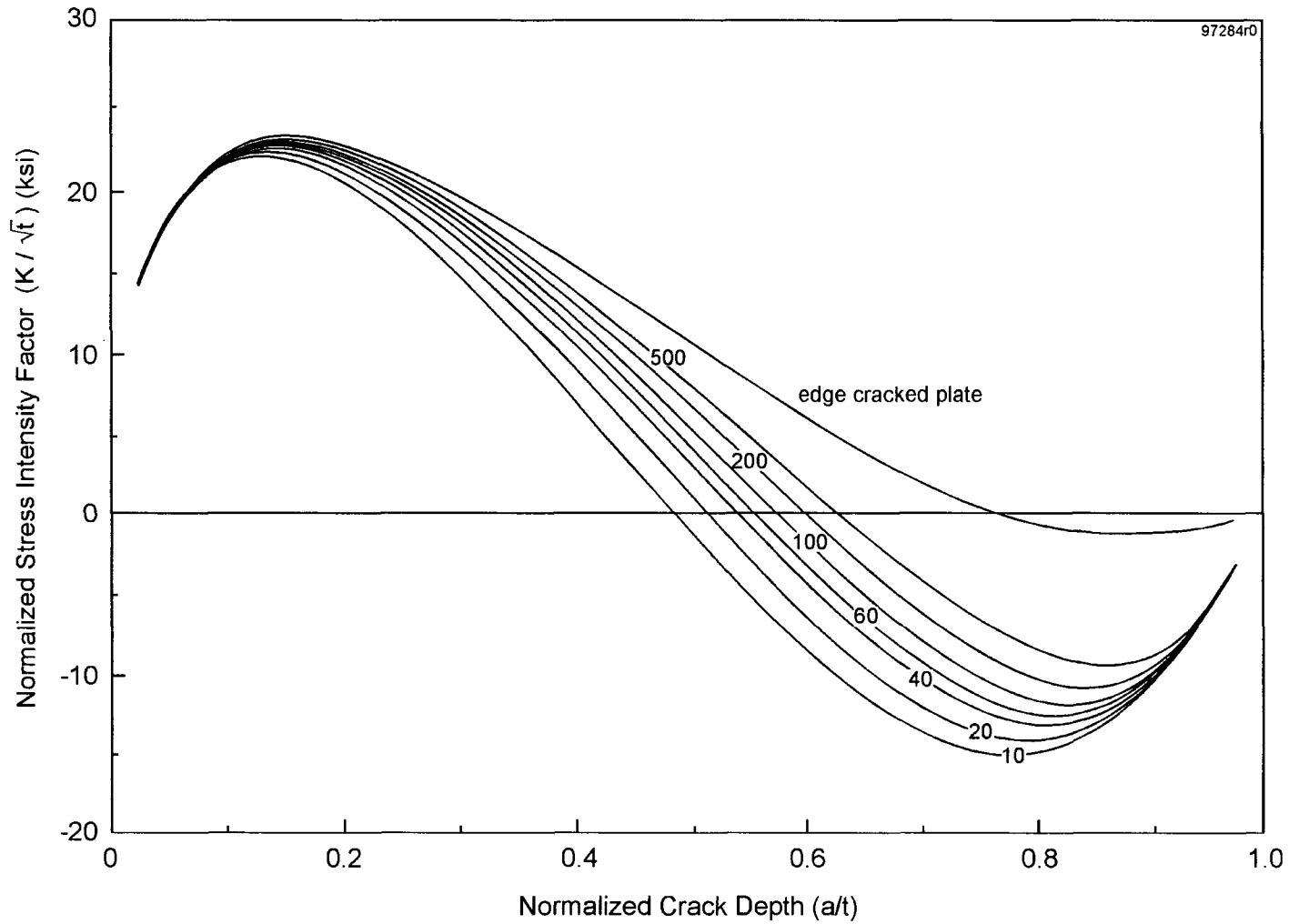


Figure 5-2
Normalized Stress Intensity Factor Magnification Factors for Circumferential Crack in Cylinder ($t/R = 0.1$) [16] K_1 for BWR Shroud Axial Weld Residual Stress Distribution (R/t Varying Between 10 and 500) [23]

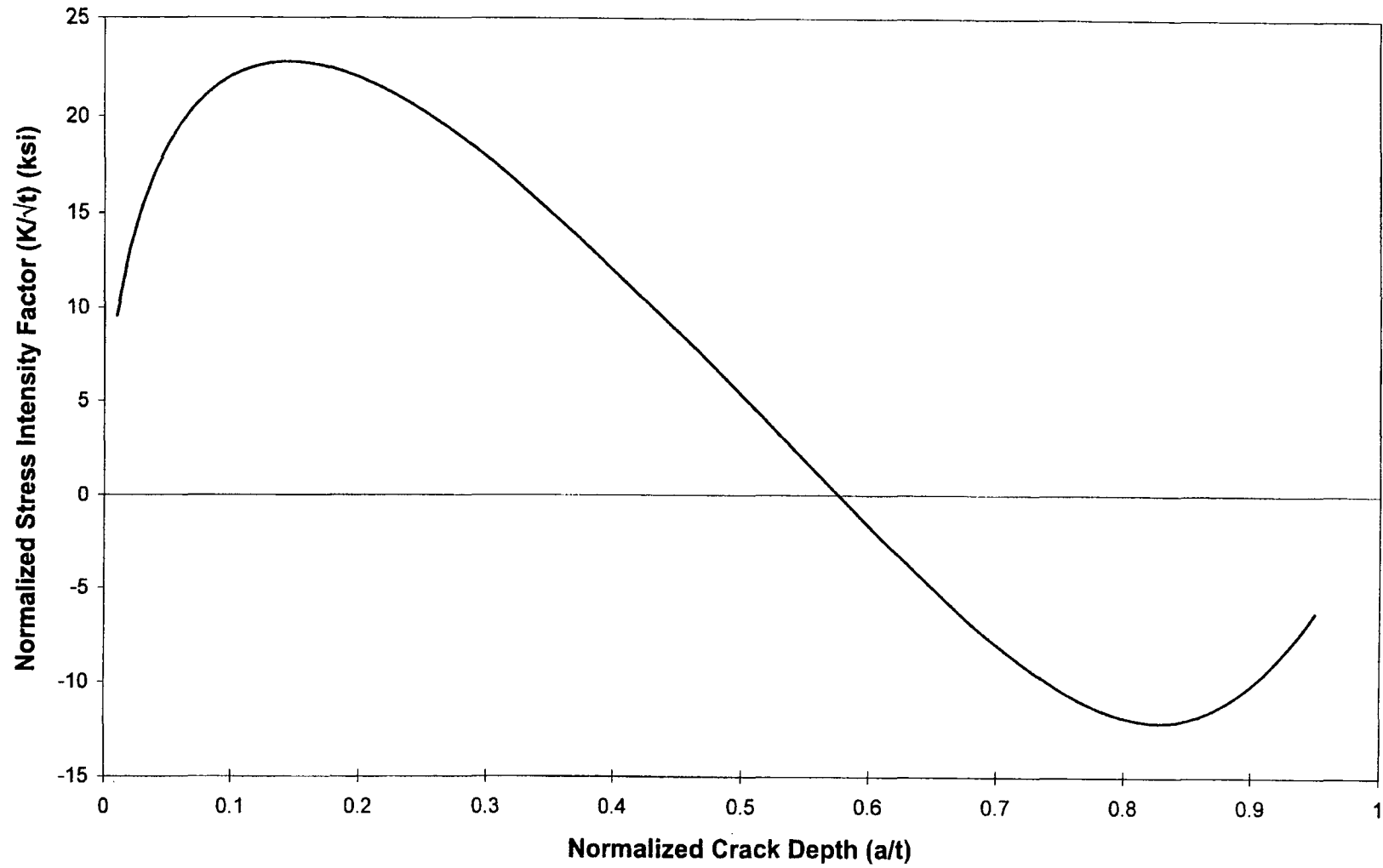


Figure 5-3
Generic K_I Distribution for BWR Shroud Axial Residual Stress (Based on $R/t = 60$)

Table 5-1
Normalized Through-Wall Stress Intensity Factor Distribution for BWR Shroud Welds

**Content Deleted –
EPRI Proprietary Information**

The K_I distribution shown in Figure 5-2 and Table 5-1 is applicable to both the shell-to shell and shell-to-ring welds. Justification for applying the same K_I distribution to both configurations is provided in Appendix O.

As discussed above, the fracture mechanics model used to obtain the K_I distribution for the weld residual stresses assumes a 360° flaw. There may be situations where this assumption may be overly conservative and some relief may be required to account for short flaws. A conservative way to account for finite flaw length is to assume that the K_I distribution for a particular flaw length will be reduced, based on the reduction of the F_I factor, shown in Figure 5-1 for that flaw length relative to the 360° flaw. As an example, if we consider a flaw with $a/t = 0.8$ in Figure 1, and $\theta/\pi = 0.2$, the reduction of the K_I value as determined with the above methodology will be $(2.1/2.6) = 0.81$. This implies a 19% reduction in K values considering the 360° flaw shown in Figure 5-4. Figure 5-4 provides the distribution of these flaw reduction factors as a function of a/t and θ/π .

**Content Deleted –
EPRI Proprietary Information**

**Figure 5-4
Flaw Reduction Factors for Determination of K_I for Weld Residual Stresses in BWR Shrouds with Part-Circumference Flaws**

5.3 Effect of Localized Stresses on Stress Intensity Factor Distribution

As discussed in Section 4-7, localized stresses are conservatively accounted for by superimposing a membrane stress of 3.2 ksi and a surface residual stress to the generic weld residual stress distribution. The combined stress distribution is presented in Figure 4-13. Using the methodology outlined in Section 5.2, the K distribution for this combined stress distribution is determined and presented in Figure 5-5. The K distribution is presented for three R/t ratios which bound the BWR fleet. As can be seen from this figure, no crack arrest is predicted. As noted earlier in Section 5.2, the K distribution for R/t = 60 can be used on a generic basis.

Thin-walled cylinders due to combined stresses with double max. membrane stress

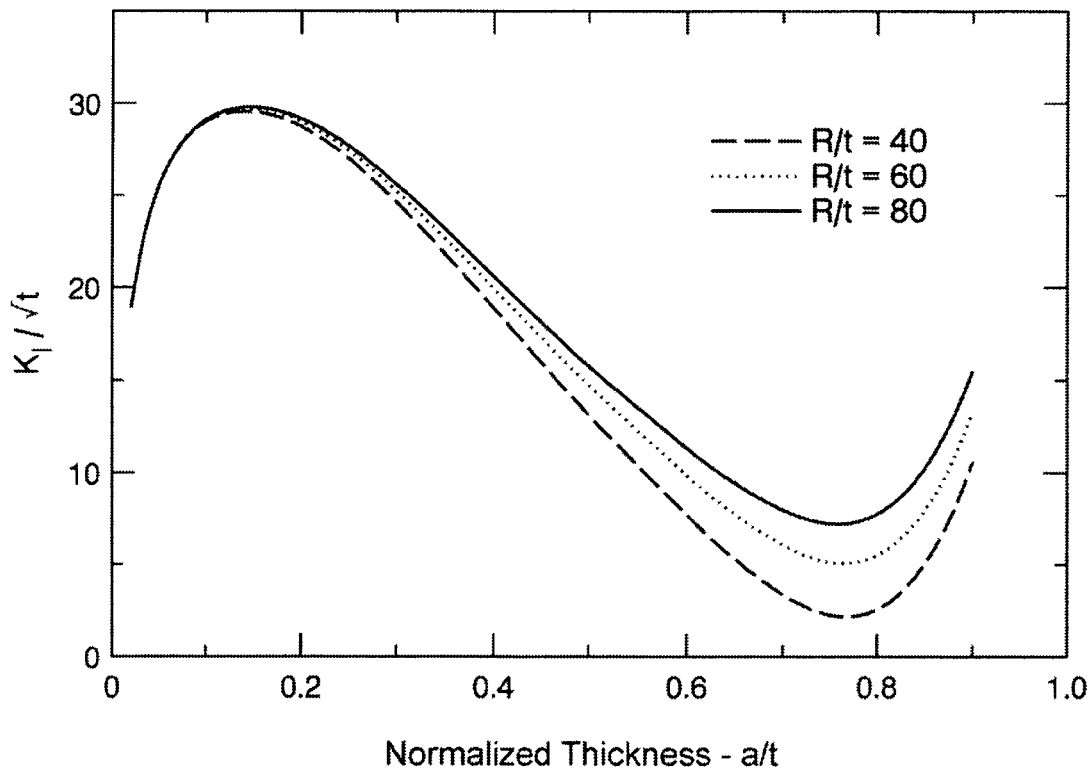


Figure 5-5
K Distribution for a Combination of Weld Residual Stress, Surface Residual Stress and 3.2 ksi Membrane Stress [26]

5.4 Allowable Flaw Size for BWR Shroud

As discussed earlier in this report, all existing BWR shrouds were fabricated from austenitic stainless steels. Several studies that have been performed to support the BWR pipe cracking problem have shown that stainless steels possess adequate toughness such that they fail in a ductile manner. As such, the net section plastic collapse principle, whereby the remaining ligament of the flawed pipe becomes fully plastic subsequent to failure, has been used as a failure mechanism in determining the allowable flaw sizes in ASME Code Section XI for austenitic stainless steels. It is expected that this should also be the case for the shroud welds which are remote from the highly irradiated regions.

Specific analyses that have been performed to support the evaluation of several flawed BWR shrouds using this methodology have shown that for the shroud welds which are not highly irradiated, the allowable flaw size even assuming a 360° circumferential flaw is at least 90% of the thickness of the shroud [20]. This very favorable allowable flaw size is not surprising since the applied loads on the shroud are relatively small, as shown in Section 4.1.

For the shroud welds in the high fluence region of the shroud (Weld H4), linear elastic fracture mechanics principles have typically been used to determine the allowable flaw size, since the toughness has been diminished slightly in this region due to irradiation. This approach is believed to be very conservative, for fluences at or below 1×10^{21} n/cm² (E >1.0 MeV). Evaluations that have been performed on several BWR shrouds using this approach have shown that the allowable flaw size is at least 70% of the thickness of the shroud.

6

EVALUATION METHODOLOGY FOR CORE SHROUD CRACK GROWTH

The information developed in the prior three sections of this report is utilized in this section to illustrate the manner in which the crack growth data and correlation can be employed in a crack growth analysis of a typical BWR core shroud. Section 6.1 describes three alternative evaluation procedures for core shroud crack growth analysis. Section 6.2 provides an example illustrating the plant-specific evaluation procedure for a core shroud weld.

6.1 Evaluation Procedure

Three alternate approaches can be used for the evaluation of crack growth in flawed stainless steel BWR shrouds. As stated in Reference 27, these three approaches are applicable to fluences of $\leq 5 \times 10^{20}$ n/cm² ($E > 1.0$ MeV) since the CGR database is presently based only on unirradiated materials. Any of these approaches can be used in the evaluation. It is recognized that there are other models and other approaches available that can also be used to resolve the BWR shroud cracking issue especially with regards to sensitization and radiation effects.

If any of the three approaches described below provide the desired continued operating interval for the bounding flawed core shroud weld, the analysis is complete. If the result is unacceptable, the utility must take some action consistent with the BWRVIP guidelines, but which are outside the scope of this document. As stated previously, for the purposes of crack growth evaluation approaches discussed in Sections 6.1.1 and 6.1.2, NWC and HWC/NMCA environments are defined as follows:

NWC: ECP of stainless steel > -230 to $+200$ mV(SHE), average coolant conductivity < 0.15 μ S/cm

HWC/NMCA: ECP of stainless steel ≤ -230 mV(SHE), average coolant conductivity < 0.15 μ S/cm with at least 80% HWC availability.

Note that the conductivity of 0.15 μ S/cm used to derive the crack growth rates for the K-independent (Section 6.1.1) and K-dependent (Section 6.1.2) approaches was chosen to bound the mean fleetwide conductivity of 0.1 μ S/cm as described in the BWR Water Chemistry Guidelines 2004 Revision (BWRVIP-130) [38].

The three approaches for determining crack growth rate are presented in the following sections.

6.1.1 Stress Intensity Factor (K) Independent Approach

In this approach, a K independent crack growth rate is provided separately for NWC and HWC/NMCA:

For NWC: $da/dt = 2.2 \times 10^{-5}$ in/hr **Equation 6-1**

For HWC/NMCA: $da/dt = 1.1 \times 10^{-5}$ in/hr **Equation 6-2**

Note: If the conductivity is greater than 0.15 $\mu\text{S/cm}$ but less than or equal to 0.3 $\mu\text{S/cm}$, then a crack growth rate of 5.0×10^{-5} in/hr can be used. Alternatively, the crack growth rate determined from Equation 6-5 (or Equation 6-6) can be used.

While the K-independent approach is simple to use, it is conservative in that it takes no credit for the reduction in crack growth rate due to decreasing K.

The NWC crack growth rate is based on the 95th percentile correlation crack growth rate with a stress intensity factor of 25 $\text{ksi}\sqrt{\text{in}}$ and the environmental conditions stated in Figure 3-9 (ECP = 200 mV[SHE] and average conductivity = 0.15 $\mu\text{S/cm}$). It should be noted that the use of the constant stress intensity factor of 25 $\text{ksi}\sqrt{\text{in}}$ is conservative for a typical shroud thickness of 1.5 inches considering the average stress intensity factor from the distribution presented in Figure 5-5.

The HWC/NMCA crack growth rate is a factor of 2 lower than that for NWC.

6.1.2 Stress Intensity Factor (K) Dependent Approach

The second approach uses the 95th percentile empirical model as presented in Equation 3-4 with K dependence but with fixed values of ECP, conductivity and temperature. The crack growth rates for NWC and HWC/NMCA conditions are as follows:

NWC:

1. For flaw depths less than or equal to 80% through wall:

$da/dt = 1.966 \times 10^{-8} K^{2.181}$ **Equation 6-3**

where K is the stress intensity factor in units of $\text{ksi}\sqrt{\text{in}}$ and da/dt is crack growth rate in in/hr.

2. For flaw depths greater than 80% through wall, use the K-independent value (Equation 6-1)

Note: If the conductivity is greater than 0.15 $\mu\text{S/cm}$ but less than or equal to 0.3 $\mu\text{S/cm}$, then a crack growth rate of 5.0×10^{-5} in/hr can be used. Alternatively, the crack growth rate determined from Equation 6-5 (or Equation 6-6) can be used.

HWC/NMCA:

1. For flaw depths less than or equal to 80% through wall:

$da/dt = 0.983 \times 10^{-8} K^{2.181}$ **Equation 6-4**

where K is the stress intensity factor in units of $\text{ksi}\sqrt{\text{in}}$ and da/dt is crack growth rate in in/hr .

2. For flaw depths greater than 80% through wall, use the K -independent value (Equation 6-2)

The NWC crack growth rate in this approach is based on Equation 3-4 with a fixed ECP of 200 mV[SHE], a fixed conductivity of 0.15 $\mu\text{S/cm}$ and a temperature of 288°C (561°K). The HWC/NMCA crack growth rate is a factor of 2 lower than that for NWC.

Use of the K -dependent model is limited to flaw depths up to 80% (a flaw growing in one direction) of the shroud wall for the following reasons (see Appendix K for details):

1. The loads on the core shroud are relatively small compared to Class 1 piping loads. It is expected that the allowable flaw depth in most cases is greater than 90% of wall thickness for a 360-degree flaw in BWR shrouds. A limit of 80% flaw depth for applicability of the K -dependent model assures that the allowable flaw depth will not be encroached upon during crack growth.
2. It is recognized that the ASME Code, Section XI, IWB-3600, allows a maximum flaw depth of 75% for defects in austenitic primary pressure boundary piping. However, this limit is not based upon structural integrity concerns but rather to avoid leakage in the pressure boundary component. For the core shroud, the consequences of leakage are not nearly as significant as for primary pressure boundary piping, and therefore an average flaw depth up to 80% is justified.
3. The fracture mechanics model used for the determination of K is limited to 90% of wall. Hence, the choice of 80% ensures that the limit of the model is not reached during K -dependent crack growth. As can be seen from Figure 5-5, K remains relatively low between 80 and 90% of wall and even when extrapolated to 95% of wall, K is less than 25 $\text{ksi}\sqrt{\text{in}}$ even for a 2-inch thick shroud (which formed the basis for the constant rate of 2.2×10^{-5} in/hr).

6.1.3 Stress Intensity Factor (K) and Environment Dependent Approach

In this third approach, the 95th percentile crack growth model presented by Equation 3-4 is used with plant specific values of ECP and conductivity to calculate the crack growth rate. The crack growth rate is calculated as follows:

$$\ln da/dt = 2.181 \ln (K) - 0.787 \text{Cond}^{-0.586} + 0.00362\text{ECP} + 6730/T_{\text{ABS}} - 33.235 \quad \text{Equation 6-5}$$

where da/dt is the CGR in mm/sec

K = stress intensity factor in units of $\text{MPa}\sqrt{\text{m}}$

Cond = conductivity in units of $\mu\text{S/cm}$

ECP = ECP in units of mv[SHE]

T_{ABS} = Temperature in units of degrees Kelvin

Alternatively, the crack growth rate in British units can be stated as:

$$\ln da/dt = \frac{2.181 \ln(K) - 0.787 \text{Cond}^{0.586} + 0.00362\text{ECP} + 6730/}{(0.5556T_f + 255.2) - 28.073} \quad \text{Equation 6-6}$$

where da/dt is the CGR in in/hr

K = stress intensity factor in units of ksi√in

Cond = conductivity in units of μS/cm

ECP = ECP in units of mv[SHE]

T_f = Temperature in units of degrees F

Plant specific values of ECP and conductivity used in Equation 6-5 or 6-6 must be justified. The maximum conductivity level for use in Equation 6-5 (or Equation 6-6) is 0.3 μS/cm which corresponds to the limit defined in Action Level 1 in the 2004 Water Chemistry Guidelines (BWRVIP-130) [38].

The above K-dependent crack growth laws are applicable for flaw depths less than or equal to 80% of through wall (flaw growing in one direction). For flaw depths greater than 80% through wall, the K-independent values (Equations 6-1 and 6-2) should be used subject to the definitions of NWC and HWC/NMCA in section 6.1.

The NRC is reviewing the report “Technical Basis for Inspection Relief for BWR Components with Hydrogen Injection (BWRVIP-62)” [34]. The use of environmental parameters in this approach will be revisited after the NRC had completed its review of BWRVIP-62. In the interim, it is appropriate to use the initial NRC Safety Evaluation for BWRVIP-62 issued on January 30, 2001.

6.2 Example of Application of K and Environment Dependent Approach

An analysis of a flawed core shroud weld using the stress intensity factor (K) and environment dependent approach (see Section 6.1.3) is presented as follows. The analysis was performed under both normal water chemistry (NWC) and hydrogen water chemistry (HWC/NMCA) conditions. The analysis was also performed under varying membrane stress to determine the sensitivity of the crack growth to the membrane stress. This example was also presented in Reference [26].

Shroud Thickness:	1.25 inches
Flaw Characteristics:	10% through-wall by 360° around circumference on inside surface
Weld Type:	H5
Applied Membrane Stress:	0 to 10 ksi
Residual Stress:	Use Shell-to-Shell Distribution (Figure 4-7)
Surface Stress:	Use Distribution Shown in Figure 4-12
ECP:	200 mV(SHE) and -230 mV (SHE)
Average conductivity:	0.15 μS/cm

Temperature: 288°C

The first step in the analysis process is to determine the through-wall stress intensity factor (K) distribution for the applied stresses and the weld residual stresses. The applied stresses are assumed to be all tensile in calculating the K distribution. In this example, the applied stress used for crack growth varied between 0 and 10 ksi to determine the sensitivity even though the maximum applied stress as discussed in Section 4-6 is bounded by 3.2 ksi. For calculation of K, the formulation presented in Section 5.2 (Table 5-1) was used. The K for the applied stress was factored appropriately from Table 5-1 for the various values and was combined with the K for the weld residual stress and the surface residual stress. The initial flaw size was assumed to be 10% of wall and 360° around the circumference.

The 95th percentile crack growth correlation, represented by Equation 6-5, is then employed to determine the crack growth with time to 90% of the wall. The results of the evaluation are shown in Figure 6-1. As can be seen in this figure, with the membrane stress of 3.2 ksi in addition to the weld residual stress and the local surface stress distributions, crack arrest is not predicted. Based upon this stress distribution, it is predicted that it takes about 30 years for an initial 10% throughwall flaw to reach 90% of wall which is consistent with field observations. The results are even more favorable for the case with hydrogen water chemistry.

Note that the use of the K and Environmental dependent approach is limited to 80% of wall. In this example, it was extended to 90% of wall. In actual plant application, the K-independent value should be used after 80% of wall with this approach.

**Content Deleted –
EPRI Proprietary Information**

Figure 6-1
Crack Growth Results for Normal and Hydrogen Water Chemistry Based on Combined K Distribution Shown in Figure 5-5 and Table 5-1

6.3 Comparison of Analytical Crack Growth Prediction With Field Data

The crack growth predictions based on the generic K distribution shown in Figure 5-5 are consistent with field crack growth data. This was previously shown in Section 3.5 (Figure 3-9). The field data was compared with the K independent and the K dependent approaches in Figure 3-9 and both approaches were found to be reasonably conservative.

The K and environment dependent approach has also been used in this section to predict crack extensions. This is illustrated in Figure 6-2 that compares the calculated K and environment (ECP & conductivity) dependent crack growth predictions with measured crack growth in several plants. The plant data used for the determination of K and the crack growth is shown in Table 6-1. Table 6-2 also provides tabular form of the crack growth results. The scatter of the calculated crack growth predictions in Figure 6-2 takes into account the effect of UT inspection uncertainty of ± 0.1 inch on the calculated K and crack extensions. In most cases, the predictions are conservative or are within the inspection uncertainty band. It is expected that the field cracking data shown in Figure 6-2 include locations of weld repair that are associated with regions of higher residual stresses. The good comparison between the field data and the analytical predictions in Figure 6-2 indicates that the analytical approach used in this report reasonably accounts for the effects of localized stresses including weld repairs.

**Content Deleted –
EPRI Proprietary Information**

Figure 6-2
Comparison of Through-Thickness Crack Growth Calculated With BWRVIP-14 K and Environment Dependent Model with Measured Crack Growth for Several Plants

Table 6-1
BWR Plants Core Shroud Crack Growth Data

**Content Deleted –
EPRI Proprietary Information**

Table 6-2
BWR Plant-Specific Core Shroud Crack Growth Results

**Content Deleted –
EPRI Proprietary Information**

7

SUMMARY AND CONCLUSIONS

The following provides a summary and conclusions of the work performed in this report.

- An empirical through-wall crack growth correlation has been developed in this report for use in the evaluation of BWR stainless steel internals, based on extensive crack growth data collected from several sources.
- The crack growth correlation accounts for the environmental conditions. Components exposed to relatively low oxidizing potential and low conductivities are predicted to have a reduced crack growth, whereas those exposed to higher oxidizing potentials and higher average conductivity are expected to have higher crack growth rates.
- The 95th percentile curve developed as part of the empirical correlation reasonably accounts for the field data that have been collected to date demonstrating that the correlation can be conservatively used for crack growth assessment of the shroud and other stainless steel internals.
- A comprehensive scope of work was performed to determine the residual stress distribution for the various shroud welds. These included the H3, H4, H5, H6a, and H6b welds. Both surface and through-wall residual stress distributions were determined both experimentally and analytically. There was good trend between the measured and analytical results. There was consistency in the trend between analytical and measured values. A single weld residual stress curve was selected to account for the general shape of the surface and through-wall distributions in shell-to-shell and ring-to-shell welds.
- Based on the measured and analytically determined residual stresses, recommendations were provided for the through-wall residual stress distributions to be used in the crack growth assessment of the shroud welds. A single recommendation was made for the shell-to-shell welds and the shell-to-ring welds. The recommendation is very similar to the one currently proposed by the USNRC for large diameter piping in NUREG-0313, Revision 2. The middle half of the curve is compressive while the outer ends are tensile.
- In addition to the weld residual stress, a conservative membrane stress of 3.2 ksi and a surface stress distribution are included in the final shroud weld through-wall stress distribution to account for localized stresses due to fit-up stresses, weld joint geometries, welding parameters such as heat input, welding sequence, welding starts and stops and repairs.
- The through-wall distribution of all stresses was used in a fracture mechanics model to develop the K distribution for both outside diameter and inside diameter initiated flaws. Because of the shape of the through-wall residual stress distribution, higher K values are obtained near the wall surface indicating high crack growth rates. K diminishes as the crack propagates into the wall leading to significantly lower crack growth rates.

- Analysis of inspection data from several plants supports the conclusion that as cracks grow deeper they slow down or arrest.
- A representative example problem was used to illustrate how all the developments in this report can be used to perform a flaw evaluation of the shroud. The ECP and average conductivity assumed in this example were conservative for BWR shroud evaluations. Both NWC and HWC/NMCA conditions were considered. The results of this analysis confirmed that a flawed shroud can operate for a significant amount of time before the ASME Section XI safety margins are compromised.
- For BWR plants operating under moderate HWC conditions, lower ECPs may be justified and are expected to yield lower crack growth rate estimates.
- Based on the work contained in this report, three alternate methods have been developed for through-wall crack growth evaluation of horizontal HAZs in BWR stainless steel shrouds. These approaches are discussed in Section 6. In the first approach, the K-independent crack growth rate is used separately for NWC and HWC conditions. For NWC conditions, a crack growth rate of 2.2×10^{-5} in/hr is utilized. This crack growth rate represents the highest crack growth rate with a stress intensity factor of 25 ksi $\sqrt{\text{in}}$ and the 95th percentile curve of the model with an average conductivity of 0.15 $\mu\text{S/cm}$ and ECP of 200 mV(SHE). The K-independent crack growth rate for HWC conditions is 1.1×10^{-5} in/hr. The second approach involves the use of the 95th percentile curve of the model with K-dependence up to 80% of wall after which the K-independent crack growth rate is used. For NWC conditions, ECP = 200 mV(SHE) is used in the model. The K-dependent crack growth for HWC conditions is half that of NWC. The third approach involves the use of the 95th percentile crack growth curve with K and ECP dependence. Any of these approaches are acceptable for evaluation of crack growth of BWR stainless steel shrouds.

8

REFERENCES

1. Eason, E. D. and Nelson, E. E., *Correlations Between Grain Boundary Compositions and IASCC Susceptibility in Austenitic Stainless Steel*. April 1994. EPRI Report TR-103508.
2. Eason, E. D., Wright J. E., and Nelson, E. E., "Multi-variable Modeling of Pressure Vessel and Piping J-R Data," NUREG/CR-5729, May 1991.
3. Hazelton, W. S. and Koo, W. H., "Technical Report on Material Selection and Processing Guidelines for BWR Coolant Pressure Boundary Piping," NUREG-0313, Revision 2, Nuclear Regulatory Commission, January 1988.
4. Ford, F. P., et al., *Corrosion-Assisted Cracking of Stainless and Low-Alloy Steels in LWR Environments*. February 1987. EPRI Report NP-5064.
5. Gordon, B. M. and Horn, R. M., Personal Communication, September 1995.
6. Harris, D. O., Dedhia, D. D., Eason, E. D. and Patterson, S. D., "Probability of Failure in BWR Reactor Coolant Piping," NUREG/CR-4792, Vol. 3, December 1986, pp. 8-9.
7. USNRC Document NUREG-1061, Volume 1, "Report of the U.S. Nuclear Regulatory Commission Piping Review Committee - Investigation and Evaluation of Stress Corrosion Cracking in Piping of Boiling Water Reactor Plants," August 1984.
8. *Measurement of Residual Stresses in Type 304 Stainless Steel Piping Butt Weldments*. June 1980. EPRI Document NP-1413.
9. *Computational Residual Stress Analysis of Induction Heating of Welded BWR Pipes*. December 1982. EPRI Document NP-2662-LD.
10. ASTM Standard E837-94, 'Determining Residual Stresses by the Hole-Drilling Strain Gage Method,' American Society for Testing and Materials, Philadelphia, 1994.
11. ANSYS Finite Element Program, Version 5.1, Swanson Analysis System, Inc., 1994.
12. *BWR Recirculation Piping System Replacement*. EPRI Report NP-6723-D. Volume 3 – Supporting Documentation for Final Report, June 1990.
13. BWRVIP letter from Larry Nelson to Raj Pathania, "Stress Relaxation Due to Irradiation," November 10, 1995.
14. Sim, R. G. and Giannuzzi, A. J., "A Study of Stress Relaxation in AISI 304 Stainless Steel," General Electric Document NEDE 13334, April 1973.
15. Giannuzzi, A. J., *Studies on AISI Type 304 Stainless Steel Piping Weldments for Use in BWR Applications*. December 1978. EPRI Report No. NP-944.
16. Zahoor, A., *Ductile Fracture Handbook, Volume II*. June 1989. EPRI Report No. NP-6301-D.

References

17. Cheng, W. and Finnie, I., "On the Prediction of Stress Intensity Factors for Axisymmetric Cracks in Thin-Walled Cylinders From Plane Strain Solutions," *Journal of Engineering Materials and Technology*, Vol. 106, 227-231, 1985.
18. Cheng, W., Finnie, I., and Vardar, O., "Deformation of an Edge-Cracked Strip Subjected to Normal Surface Traction on the Crack Faces," *Engineering Fracture Mechanics*, Vol. 42, 97-108, 1992.
19. Buchalet, C.B., and Bamford, W. H., "Stress Intensity Factor Solutions for Continuous Surface Flaws in Reactor Pressure Vessels," *Mechanics of Crack Growth*, ASTM STP S90, American Society for Testing and Materials, 1976, pp. 385-402.
20. USNRC, "Safety Evaluation by the Office of Nuclear Reactor Regulation Related to Core Shroud Cracking; Commonwealth Edison Company and Iowa-Illinois Gas and Electric Company; Dresden Nuclear Power Station, Unit 3; Quad Cities Nuclear Power Station Unit 1, Docket Nos. 50-249 and 50-254," July 21, 1994.
21. *BWR Vessels and Internals Project, Evaluation of Crack Growth in BWR Stainless Steel RPV Internals (BWRVIP-14)*. March 1996. EPRI Report TR-105873.
22. Letter from C. E. Carpenter (USNRC) to J. T. Beckham Jr. (BWRVIP), "Proprietary Request for Additional Information – Review of BWR Vessel and Internals Project Proprietary Report, *BWR Vessel and Internals Project, Evaluation of Crack Growth in BWR Stainless RPV Internals (BWRVIP-14)*," December 9, 1996.
23. Letter from V. Wagoner (BWRVIP) to C. E. Carpenter (USNRC), BWRVIP Document 97-651 "BWRVIP Response to NRC Request for Additional Information on BWRVIP-14," July 28, 1997.
24. Letter from G. C. Lucas (USNRC) to C. Terry (BWRVIP), "Safety Evaluation of the BWR Vessel and Internals Project BWRVIP-14 Report (TAC No. M94975)" and enclosure, June 8, 1998.
25. W. J. Shack (Argonne National Laboratory), *BWR Vessels and Internals Project, Evaluation of Crack Growth in BWR Stainless Steel RPV Internals*. January 27, 1998. *Technical Evaluation Report on EPRI TR-105873*.
26. Letter from C. Terry (BWRVIP) to C. E. Carpenter (USNRC) BWRVIP Document 98-458, "BWRVIP Response to NRC Safety Evaluation of BWRVIP-14," November 24, 1998.
27. Letter from J. Strosnider (USNRC) to C. Terry (BWRVIP), "Final Safety Evaluation of the BWR Vessel and Internals Project BWRVIP-14 Report (TAC No. M94975)," December 3, 1999 (with enclosure TER on Project 704).
28. W. J. Shack, O. K. Chopra, S. Majumdar (Argonne National Laboratory), "Technical Evaluation Report on Project No. 704 - BWRVIP Response to NRC Safety Evaluation of BWRVIP-14," August 5, 1999.
29. BWRVIP Document 2000-049, "Summary of February 17, 2000 BWRVIP/NRC Meeting," February 29, 2000.
30. Letter from C. Terry (BWRVIP) to C. E. Carpenter (USNRC) BWRVIP Document 200-198, "Project No. 704 – BWRVIP Response to NRC Final Safety Evaluation of BWRVIP-14," July 11, 2000.

31. Letter from J. R. Strosnider (USNRC) to C. Terry (BWRVIP), "BWRVIP Response to NRC Final Safety Evaluation of BWRVIP-14 (TAC No. M94975)," May 13, 2001.
32. Letter from W. H. Bateman (USNRC) to C. Terry (BWRVIP), "Clarification to NRC Letter Regarding BWRVIP Responses to BWRVIP-14 Final Safety Evaluation (TAC No. M94975)," July 20, 2001.
33. *BWR Vessels and Internals Project – BWR Core Shroud Inspection and Flaw Evaluation Guidelines, Revision 2 (BWRVIP-01)*. October 1996. EPRI-TR-107079.
34. *BWR Vessels and Internals Project – Technical Basis for Inspection Relief of BWR Internal Components with Hydrogen Injection (BWRVIP-62)*. December 1998. EPRI-TR-108705.
35. W. J. Shack and S. W. Tam (Argonne National Laboratory), "Technical Evaluation Report on BWRVIP-14-A, BWR Vessels and Internals Project, Evaluation of Crack Growth in BWR Stainless Steel RPV Internal," Draft, July 30, 2004.
36. Letter from W. A. Eaton (BWRVIP Chairman) to M. Khana (NRC), "PROJECT NO. 704 – BWRVIP Response to Draft Technical Evaluation Report on BWRVIP-14-A (Evaluation of Crack Growth in BWR Stainless Steel RPV Internals)," September 12, 2005, (BWRVIP Correspondence File Number 2005-364).
37. Letter from M. A. Mitchell (NRC) to R. Libra (BWRVIP Chairman), "Staff Evaluation of BWRVIP Response to Nuclear Regulatory Commission Safety Evaluation of "BWR Vessel and Internals project, Evaluation of Crack Growth in BWR Stainless Steel RPV Internals," (TAC NO. MC2738)," August 22, 2007, (BWRVIP Correspondence File Number 2007-261).

A

CRACK GROWTH RATE DATA: ABB ATOM AND ARGONNE NATIONAL LABORATORIES

**Entire Appendix Deleted -
EPRI Proprietary Information**

B

CRACK GROWTH RATE DATA: GE NUCLEAR ENERGY

**Entire Appendix Deleted -
EPRI Proprietary Information**

C

CRACK GROWTH RATE CORRELATION

**Entire Appendix Deleted -
EPRI Proprietary Information**

D

RIVER BEND SHROUD MATERIAL PROPERTIES

**Entire Appendix Deleted -
EPRI Proprietary Information**

E

NEAR SURFACE RESIDUAL STRESS MEASUREMENTS AT RIVER BEND NUCLEAR STATION

**Entire Appendix Deleted -
EPRI Proprietary Information**

F

**THROUGH-THICKNESS RESIDUAL STRESS
MEASUREMENT ON RIVER BEND CORE SHROUD**

**Entire Appendix Deleted -
EPRI Proprietary Information**

G

NEAR SURFACE RESIDUAL STRESS MEASUREMENTS AT GRAND GULF NUCLEAR STATION

**Entire Appendix Deleted -
EPRI Proprietary Information**

H

ANALYTICAL PREDICTION OF RESIDUAL STRESSES IN BWR SHROUD WELDS

**Entire Appendix Deleted -
EPRI Proprietary Information**

/ **IN-PLANT CRACK EXTENSION DETERMINATION FROM SUCCESSIVE UT EXAMINATIONS**

**Entire Appendix Deleted -
EPRI Proprietary Information**

J

USNRC FINAL SAFETY EVALUATION OF BWRVIP-14



UNITED STATES
NUCLEAR REGULATORY COMMISSION
WASHINGTON, D.C. 20555-0001

99-496

December 3, 1999

Carl Terry, BWRVIP Chairman
Niagara Mohawk Power Company
Post Office Box 63
Lycoming, NY 13093

SUBJECT: FINAL SAFETY EVALUATION OF PROPRIETARY REPORT TR 105873 "BWR VESSEL AND INTERNALS PROJECT, EVALUATION OF CRACK GROWTH IN BWR STAINLESS STEEL INTERNALS (BWRVIP-14)" (TAC NO. M94975)

Dear Mr. Terry:

The NRC staff has completed its review of the proposed revisions to the Electric Power Research Institute (EPRI) proprietary report TR-105873, "BWR Vessel and Internals Project, Evaluation of Crack Growth in BWR Stainless Steel Internals (BWRVIP-14)," dated March 1996. This report was submitted by letter dated July 28, 1997, as supplemented by letter dated July 28, 1997, for NRC staff review and approval.

On June 8, 1998, the NRC staff issued its initial safety evaluation (SE) of the BWRVIP-14 report, which found the BWRVIP-14 evaluation of crack growth to be acceptable for use except where the staff's conclusions differed from the BWRVIP's. The BWRVIP was requested to resolve the open issues raised in the staff's initial SE. By letter dated November 24, 1998, you provided a response which proposed to resolve the issues.

The NRC staff, with assistance from the Argonne National Laboratory (ANL), has reviewed your responses to the staff's initial SE and finds, in the enclosed technical evaluation report (TER) prepared by ANL, with one exception, that your response to the open issues is acceptable. The exception is your conclusion that the use of the generic stress intensity factors, provided in Figure 4 of the response, avoids the need to document weld repairs when using a K based approach for estimating crack growth rates (CGR).

Specifically, the generic stress intensity factor distributions proposed in your response will generally be conservative for cylinder-to-cylinder horizontal welds and cylinder-to-edge-ring welds. However, because local weld repairs inherently introduce three dimensional effects, this is an artificial constraint and may lead to nonconservative estimates of the local stresses. In most cases, such local effects would have little impact on the overall structural integrity of the components, but, as the extent of the cracking increases, the uncertainties introduced by such local effects could become more significant and cannot be ignored. If the extent of weld repairs cannot be documented, the bounding CGR approach should be used for safety evaluations.

Carl Terry

- 2 -

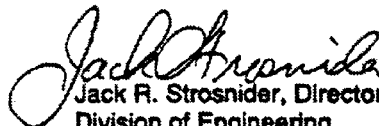
We believe that, by using an appropriately reduced value for the CGR from the 5×10^{-6} in/hr value found in NUREG-0313, Rev. 2, it would be possible for licensees to get credit for improved water chemistry and other measures to mitigate cracking, e.g., hydrogen water chemistries (HWC) and/or noble metal additions. The revised CGR of 2.2×10^{-6} in/hr corresponds to water chemistries with a conductivity of ≤ 0.15 μ S/cm and an electro-chemical potential (ECP) of +200 mV. The BWRVIP-14 correlation indicates that this bounding CGR could be reduced for HWC with ECP ≤ -230 mV. The staff finds acceptable a reduction in the CGR from 2.2×10^{-6} in/hr to 1.1×10^{-6} in/hr for plants with HWC. The crack growth rates stated are only applicable to components with fluences $< 5 \times 10^{20}$ n/cm² ($E > 1$ MeV) since the CGR database is presently based only on unirradiated materials.

The above is discussed in greater detail in the enclosed TER, and was discussed with members of the BWRVIP during a telephone call on October 18, 1999. Therefore, based on the information you have provided, the staff has concluded that licensee usage of the BWRVIP-14 guidelines as revised is acceptable.

The staff requests that you incorporate the staff's recommendation regarding the above issue on generic stress intensity factors, as well as your response to other issues raised in the staff's initial SE, into a revised, final BWRVIP-14 report. Please inform the staff within 90 days of the date of this letter as to your proposed actions and schedule for such a revision.

Please contact C. E. (Gene) Carpenter, Jr., of my staff at (301) 415-2169 if you have any further questions regarding this subject.

Sincerely,


Jack R. Strosnider, Director
Division of Engineering
Office of Nuclear Reactor Regulation

Enclosure: TER

cc: See next page

cc:

Bill Eaton, Executive Chair
Inspection Committee
Entergy Operations, Inc.
PO Box 756, Waterloo Rd
Port Gibson, MS 39150-0756

H. Lewis Sumner, Executive Chairman
BWRVIP Mitigation Task
Southern Nuclear Operating Co.
M/S BIN B051, PO Box 1295
40 Inverness Center Parkway
Birmingham, AL 35201

Harry P. Salmon, Executive Chairman
BWRVIP Integration Task
New York Power Authority
123 Main St., M/S 11 D
White Plains, NY 10601-3104

George T. Jones, Executive Chair
BWRVIP Repair Task
Pennsylvania Power & Light, Inc.
M/S GEN A 61
2 N 9th Street
Allentown, PA 18101-1139

Robert Carter, EPRI BWRVIP
Assessment Manager
Greg Selby, EPRI BWRVIP
Inspection Manager
EPRI NDE Center
P. O. Box 217097
1300 W. T. Harris Blvd.
Charlotte, NC 28221

Joe Hagan, BWRVIP Vice Chairman
PEPCO Energy Co.
MC 62C-3
965 Chesterbrook Blvd
Wayne, PA 19807-5691

Steve Lewis, Technical Chairman
BWRVIP Assessment Task
Entergy
P. O. Box 756
Waterloo Road
Port Gibson, MS 39150

Carl Larsen, Technical Chairman
BWRVIP Inspection Task
P.O. Box 157
Vernon, VT 05354

John Wilson, Technical Chairman
BWRVIP Mitigation Task
Clinton Power Station, M/C T-31C
P.O. Box 678
Clinton, IL 61727

Vaughn Wagoner, Technical Chairman
BWRVIP Integration Task
Carolina Power & Light Company
One Hannover Square 9C1
P.O. Box 1551
Raleigh, NC 27612

Bruce McLeod, Technical Chairman
BWRVIP Repair Task
Southern Nuclear Operating Co.
Post Office Box 1295
40 Inverness Center Parkway
Birmingham, AL 35201

Tom Mufford, EPRI BWRVIP
Integration Manager
Raj Pathania, EPRI BWRVIP
Mitigation Manager
Ken Wolfe, EPRI BWRVIP
Repair Manager
Electric Power Research Institute
P. O. Box 10412
3412 Hillview Ave.
Palo Alto, CA 94303

James P. Palletier, BWRVIP Liaison
to EPRI Nuclear Power Council
Nebraska Public Power District
1200 Prospect Avenue
PO Box 98
Brownville, NE 68321-0098

**Technical Evaluation Report on
Project No. 704—BWRVIP Response to
NRC Safety Evaluation of BWRVIP-14**

August 5, 1999

**Prepared by
W. J. Shack
O. K. Chopra
S. Majumdar**

**Argonne National Laboratory
9700 South Cass Avenue
Argonne, IL 60439**

**Technical Monitor
Donald Naujock
USNRC Office of Nuclear Reactor Regulation**

Introduction

This technical evaluation report reviews Project 704, *BWR Vessels and Internals Project, Response to NRC Safety Evaluation of BWRVIP-14*. The overall conclusions of the ANL Assessment are:

1. We agree with the BWRVIP conclusion that the crack growth rate of 2.2×10^{-5} in/hr is sufficiently conservative that it should bound crack growth in cylinder-to-cylinder horizontal welds, shroud vertical welds, and cylinder-to-edge-ring welds. These would include the H1-H7 welds for BWR 3/4 models (Fig. 1-2 of BWRVIP-14) and the H3-H7 welds for BWR 6 models (Fig. 1-3 of BWRVIP-14).
2. We do not agree with the BWRVIP conclusion that the use of the generic stress intensity factor factors provided in Fig. 4 of the response avoids the need to document weld repairs when using a K based approach for estimating CGRs. The generic stress intensity factor distributions proposed in the BWRVIP response will generally be conservative for cylinder-to-cylinder horizontal welds and cylinder-to-edge-ring welds. However, it restricts the local stress distributions to be self-equilibrating at every azimuth. Because local weld repairs inherently introduce three dimensional effects, this is an artificial constraint and may lead to nonconservative estimates of the local stresses. In most cases such local effects would have little impact on the overall structural integrity of the shroud, but as the extent of the cracking increases the uncertainties introduced by such local effects could become more significant and cannot be ignored. If the extent of weld repairs cannot be documented, the bounding CGR approach should be used for safety evaluations.

We believe that by using an appropriately reduced value for the bounding CGR, it still would be possible for licensees to get credit for improved water chemistry and other measures to mitigate cracking such as noble metal additions. The bounding crack growth rate of 2.2×10^{-5} in/hr corresponds to water chemistries with a conductivity of ≤ 0.15 $\mu\text{S}/\text{cm}$ and an ECP of 200 mV. The BWRVIP-14 correlation indicates that this bounding CGR could be reduced by a factor of 4.5 for hydrogen water chemistries (HWC) with ECP ≤ -230 mV. The staff has already concluded in its SER that the estimates of the benefits of improved water chemistry provided by the BWRVIP-14 correlation are conservative, and hence we believe that it can be used to determine appropriate factors of reduction in the current bounding CGR.

3. As the BWRVIP has noted in its response to an earlier RIA on BWRVIP-14 and in the response to the staff SER, the stress intensity factor solutions in BWRVIP-14 using the Bamford and Buchelet weight functions, which were determined for $R/t = 10$, may give significantly nonconservative values for K and should not be used. The BWRVIP has presented improved stress intensity factor solutions based on the work of Cheng and Finnie. These solutions take into account the R/t ratio and have been benchmarked with the solutions by Labbens and Bamford and Buchelet for $R/t = 10$ and the limiting case of the flat plate ($R/t = \infty$).

Discussion

The BWRVIP response to the NRC Safety Evaluation of BWRVIP-14 discusses a number of issues. These are addressed on a point by point basis.

BWRVIP Response to Issues Identified in the NRC Safety Evaluation Report

1. Item 1, pg. 2: The BWRVIP argues that the effect of weld repairs, fit-up stresses can be bounded for core shroud horizontal and vertical welds and that the bounding crack growth rate of 2.2×10^{-5} in/hr should be applicable for these welds without plant specific NRC review of weld repairs and residual stress distributions. (Item 1 of the BWRVIP response essentially also includes their Item 3 which rephrases the argument to consider vertical welds.)

Assessment:

We agree with the BWRVIP conclusion that the crack growth rate of 2.2×10^{-5} in/hr is sufficiently conservative that it should bound crack growth in cylinder-to-cylinder horizontal welds, shroud vertical welds, and cylinder-to-edge-ring welds.

This conclusion is supported by detailed analyses of the residual stresses and crack growth for these geometries which show that typically the crack growth rates should be much less than 2.2×10^{-5} in/hr. Because a CGR of 2.2×10^{-5} in/hr corresponds to growth of a throughwall crack in about 7 years, field experience suggests that even in situations where high local residual stresses are present so that crack arrest does not occur, this is still a conservative estimate of the average throughwall CGR.

BWRVIP-14 presents residual stress calculations and measurements on a number of core shroud cylinder-to-cylinder welds and cylinder-to-edge-ring welds. It also defines a generic residual stress distribution for such welds. The calculated and measured distributions are compared in Figs. 4-4 through 4-11. It can be difficult to interpret whether one throughwall residual stress distribution is conservative with respect to another. It is much more meaningful to compare the corresponding distributions of K , because it really controls the crack growth. The throughwall variation of the stress intensity factors which correspond to the various throughwall residual stress distributions given in BWRVIP-14 are shown in Fig. 1. The K solution corresponding to the "generic" BWRVIP residual stress distribution is bounding in the sense that it predicts crack arrest at a larger depth than all but one of the distributions, the values in the positive portion of the curve are greater than those of the other distributions at most locations, and it is less compressive for deep cracks so that any prediction of crack arrest in the presence of additional stresses is conservative.

2. Item 2, pg. 2: The BWRVIP notes that although the NRC SER indicates that an electrochemical potential (ECP) of 200 mV (SHE) for stainless steel was typical of BWRs operating under moderate hydrogen water chemistry, this ECP is actually typical of normal water chemistry operations.

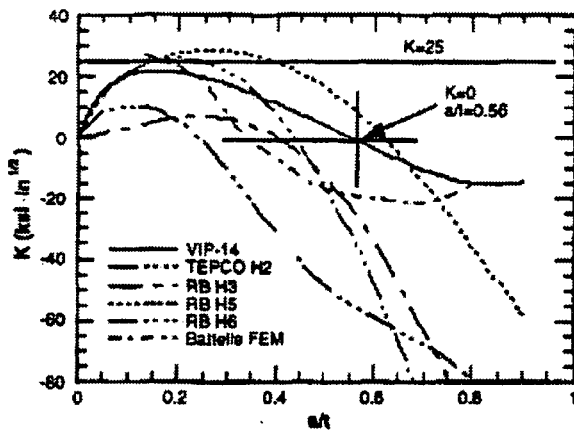


Figure 1
Throughwall variation of the stress intensity factor K for various cylinder-to-cylinder and cylinder to edge-ring welds based on the corresponding residual stress distributions reported in BWRVIP-14 and in independent calculations by Battelle.

Assessment:

The BWRVIP observation is correct. An ECP of 200 mV would be typical (perhaps somewhat conservative) for the core shroud for normal water chemistry conditions.

- Item 3 pg.2: The BWRVIP argues that the residual stress distributions for vertical double V groove welds are similar to those for double V groove horizontal welds for which more measurements and calculations are available. Hence the CGR of 2.2×10^{-5} in/hr is also bounding for these welds.

Assessment:

We agree with BWRVIP argument and believe, as noted in our assessment of Point 1, that the crack growth rate of 2.2×10^{-5} in/hr is sufficiently conservative that it should bound crack growth shroud vertical welds as well as in cylinder-to-cylinder horizontal welds and cylinder-to-edge-ring welds.

- Item 4 pg.2: The BWRVIP in its response defines a new K distribution (Fig. 4 of the BWRVIP response) that it argues can be used on a generic basis for core shroud horizontal welds to determine K distributions that can be used with K dependent CGR models such as the BWRVIP-14 correlation or PLEDGE.

Assessment:

Despite the arguments of the BWRVIP, we believe that if the extent of weld repairs cannot be documented, then for safety evaluations the bounding CGR approach should be used rather than a K dependent CGR approach. For its own planning purposes the licensee may choose to use the conservative, but not necessarily bounding, K distributions proposed by the BWRVIP.

It would still be possible for the licensee to take credit for improved water chemistry and other measures to mitigate cracking by reducing the bounding CGR appropriately. The bounding CGR, 2.2×10^{-5} in/h, corresponds to water chemistries with a conductivity

of $\leq 0.15 \mu\text{S}/\text{cm}$ and an ECP of 200 mV. The BWRVIP-14 correlation indicates that this bounding CGR could be reduced by a factor of 4.5 for hydrogen water chemistries (HWC) with ECP ≤ -230 mV.

The new K distribution is based on a stress distribution (Figs. 1 and 2 of 704) that consists of the generic residual stress distribution given in BWRVIP-14, plus a conservative estimate of the membrane stresses acting on the shroud, and plus an estimate of the local stresses due to weld repair. The overall stress state is still dominated by the welding residual stresses. As noted in the assessment of Item 1, we agree that the generic welding residual stress distribution given in BWRVIP-14 is conservative for cylinder-to-cylinder horizontal welds, shroud vertical welds, and cylinder-to-edge-ring welds. The estimate of the membrane stresses is also clearly conservative. However, the basis for the selection of the surface residual stress distribution used to account for weld repairs and other local phenomena is unclear. There is a reference in the BWRVIP response to FEA of the effects of weld repairs performed as part of the BWRVIP-14 study (pg. 6), but the results of those analyses do not appear to be included in the BWRVIP-14 report.

The local residual stress distribution proposed by the BWRVIP is forced to be self-equilibrating through the thickness, i.e., the distribution is self-equilibrating at every azimuth. However, local weld repairs lead to three dimensional nonaxisymmetric stress states, and in such case the axial stresses need not be self-equilibrating at every azimuth and it is certainly possible that at some azimuths high tensile stresses persist to greater depths than assumed in the BWRVIP estimate.

The BWRVIP response does recognize that the proposed distribution need not be bounding at every location. They argue that the local regions where the stresses could be higher are limited in extent and hence do not affect the overall structural integrity. If the cracking is limited in extent and the crack size much smaller than the critical size for failure, the BWRVIP argument is valid, but in such cases one could probably just use the bounding CGR approach. If the crack size is close to critical, then the sizes and nature of the local regions in which the stresses are more severe than assumed by the BWRVIP could be more important. Local perturbations in stress can have dramatic effects on CGRs. From Figure 5 in the BWRVIP response, it can be seen that an increase of 1 ksi in the average throughwall stress could reduce the time required for the crack to grow throughwall from 30 years to 5 years.

There is substantial experience in the calculation and measurement of residual stresses for "good" welds. There is much less information available on the nature and distribution of the local stresses due to repairs. In the ANL TLR on BWRVIP-14, the approach taken was to assume that experience permits a good estimate of a bounding CGR, in particular 2.2×10^{-5} in/h, which corresponds to 0.2 in/y. The throughwall average stress which had to be added to the generic welding residual stress to obtain this average CGR was ≈ 10 ksi. As the BWRVIP response notes such a stress state could not exist over the entire circumference, but it was intended to be used to estimate CGR only in local weld repair regions. It probably would have been simpler to just state that the bounding CGR should be used in local weld repair regions and a "best estimate" CGR used elsewhere.

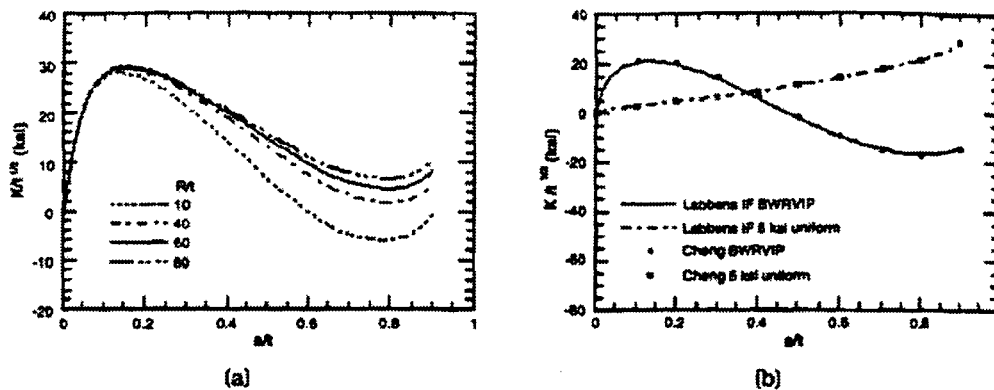


Figure 2 (a) Distributions of $K/t^{1/2}$ for the proposed generic stress distribution in the BWRVIP response for $R/t = 10, 40, 60, 80$. (b) Comparison of influence function solutions for K for a uniform stress and the BWRVIP-14 residual stress distribution with the Cheng and Finnie solutions for these distributions.

As the BWRVIP has noted in its response to an earlier RIA on BWRVIP-14 and in the response to the staff SER, the stress intensity factor solutions in BWRVIP-14 using the Bamford and Buchelet weight functions, which were determined for $R/t = 10$ may give significantly nonconservative values for K and should not be used. The BWRVIP has presented improved stress intensity factor solutions based on the work of Cheng and Finnie. These solutions take into account the R/t ratio and have been benchmarked with the solutions by Labbens and Bamford and Buchelet for $R/t = 10$ and the limiting case of the flat plate ($R/t = \infty$) for a variety of stress distributions. In Fig 2a are shown the K solutions for $R/t = 10, 40, 60, 80$ for the proposed generic weld residual stress in the BWRVIP response to the SER. The solutions for $R/t = 10$ are nonconservative. They predict arrest for the new generic stress distribution, whereas the solutions for $R/t \geq 40$ predict throughwall crack growth.

These Cheng and Finnie solutions take into account the R/t ratio and have been benchmarked with the solutions by Labbens and Bamford and Buchelet for $R/t = 10$ and the limiting case of the flat plate ($R/t = \infty$). Comparisons with the Labbens influence function solutions for a uniform stress and the BWRVIP-14 residual stress with the corresponding Cheng and Finnie solutions for $R/t=10$ are shown in Fig. 2b.

5. Item 5 pg. 2: The BWRVIP concurs that application of BWRVIP-14 above a fluence level of 5×10^{20} n/cm² requires plant specific analysis.

BWRVIP Response to NRC Evaluation and Observations

1. Item 1, pg. 4: The BWRVIP observes that in most cases the value of 2.2×10^{-5} in/h will be very conservative for core shrouds. They state that "In view of the conservatism associated with this number, the BWRVIP believes that where significant improvement in the water chemistry and ECP are maintained by the plant, this CGR rate can be substantially reduced by use of the empirical model in BWRVIP-14."

Assessment

We agree that the CGR of 2.2×10^{-5} in/h is expected to be conservative for most locations. Indeed, away from weld repairs, crack growth in the core shroud would be expected to arrest about half way through the wall.

It is not clear to us exactly what is being argued in the last sentence of the paragraph. For a plant with normal water chemistry, but low conductivity and for which the regions of local weld repair can be appropriately characterized, that the empirical model in BWRVIP-14 can be applied and will in general predict lower crack growth rates. We do not agree as discussed previously under element 4 that the generic residual stress/K solutions provided in the BWRVIP response can be assumed to be bounding without additional knowledge of the weld repair history. If local weld repairs can't be characterized, we believe that credit can still be given for improved water chemistries such as hydrogen water chemistry by using an appropriately reduced value of the bounding CGR. For example, for a plant with HWC so that the conductivity is ≤ 0.15 $\mu\text{S}/\text{cm}$ and ECP ≤ -230 mV the empirical model in BWRVIP-14 predicts that the CGR is a factor of 4.5 than a plant with an ECP = 200 mV. For such a plant an appropriate bounding CGR might be:

$$2.2 \times 10^{-5} / 4.5 = 4.9 \times 10^{-6} \text{ in/h.}$$

The reduction factor for the lower ECP predicted by the BWRVIP-14 model is quite conservative compared with the reductions predicted by other models such as PLEDGE and observed in most laboratory and in-reactor tests.

2. Item 2, pg. 4: The bounding CGR of 2.2×10^{-5} in/h is appropriate for BWRs under normal water chemistry in which case the in-core ECP would be expected to be on the order of 200 mV. Hydrogen water chemistry conditions are not required for use of this bounding CGR.

Assessment

We agree.

3. Item 3, pg. 4: The BWRVIP cites data from NDE measurements at a Swiss BWR at a fluences up to 1×10^{21} n/cm² indicating that little or no crack growth was occurring. They argue that these data suggest that the effects of irradiation on IGSCC crack growth are limited and may be bounded by thermally sensitized data.

Assessment

We do not believe any conclusion can be drawn from the cited data on the effects of irradiation on IGSCC crack growth.

The slow crack growth in the Swiss core shroud could well be due to a favorable residual stress distribution. It is almost impossible to deduce anything about the basic crack growth response of a material from such measurements because the effects of other variable like the residual stresses cannot be isolated. It is probably true that chromium depletion levels due to irradiation are bounded by those in heavily thermally sensitized

materials. Irradiation, however, also has profound effects on mechanical properties which could strongly affect crack tip strain rates, and without additional data it is premature to conclude that the CGRs on thermally sensitized materials bound those for irradiated materials. The limited data on IASCC CGRs currently available seem to indicate that for equivalent environmental and loading conditions the CGRs for irradiated materials may be greater than those in materials thermally sensitized by typical welding practices.

4. Item 4, pg. 5: BWRVIP argues again that the generic welding residual stress in BWRVIP-14 is applicable to both cylinder-to-cylinder horizontal welds and cylinder-to-ring welds.

Assessment

We agree.

As noted in our assessment of Item 1, pg. 2, BWRVIP-14 presents residual stress calculations and measurements on a number of core shroud cylinder-to-cylinder welds and cylinder-to-edge-ring welds. It also defines a generic residual stress distribution for such welds. The K solution corresponding to the "generic" BWRVIP residual stress distribution is appropriately bounding, and hence we agree that the generic residual stress distribution is applicable to both cylinder-to-cylinder horizontal welds and cylinder-to-ring welds.

5. Item 5, pg. 5: The BWRVIP seems to believe the use of a bounding CGR is appropriated only for plants with normal water chemistry and that plants using hydrogen water chemistry will use K dependent CGRs based on the BWRVIP-14 correlation.

Assessment

The BWRVIP seems to make the distinction between whether a plant uses the bounding approach or a K dependent CGR approach based on the water chemistry. We believe that the decision of whether to use the bounding approach or a K dependent approach depends on knowledge of residual stresses not water chemistry. The use of a K dependent CGR requires that residual stresses be characterized. We do not believe that this can be done adequately without knowledge of the weld repairs.

As noted previously a bounding CGR approach can be used for both plants on normal water chemistry and those on hydrogen water chemistry. The value of the bounding CGR can be adjusted appropriately. The bounding CGR would be much lower in plants operating on HWC. The staff has already concluded in its SER that the estimates of the benefits of improved water chemistry provided by the BWRVIP-14 correlation are conservative, and hence we believe that it can be used to determine appropriate factors of reduction in the current bounding CGR.

6. Item 6, pg. 5: The BWRVIP proposes a generic stress distribution that includes the welding residual stresses, a conservative estimate of the membrane stresses due to loads on the shroud, and a surface stress distribution intended to represent the effect of local weld repairs.

Assessment

We do not agree with the BWRVIP conclusion that the residual stress distribution given in Fig. 1 of the response and the corresponding K solutions given in Fig. 4 are sufficiently conservative that they can be used to estimate CGRs with no additional knowledge of weld repairs.

The intent of the BWRVIP proposal is to avoid having to document weld repairs. As discussed in the assessment of Item 4 pg.2 of the BWRVIP response, the proposed distribution appears reasonable "on the average." However, it restricts the local stress distributions to be self-equilibrating at every azimuth. Because local weld repairs inherently introduce three dimensional effects, this is an artificial constraint and may lead to nonconservative estimates of the local stresses. In most cases such local effects will not be important for the overall structural integrity of the shroud. In any given case, however, it is difficult to ensure integrity without knowing more about the extent and nature of any weld repairs. Without knowledge of the repairs, we believe it is prudent to use a bounding CGR approach for safety analyses.

K

BWRVIP RESPONSE TO NRC FINAL SAFETY EVALUATION OF BWRVIP-14

BWRVIP

BWR Vessel & Internals Project

2000-198

July 11, 2000

Document Control Desk
U. S. Nuclear Regulatory Commission
11555 Rockville Pike
Rockville, MD 20852

Attention: C. E. Carpenter

Subject: PROJECT NO. 704 – BWRVIP Response to NRC Final Safety Evaluation of BWRVIP-14

Reference: Letter from Jack Strosnider (NRC) to Carl Terry (BWRVIP Chairman), "Final Safety Evaluation of Proprietary Report TR 105873 'BWR Vessel and Internals Project, Evaluation of Crack Growth in BWR Stainless Steel Internals (BWRVIP-14)' (TAC NO. M94975)," dated December 3, 1999.

Enclosed are 10 copies of the BWRVIP response to the issues identified in the NRC Final Safety Evaluation (SE) on the BWRVIP report "BWR Vessel and Internals Project, Evaluation of Crack Growth in BWR Stainless Steel Internals (BWRVIP-14)" transmitted by the NRC letter referenced above.

The enclosed information concerns a report that the NRC staff has found to be proprietary in nature. Therefore, the enclosed information is also proprietary and should be withheld from public disclosure.

If you have any questions on this subject please contact Rich Ciemiewicz of PECO Energy (BWRVIP Assessment Committee Technical Chairman) by telephone at 610.640.6419.

Sincerely,



Carl Terry
Niagara Mohawk Power Corp.
Chairman, BWR Vessel and Internals Project

Enclosure

EPRI Proprietary Information

BWRVIP Proposed Resolutions to Issues Identified in NRC Safety Evaluation of BWRVIP-14 and Technical Evaluation Report on Project No. 704

Introduction

The NRC issued the final safety evaluation (SE) of proprietary report TR-105873 "BWR Vessel and Internals Project, Evaluation of Crack Growth in BWR Stainless Steel Internals (BWRVIP-14)" on December 3, 1999. The NRC SE was issued along with a Technical Evaluation Report on Project No. 704 prepared by the Argonne National Laboratory (ANL). A meeting was held on February 17, 2000 at Argonne National Laboratories (Argonne, Illinois) between representatives of the USNRC, ANL and BWRVIP, at which several issues related to the USNRC Safety Evaluation of BWRVIP-14 and Technical Evaluation Report on Project No. 704 were discussed [1]. This document proposes a resolution of the NRC concern about the BWRVIP-14 K-dependent crack growth model based on the February 17, 2000 meeting. It also proposes an interim approach to address crack growth issues for plants on moderate hydrogen water chemistry (HWC-M) or Noble Metal Chemical Application (NMCA) pending NRC review of BWRVIP-62.

Use of BWRVIP-14 K-dependent Crack Growth Model

In the SE, the NRC took exception to the BWRVIP conclusion that the use of the generic stress intensity factors proposed in Figure 4 of the November 24, 1998 RAI response [2] avoids the need to document weld repairs when using a K-based approach for estimating crack growth rates. During the meeting, the BWRVIP stated that the generic stress intensity factor (K) distribution proposed by BWRVIP in November 1998 was conservative because of the following factors:

- Inclusion of the radius to thickness ratio effect.
- Inclusion of a surface stress to account for repair weld effects.
- Inclusion of a 3.2 ksi membrane stress to account for operating stresses (typically 0.5 ksi) and local repair weld effects.

The generic K distribution is shown in Figure 1. It is more conservative than a distribution based on the Bamford-Buchalet model (which includes a membrane stress of 10 ksi). The generic K distribution remains positive through the thickness and predicts crack retardation but not arrest. This prediction is conservative because inspection data from core shrouds shows evidence of crack arrest.

The BWRVIP further stated that the generic K distribution addresses local weld repair effects with reasonable conservatism by not assuming that they are self equilibrating at all locations. Weld repairs produce significantly higher residual stresses only for short repairs which have little impact on the overall structural integrity of the shroud. As the repairs become longer the restraints on repair welds are similar to the original weld and therefore the residual stress

EPRI Proprietary Information

distributions should also be similar. A requirement to document weld repairs in the core shrouds is very difficult to implement as in-process repairs are generally not reported.

The crack growth predictions based on the generic K distribution shown in Figure 1 are consistent with field crack growth data. This is illustrated in Figure 2 which compares the calculated K-dependent crack growth predictions with measured crack growth in several plants. In most cases, the predictions are conservative or are within the inspection uncertainty band. If the locations of weld repair are regions of higher residual stress, field cracking experience should include many of these locations.

The NRC pointed out that the local weld repair concerns could be further addressed by recommending a range of flaw depths for which the K-dependent model would be applicable. The BWRVIP proposes the following changes to BWRVIP-14:

Use of the K-dependent model will be limited to flaw depths up to 80% of the shroud wall thickness. This maximum limiting flaw depth is selected for the following reasons:

- (a) The loads on the core shroud are relatively small compared to Class 1 piping loads. It is expected that the allowable flaw depth in most cases is greater than 90% of wall thickness for a 360-degree flaw in BWR shrouds. A limit of 80% flaw depth for applicability of the K-dependent model assures that the allowable flaw depth will not be encroached upon during crack growth.
- (b) It is recognized that the ASME Code, Section XI, IWB-3600, allows a maximum flaw depth of 75% for defects in austenitic primary pressure boundary piping. However, this limit is not based upon structural integrity concerns but rather to avoid leakage in the pressure boundary component. For the core shroud, the consequences of leakage are not nearly as significant as for primary pressure boundary piping, and therefore an average flaw depth up to 80% is justified.
- (c) As can be seen from Figure 1, the fracture mechanics model used for the determination of K is limited to 90% of wall. Hence, the choice of 80% ensures that the limit of the model is not reached during K-dependent crack growth. It can be seen from Figure 1 that K remains relatively low between 80 and 90% of wall and even when extrapolated to 95% of wall, K is less than 25 ksi $\sqrt{\text{in.}}$ for a 2-inch thick shroud (which formed the basis for the constant rate of 2.2×10^{-5} inch per hour).

Application of the BWRVIP-14 Stainless Steel Crack Growth Model to Plants Under Normal Water Chemistry

1. For average flaw depths up to 80% through-wall, use the K-dependent model for NWC plants (ECP = +200 mV, SHE).
2. For average flaw depths greater than 80%, but less than the allowable flaw size (presented in BWRVIP-01 and supplemented by BWRVIP-76), use the K-independent crack growth

EPRI Proprietary Information

rate of 2.2×10^{-5} in /hr for NWC plants (ECP= +200 mV, SHE, conductivity ≤ 0.15 $\mu\text{S/cm}$).

Application of the BWRVIP-14 Stainless Steel Crack Growth Model to Plants Under Hydrogen Water Chemistry

The NRC is reviewing the report entitled, "Technical Basis for Inspection Relief for BWR Components with Hydrogen Injection" (BWRVIP-62). The NRC stated at the meeting that in the interim, the crack growth rate for plants under hydrogen chemistry (HWC) or Noble Metal Chemical Application (NMCA) can be reduced by a factor of 2 if HWC availability is at least 80% and ECP is ≤ -230 mV, SHE.

The BWRVIP proposes the following crack growth model be used for plants when HWC availability is at least 80% and ECP is ≤ -230 mV, SHE:

1. For an average flaw depth of up to 80% through-wall, use the K-dependent crack growth model of BWRVIP-14 for NWC plants and reduce it by a factor of 2 for HWC/NMCA plants (ECP ≤ -230 mV, SHE)
2. For average flaw depths greater than 80%, but less than the allowable flaw size (presented in BWRVIP-01 and supplemented by BWRVIP-76), use the K-independent crack growth of 1.1×10^{-5} in /hr for HWC/NMCA plants (ECP ≤ -230 mV, SHE, conductivity ≤ 0.15 $\mu\text{S/cm}$).

The use of the BWRVIP-14 crack growth model at various ECPs and HWC availabilities to calculate factors of improvements as shown in Figure 4-1 of BWRVIP-62 will be revisited after the NRC has completed its review of BWRVIP-62 report.

References

1. Summary of February 17, 2000 BWRVIP/NRC Meeting, BWRVIP Document 2000-049, February 29, 2000.
2. BWRVIP Response to NRC Safety Evaluation of BWRVIP-14, BWRVIP Document 98-458, November 24, 1998.

EPRI Proprietary Information

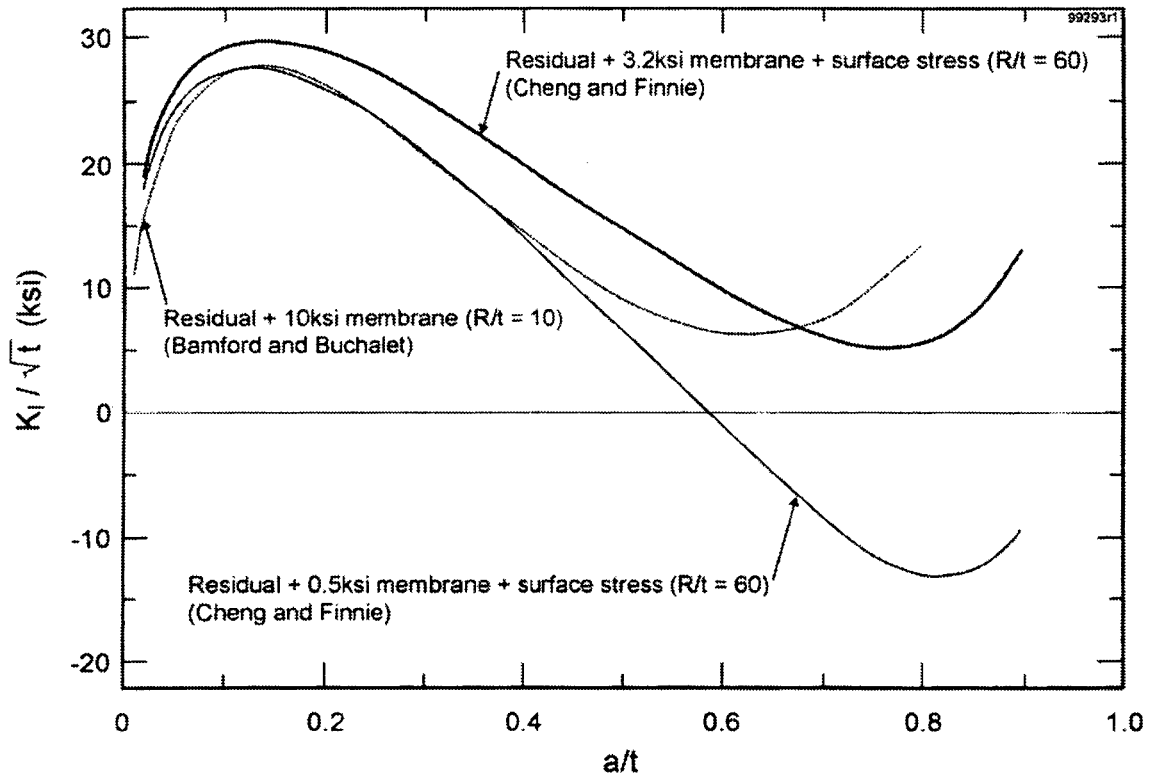


Figure1: BWRVIP Generic Stress Intensity Factor Distribution for Core Horizontal Core Shroud Welds (Residual +3.2 ksi Membrane Stress + Surface Stress)

**Content Deleted –
EPRI Proprietary Information**

**Figure 2: Comparison of Through-thickness Crack Growth Calculated with BWRVIP-14 K
Dependent Model with Measured Crack Growth for Several Plants**

L

USNRC POSITION ON BWRVIP RESPONSE TO NRC FINAL SAFETY EVALUATION OF BWRVIP-14



UNITED STATES
NUCLEAR REGULATORY COMMISSION
WASHINGTON, D.C. 20555-0001

2001-163A

May 13, 2001

FILE COPY

Carl Terry, BWRVIP Chairman
Niagara Mohawk Power Company
Post Office Box 63
Lycoming, NY 13093

SUBJECT: BWRVIP RESPONSE TO NRC FINAL SAFETY EVALUATION OF BWRVIP-14
(TAC NO. M94975)

Dear Mr. Terry:

By letter dated July 11, 2000, you provided the BWR Vessel and Internals Project's (BWRVIP) response to the staff's December 3, 1999, final safety evaluation report (FSER) of the Electric Power Research Institute's (EPRI) proprietary report TR-105873, "BWR Vessel and Internals Project, Evaluation of Crack Growth in BWR Stainless Steel Internals (BWRVIP-14)," dated March 1996. This letter provided additional information regarding the use of the BWRVIP-14 K-dependent crack growth model based on a February 17, 2000, meeting between members of the BWRVIP and the staff.

In the December 3, 1999, FSER, the staff had taken exception to your conclusion that the use of the generic stress intensity factors, provided in Figure 4 of the response, avoids the need to document weld repairs when using a K based approach for estimating crack growth rates (CGR). Specifically, the staff raised a concern regarding the uncertainties introduced by local effects if the extent of weld repairs cannot be documented, and the FSER stated that, in such cases, the bounding CGR approach should be used for safety evaluations.

The NRC staff, with assistance from the Argonne National Laboratory (ANL), has reviewed your response to the staff's FSER and finds that you have provided sufficient additional information such that the staff's original concern with the BWRVIP-14 report's K-dependent crack growth model has been satisfied. Licensee implementation of this revised BWRVIP-14 report will provide an acceptable level of quality for determining inspection frequencies for the safety-related BWR internal components under normal water chemistry (NWC) conditions. In revising the BWRVIP-14 report to address the staff's concerns in the June 8, 1998, initial safety evaluation and the December 3, 1999, FSER, please include your July 11, 2000, letter and this response in the revised BWRVIP-14 report.

In your July 11, 2000, letter, you address plants implementing hydrogen water chemistry (HWC). Please address factors of improvements described in this letter in your future response to the staff's January 30, 2001, initial SE regarding the EPRI proprietary report TR-108705, "BWR Vessel and Internals Project, Technical Basis for Inspection Relief for BWR Internal Components with Hydrogen Injection (BWRVIP-62)," dated December 1998.

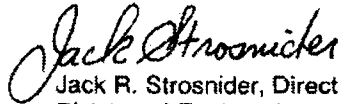
Carl Terry

-2-

The staff requests that you incorporate the staff's recommendations, as well as your responses to other issues raised in the staff's initial SE and FSER, into a revised, final BWRVIP-14 report. Please inform the staff within 90 days of the date of this letter as to your proposed actions and schedule for such a revision.

Please contact C. E. (Gene) Carpenter, Jr., of my staff at (301) 415-2169, if you have any further questions regarding this subject.

Sincerely,



Jack R. Strosnider, Director
Division of Engineering
Office of Nuclear Reactor Regulation

cc: See next page

M

USNRC CLARIFICATION TO POSITION ON BWRVIP RESPONSE TO NRC FINAL SAFETY EVALUATION OF BWRVIP-14



UNITED STATES
NUCLEAR REGULATORY COMMISSION

WASHINGTON, D.C. 20555-0001

July 20, 2001

2001-243A

FILE COPY

Carl Terry, BWRVIP Chairman
Niagara Mohawk Power Company
Post Office Box 63
Lycoming, NY 13093

**SUBJECT: CLARIFICATION TO NRC LETTER REGARDING BWRVIP RESPONSE TO
BWRVIP-14 FINAL SAFETY EVALUATION (TAC NO. M94975)**

Dear Mr. Terry:

By letter dated May 13, 2001, the staff provided to you our findings regarding the staff's review of the July 11, 2000, BWR Vessel and Internals Project (BWRVIP) response to the staff's December 3, 1999, final safety evaluation (FSER) of EPRI report TR-105873, "BWR Vessel and Internals Project, Evaluation of Crack Growth in BWR Stainless Steel Internals (BWRVIP-14)." This letter provides additional clarification in response to questions raised by BWR licensees regarding the staff's conclusions in that letter. In summary, the staff has concluded that:

- the BWRVIP has provided sufficient additional information such that the staff's original concern with the K-dependent crack growth model has been satisfied;
- the staff accepts the methodology described in the July 11, 2000, BWRVIP document on application of the stainless steel crack growth model to plants under normal water chemistry, and for plants using hydrogen water chemistry (HWC) with or without the addition of noble metal (NMCA); and,
- the staff is reviewing the acceptability of the BWRVIP-14 crack growth model to calculate factors of improvement at various electrochemical potentials (ECPs) and HWC availabilities, as shown in Figure 4-1 of the EPRI proprietary report TR-108705, "BWR Vessel and Internals Project, Technical Basis for Inspection Relief for BWR Internal Components with Hydrogen Injection (BWRVIP-62)," dated December 1998.

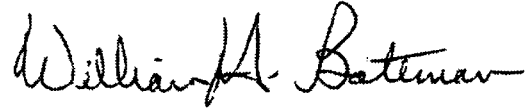
The staff requests that you incorporate the staff's recommendations, as well as your response to other issues raised in the staff's initial SE and FSER into a revised, final BWRVIP-14 report.

Carl Terry

-2-

Please contact C. E. (Gene) Carpenter, Jr., of my staff at (301) 415-2169, if you have any further questions regarding this subject.

Sincerely,

A handwritten signature in black ink that reads "William H. Bateman". The signature is written in a cursive style with a large, prominent "W" and "B".

William H. Bateman, Chief
Materials and Chemical Engineering Branch
Division of Engineering
Office of Nuclear Reactor Regulation

cc: BWRVIP Service List

cc:

Joe Hagan, BWRVIP Vice Chair
Exelon Corp.
200 Exelon Way (M/S KSA 3-N)
Kennett Square, PA 19348

George Vanderheyden, Executive Chair
Assessment Committee
Exelon Corp.
Suite 400
1400 Opus Place
Downers Grove, IL 60515-1198

Bill Eaton, Executive Chair,
Inspection Committee
Grand Gulf Gen. Mgr., Plant Operations
Energy Operations, Inc.
PO BOX 756, Waterloo Rd
Port Gibson, MS 39150-0756

H. Lewis Sumner, Executive Chair
BWRVIP Mitigation Task
Vice President, Hatch Project
Southern Nuclear Operating Co.
M/S BIN B051, PO BOX 1295
40 Inverness Center Parkway
Birmingham, AL 35242-4809

George T. Jones, Executive Chair
Repair Committee
Vice President, Nuclear Engrg. & Support
PP&L, Inc.
M/S GENA61
2 N 9th St
Allentown, PA 18101-1139

Robert Carter, EPRI BWRVIP
Assessment Manager
Greg Selby, EPRI BWRVIP
Inspection Manager
EPRI NDE Center
P. O. Box 217097
1300 W. T. Harris Blvd.
Charlotte, NC 28221

Richard Ciemiewicz, Technical Chair
Assessment Committee
Exelon Corp.
Peach Bottom Atomic Power Station
(M/S SMB3-6)
1848 Lay Road
Delta, PA 17314-9032

Carl Larsen, Technical Chair
BWRVIP Inspection Task
Vermont Yankee Nuclear Power Corp.
P.O. Box 157
Vernon, VT 05354

John Wilson, Technical Chair
BWRVIP Mitigation Task
AmerGen Energy Co.
Clinton Power Station, M/C T-31C
P.O. Box 678
Clinton, IL 61727

Vaughn Wagoner, Technical Chair
BWRVIP Integration Task
Carolina Power & Light Company
One Hannover Square 9C1
P.O. Box 1551
Raleigh, NC 27612

Bruce McLeod, Technical Chair
BWRVIP Repair Task
Southern Nuclear Operating Co.
Post Office Box 1295
40 Inverness Center Parkway
Birmingham, AL 35201

Tom Mulford, EPRI BWRVIP
Integration Manager
Raj Pathania, EPRI BWRVIP
Mitigation Manager
Ken Wolfe, EPRI BWRVIP
Repair Manager
Electric Power Research Institute
P. O. Box 10412 3412 Hillview Ave.
Palo Alto, CA 94303

N

USNRC TECHNICAL EVALUATION REPORT ON BWRVIP-14-A DATED JULY 30, 2004

Appendix N

USNRC Technical Evaluation Report on BWRVIP-14-A dated July 30, 2004

DRAFT

**Technical Evaluation Report on
BWRVIP-14-A, BWR Vessels and Internals Project, Evaluation
of Crack Growth in BWR Stainless Steel RPV Internal**

July 30, 2004

Prepared by

W. J. Shack

S. W. Tam

Argonne National Laboratory
9700 South Cass Avenue
Argonne, IL 60439

Technical Monitor

Meena Khanna

USNRC Office of Nuclear Reactor Regulation

Introduction

This technical evaluation report reviews *BWRVIP-14-A, BWR Vessels and Internals Project, Evaluation of Crack Growth in BWR Stainless Steel RPV Internals*, which presents three approaches for the evaluation of crack growth in stainless steel RPV internals and the technical bases for these approaches. This revision addresses most of the issues raised in previous reviews and the staff SER of the original version of this report.

One of the original assumptions of BWRVIP-14 was that the available database on unirradiated materials would be applicable for irradiated materials, at least up to fluence levels of 5×10^{20} n/cm². Data developed since the original publication of EPRI TR-105873 have shown that for fluence levels $\geq 1 \times 10^{21}$ n/cm² crack growth rates can be much higher than in unirradiated materials. Currently the industry proposes to use the BWRVIP-14 correlation for fluences up to 5×10^{20} n/cm², and then to "jump" to a new, higher crack growth rate curve for more highly irradiated materials. Limited data suggest that in some cases even fluence levels of 5×10^{20} n/cm² can result in significant acceleration of the crack growth rate, and hence, the BWRVIP-14 "95th percentile" curve will bound a significantly lower portion of the crack growth rates in materials irradiated to 5×10^{20} n/cm².

Although the crack growth rate curve in BWRVIP-14 may not be as conservative as originally thought, it is the conservatism of the overall crack growth rate calculation process that must be assessed including the conservatism that may be present in the BWRVIP-14 throughwall distribution for the stress intensity factor.

Conclusions and Recommendations

The BWRVIP crack growth model appears to provide a good correlation with a large database of experimental measurements of CGRs for *unirradiated* materials under a range of water chemistry conditions that bound those expected in-reactor. However, even for fluence levels as low as 5×10^{20} n/cm², the "95th percentile" curve, i.e., the BWRVIP-14 disposition curve, may bound the crack growth rate only about 70% of the time.

The BWRVIP model for the throughwall residual stress and the corresponding K distribution is judged to be sufficiently conservative for H4/H5 shell-to-shell welds that the possibility of higher crack growth rates has little impact on the analyses. For these types of welds any of the three approaches given in BWRVIP-14-A for the evaluation of crack growth:

- (1) use of a stress intensity factor (K) independent CGR of 2.2×10^{-5} in/h (1.6×10^{-10} m/s);
- (2) use of a K dependent CGR with a constant of proportionality corresponding to bounding values the conductivity (0.15 μ S/cm) and ECP (200 mV); and
- (3) use of a K dependent CGR with plant specific data for conductivity and ECP

are acceptable for materials with fluence $< 5 \times 10^{20}$ n/cm² ($E > 1$ MeV).

The residual stress distributions for other types of welds found in core shrouds (typically ring-to-shell welds, e.g., H1, H2, H3, H6a, H6b in BWR 3/4s) given in BWRVIP-14 appear to be reasonable. However, BWRVIP-14 assumes that the generic throughwall K solution derived for a shell-to-shell geometry is also applicable to ring-to-shell welds. BWRVIP-14 attempts to

justify this by considering the general character of the residual stress distributions for the two classes of welds. Broadly speaking, they are qualitatively similar, but calculations presented in this report demonstrate that "qualitatively" similar residual stress distributions can lead to quite different K distributions. Because it can be argued that a ring is like a "stiff" shell, we have assumed that the Cheng-Finnie solutions for shell-to-shell welds together with the actual residual stress distributions for ring-to-shell welds can be used to obtain conservative estimates of the K distributions for ring-to-shell welds. These estimates suggest the BWRVIP K distribution may not be conservative in all cases for such welds. Even the presumed bounding constant throughwall value of $25 \text{ ksi}\cdot\text{in}^{1/2}$ may not be conservative in all cases. Although the Cheng-Finnie solutions for the ring-to-shell welds presented in this report are believed to be conservative, confirmatory calculations for the K distributions in ring-to-shell welds would be helpful. Finite-element elastic superposition solutions based on the residual stress distributions given in BWRVIP-14 would be straightforward and give conservative results compared to the more rigorous solutions based on node release in the weld residual stress model.

Although the BWRVIP K distributions is not conservative in all cases for ring-to-shell welds, they are conservative in most cases. Similarly, the BWRVIP 95th percentile crack growth curve for unirradiated materials is expected to bound 70-95% of the crack growth rates for materials with fluences less than $5 \times 10^{-20} \text{ n/cm}^2$. The K distribution and crack growth rate are uncorrelated variables. This suggests that the crack growth predicted by the BWRVIP-14 models will be nonconservative only for a relatively small fraction of cases. If the total length of cracks in a given weld that could be addressed by these generic results were limited to say one half of the total circumference, the consequences of underestimating the crack growth would be limited. With the low applied loads that are present on shrouds, crack opening areas will be small. The structural margins for gross failures of the shrouds would still be large. For longer cracks more specific analyses for the ring-to-shell welds that take into account the actual geometry and weld sequence or a more conservative bounding growth rate ($5 \times 10^{-5} \text{ in/h}$) would be required.

General Discussion

Residual Stresses and K distributions for shell-to-shell welds

BWRVIP-14 contains a substantial amount of information on residual stresses in the shell-to-shell and ring-to-shell welds that comprise the H1-H6 welds in most BWR core shroud designs. Most of these results are based on finite-element calculations of welding residual stress. For the shell-to-shell welds, independent calculations of the residual stresses are available from work done by Battelle under subcontract to ANL as part of the work on environmentally assisted cracking supported by the USNRC Office of Research.

Rather than compare the residual stress distributions for the welds presented in BWRVIP-14 with the Battelle results, it is more meaningful to compare the resulting throughwall distributions of the stress intensity factor K since it is K that actually governs the crack growth. In Figure 1, the K distributions determined from the computed residual stresses for shell-to-shell welds given by BWRVIP-14 are compared with the K distributions determined from the residual stresses computed by Battelle. The BWRVIP-14 results are given for two values of the yield stress, 40 and 67 ksi. Although the modeling assumptions and computation approaches used for the BWRVIP-14 calculations are significantly different than those used in

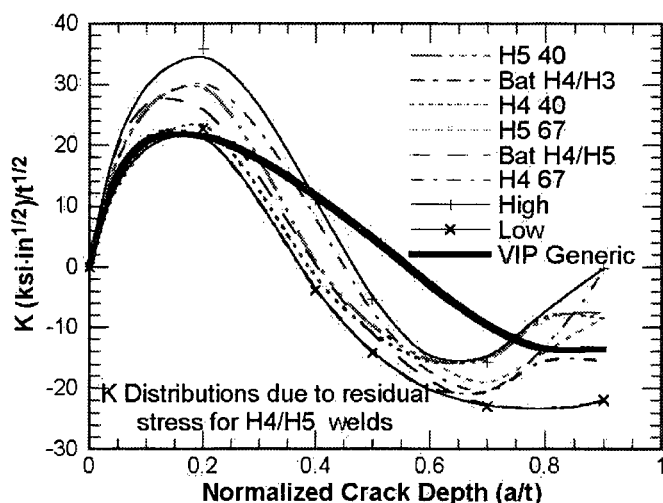


Figure 1. Normalized K for shell-to-shell H4/H5 welds. The calculated residual stresses for yield stresses of 40 and 67 ksi from BWRVIP-14 as shown as H5 40, H4 40, etc. The residual stresses calculated by Battelle on the H3 side and on the H5 side of the H4 weld, respectively are shown as Bat H4/H3 and Bat H4/H5.

the Battelle calculations, the K distributions are quite similar in character. The differences between the various solutions reflect in some cases a variation in a significant parameter (the yield stress) and in others model uncertainty. Bounding K solutions were obtained by determining the maximum and minimum values for K at each depth from the six computed solutions.

Also shown in Fig. 1 is the proposed BWRVIP generic K distribution. Compared to the actual K distributions for the shell-to-shell welds, it is nonconservative for shallow flaws, but more conservative for deeper flaws.

In addition to calculated values of residual stresses, BWRVIP-14 has measurements of residual stresses for a shell-to-shell weld from a core shroud from a cancelled plant. The measured residual stresses are compared with the computed residual stresses in Fig. 2. BWRVIP-14 states (pg. 4-10) "in general, the analytical predictions have the same through-wall shape as the experimentally measured distributions; with tensile stresses on the inside and outside surfaces and compressive stresses in the middle half of the shroud wall."

The corresponding K distributions shown in Fig. 3, however, are very different in character. The K distributions based on either the BWRVIP or the Battelle analytical predictions of the weld residual stresses suggest that there is a high likelihood that cracks will arrest approximately half way through the wall. The K distribution corresponding to the measured residual stresses suggests rapid throughwall growth.

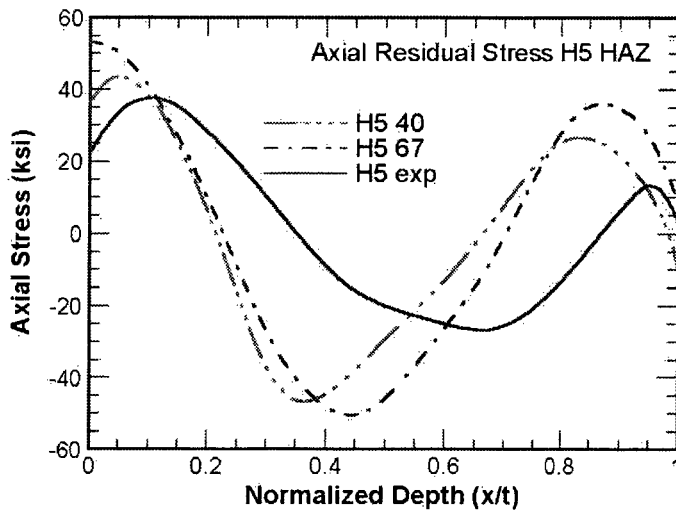


Figure 2. Computed (40 and 67 ksi yield) and measured axial residual stress in the HAZ of an H5 weld (cf. Figure 4-4 BWRVIP-14.)

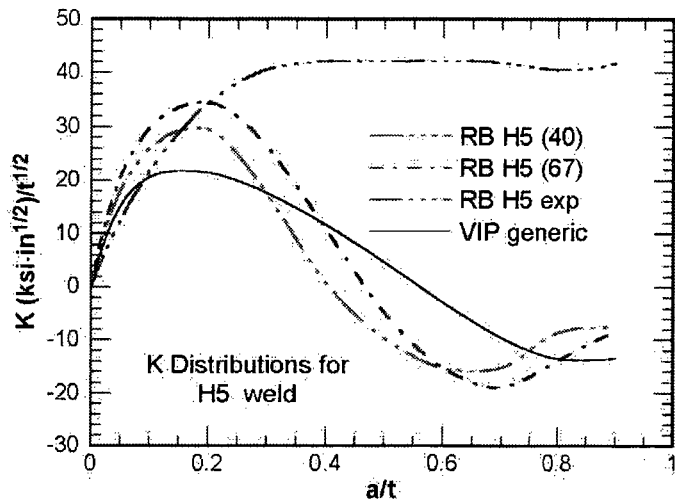


Figure 3. K distributions for the computed and measured residual stresses in H5 welds

The residual stresses measured on the H5 weld consist of a self equilibrating portion and a portion corresponding to the net moment relieved when the specimen for the throughwall analysis was removed from the shroud. The total residual stress is the sum of these two stresses. The different contributions to the residual stress are shown in Fig. 4a and the corresponding K distributions are shown in Fig. 4b.

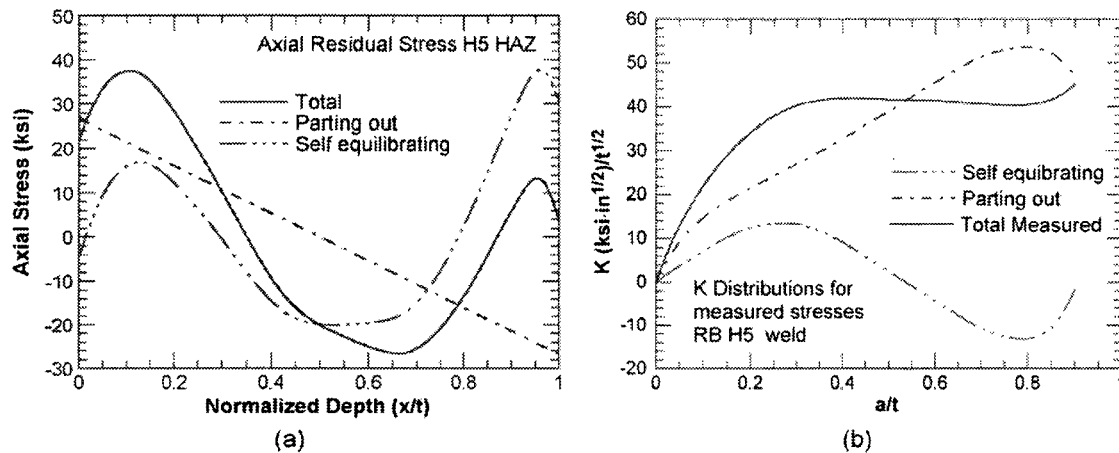


Figure 4. (a) Total, parting out, and self-equilibrating axial residual stress H5 weld; (b) K distributions corresponding to the total, parting-out, and self-equilibrating residual stresses.

The question of which K distributions are appropriate for the shell-to-shell welds, i.e., those in Fig. 1 based on the analytical predictions of the residual stress or that in Fig. 4b based on the experimentally measured stresses, obviously has a strong impact on the disposition of cracks in shell-to-shell welds. The distributions in Fig. 1 seem more consistent with field experience. Cracks seem to have high aspect ratios as described in Appendix I of BWRVIP-14, suggesting a retardation of throughwall growth. The K distribution of Fig. 4b would tend to lead to much smaller aspect ratios

In a flat plate, the net force and moment due to the residual stresses must vanish. This is not the case for a cylinder which can sustain a net moment. However, the shroud is relatively thin-walled and flexible, and one would expect the net moments to be fairly small. This is the case for the analytical solutions. The residual stress distributions have non-zero moment resultants, but they are small in magnitude, and the K distribution is largely determined by the self-equilibrating portion of the stresses. The parting out stresses depend on a single reading from a single gage during the parting out process.

For these reasons, it is assumed that the K distributions in Fig. 1 are indeed representative of those in the H5 weld and that there are unidentifiable problems with the reported residual stress measurements.

Residual Stresses and K distributions for ring-to-shell welds

BWRVIP-14 also describes residual stress calculations and measurements on ring-to-shell welds. No calculations are explicitly made for these stress distributions and weld geometries. Instead the argument is made the generic residual stress distribution is a reasonable representation of axial through-wall residual stress distribution for all the shroud welds for safety evaluation purposes. However, as shown in Figs. 5a and 5b, "reasonable" agreement between stress profiles is not a guarantee of reasonable agreement between K distributions.

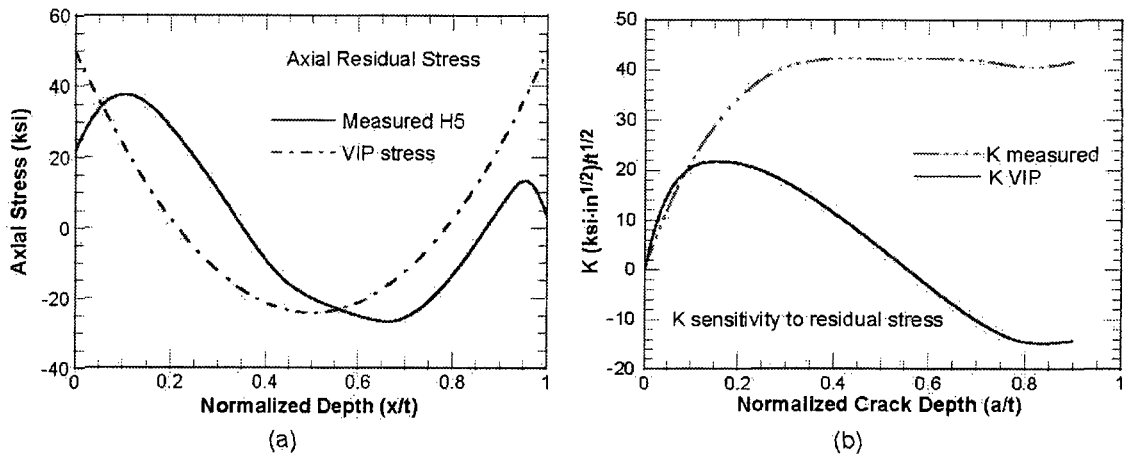


Figure 5. (a) Comparison of the BWRVIP generic weld profile and the reported measured profile for an H5 weld; (b) Comparison of the corresponding K distributions.

It is much better to compute the K distributions corresponding to the different residual stress distributions and then to determine a bounding K or a range of K values as was done in Fig. 1 for the H4 and H5 welds. It is easy to compute K for shell-to-shell welds using the Cheng-Finnie solution. The applicability of this solution to ring-to-shell welds has not been established and no other applicable type of solution for this geometry is presented in BWRVIP-14.

It seems plausible that the stiffer ring-to-shell weld is equivalent to a shell-to-shell configuration for some appropriate value of R/t . It also can be shown that for a stress distribution like those expected in the welds, a stiffer shell (smaller R/t) results in less severe K distribution, e.g., the depth at which K becomes negative, decreases. Thus it seems likely that using the Cheng-Finnie approach with $R/t = 60$ to compute K distributions (i.e., ignoring the added stiffness of the ring) should give conservative results for the K distributions for ring-to-shell welds.

Estimates of the K distributions for these welds computed using the Cheng-Finnie solution with $R/t = 60$ are shown in Figs. 6 and 7. To get some idea of the potential effect of the ring-to-shell geometry, the results for the H2, H3, and H6b welds were also computed for $R/t = 10$. Conclusions about the applicability of the BWRVIP results were based on comparisons with the more conservative of the two Cheng-Finnie solutions.

Although the VIP generic solution is conservative (i.e., becomes negative at a deeper depth and has a shallower minimum) compared to most of the distributions, it is not always conservative. These welds also show a fairly strong dependence on weld sequence and yield strength. There is no indication in BWRVIP-14 which of the welding sequences were actually used for shroud construction. It would appear that knowledge of the welding sequence could have a significant impact on the assessment of the adequacy of the BWRVIP generic residual stress or K solution. However, except for one case, a H6b weld with weld sequence 3b, a constant throughwall K of $27.5 \text{ MPa}\cdot\text{m}^{1/2}$ ($25 \text{ ksi}\cdot\text{in}^{1/2}$) would give conservative estimates of the throughwall crack growth.

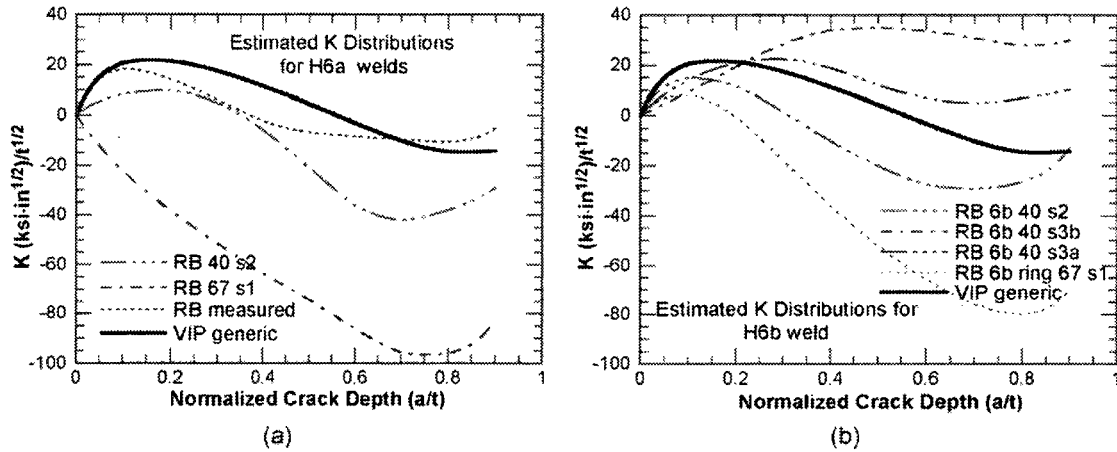


Figure 6. Estimated K distributions with $R/t = 60$ for (a) H6a and (b) H6b welds.

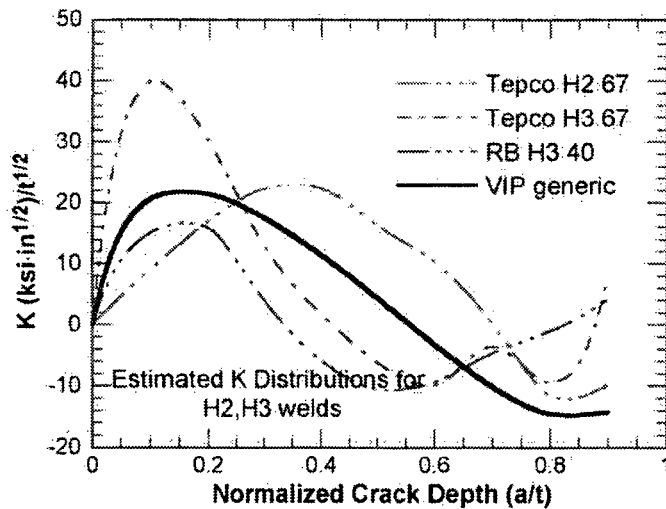


Figure 7. Estimated K distributions with $R/t = 60$ for H2 and H3 welds.

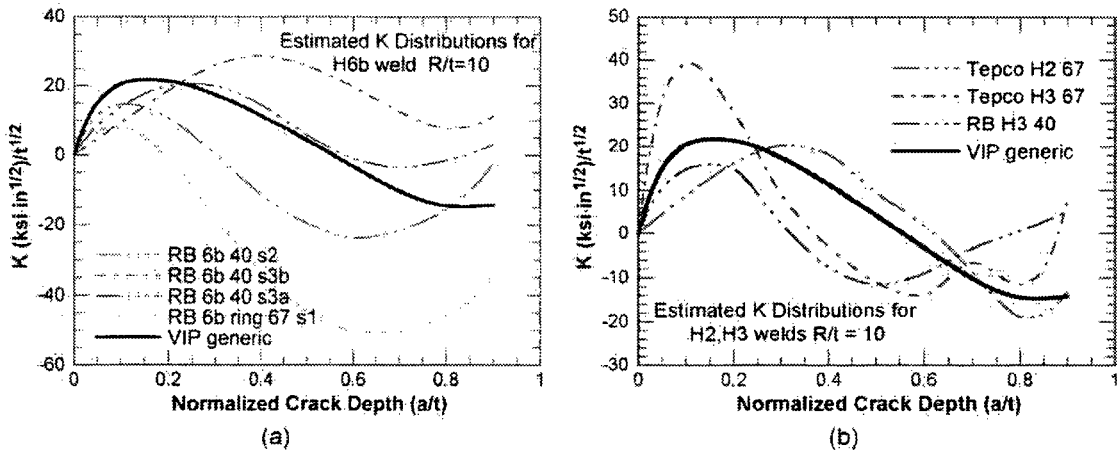


Figure 8. Estimated K distributions with $R/t = 10$ for (a) H6b and (b) H2 and H3 welds.

Total Throughwall Distribution of K for H4/H5 welds

The distribution of K shown in Fig. 1 includes only the contribution from the weld residual stresses. In addition in the BWRVIP-14 approach, there are additional surface residual stresses, an applied load of 1.6 ksi, and an additional applied load of 1.6 ksi intended to address additional stresses that may be present due weld repairs.

The additional surface stress (shown in Fig. 4-12 of BWRVIP-14) is not sufficient to account for all the discrepancies between the predicted residual stresses due to welding and the measured surface stresses, but it remains tensile over a depth greater than 10% of the wall. Although it may not be conservative in terms of estimating initiation times, it should give a conservative estimate of the effect of such stresses on crack growth. Similarly the use of a constant 1.6 ksi stress may not give a conservative estimate of the local increase in K at some depths do to weld repairs, but this choice of non-self-equilibrating stress should give a conservative estimate of the potential increase in K for deep cracks, i.e., for the potential for the crack to go throughwall rather than arrest.

The K distribution corresponding to the bounding value of K due to weld residual stresses shown in Fig. 1 and the added surface, applied, and weld repair loads is shown in Fig. 9 along with the generic BWRVIP-14 K distribution for the total stress. In the critical region in the midsection of the wall, the BWRVIP distribution is more conservative than the total K based on the bounding K solution for residual stresses in the H4/H5 welds. The VIP solution does not bound the shell-to-shell K distributions at every depth. Thus for very shallow cracks, The BWRVIP solution may underpredict the growth of shallow flaws for some period of time. However, it is more conservative than these distributions in the sense that it predicts complete throughwall growth of an initial $a/t = 0.25$ depth, while the bounding solution for the shell-to-shell welds predicts arrest of an initial $a/t = 0.25$ crack in every case. The depths for arrest based on a range of assumptions about the residual and applied stresses are shown in Table 1. The results suggest that cracks in shell-to-shell welds would be expected to arrest at depths ranging from 0.37 to 0.56 of the wall thickness. Of the reported depths for H4/H5 welds in BWRVIP-14, only one exceeds $0.56 a/t$ in depth, and that reported depth is only 0.57 so within measurements errors it is also consistent with the results in Table 1.

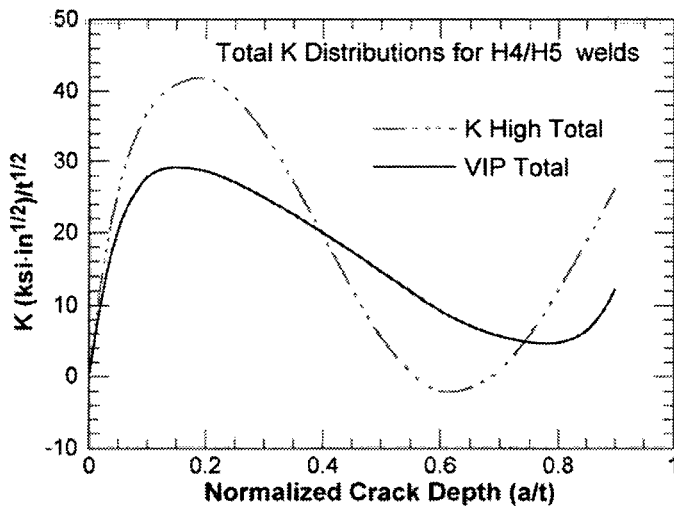


Figure 9. Distributions of total K for H4/H5 welds.

Table 1. Nondimensional arrest depth for H4/H5 welds for different assumptions about residual stresses, surface stresses, and added constant stresses

Residual Stress	Added Constant Stress	VIP Surface Stress	Arrest Depth (x/t)
High	3.2	Yes	0.56
High	1.6	Yes	0.50
Low	3.2	Yes	0.46
Low	1.6	Yes	0.41
Mean	1.6	Yes	0.47
High	-	No	0.47
Low	-	No	0.37

For the ring-to-shell welds, the BWRVIP K solution is not bounding in every case (again in the sense of predicting the subsequent growth of an $a/t = 0.25$ crack), although in many cases, arrest would be expected. In two cases, for an applied stress of 3.2 ksi, even the assumption of a constant throughwall stress intensity of $25 \text{ ksi}\cdot\text{in}^{1/2}$ does not bound the growth due to the actual K distributions. Since the assumption of the constant 3.2 ksi stress in addition to the welding residual stresses and the surface residual stress is probably conservative, the growth under an applied constant stress of 1.6 ksi was also considered. The results for the different welding residual stress profiles, applied loads, and surface stresses associated with the H2, H3, H6a, and H6b ring-to-shell welds are summarized in Table 2.

Table 2 Comparison of specific stress profiles for ring-to-welds with the BWRVIP generic profile including residual stresses, surface stresses, and either a 3.2 or 1.6 ksi constant load.

Weld	Applied stress 3.2 ksi			Applied stress 1.6 ksi		
	Arrest	VIP bounds	25 $\text{ksi}\cdot\text{in}^{1/2}$ bounds	Arrest	VIP bounds	25 $\text{ksi}\cdot\text{in}^{1/2}$ bounds
TEPCO H2 67	no	no	yes	yes	yes	yes
TEPCO H3 67	no	yes	yes	yes	yes	yes
River Bend H3 40	yes	yes	yes	yes	yes	yes
River Bend H6a 40 HAZ seq 2	yes	yes	yes	yes	yes	yes
River Bend H6a 67 HAZ seq 1	yes	yes	yes	yes	yes	yes
River Bend H6a measured	no	yes	yes	yes	yes	yes
River Bend H6b 40 HAZ seq 3b	no	no	no	no	no	no
River Bend H6b 40 HAZ seq 3a	no	no	no	no	no	yes

No field data are reported in BWRVIP-14 for H6 welds. There are seven measurements on H2 and H3 welds. The BWRVIP solution bounds the measured crack extension in all but one case. In that case the measured extension was 0.3 in., the predicted extension 0.17 in. The Chinsan-2 H3 weld had a total crack length of 209 in., but the maximum throughwall penetration was $0.50 a/t$. Clearly the throughwall growth had to be retarded by the residual stress field.

Although the BWRVIP generic K solution and the even the constant $25 \text{ ksi}\cdot\text{in}^{1/2}$ solution do not bound the K solutions for all the ring-to-shell welds, it is the conservatism of the overall crack growth prediction that must be assessed. Thus far only the conservatism in the K solutions has been addressed. The degree of conservatism in the BWRVIP crack growth model must also be considered.

Crack Growth Models

As discussed in our previous technical letter report on BWRVIP-14, the BWRVIP model for crack growth in unirradiated materials provides a reasonable description of crack growth in sensitized austenitic stainless steels. It does not explicitly address cold work or irradiation effects. Because the model does not include sensitization as a variable, it appears to adequately address cracking in cold-worked materials, at least to the level of cold work that would be encountered in an actual fabricated components, even though the data base from which it was developed did not include cold-worked materials.

It is now well established that crack growth rates in irradiated materials can substantially exceed those in unirradiated materials. The combined effects of the radiation-induced segregation and hardening appear to severely degrade the material.

Data on crack growth rates for irradiated base metal are shown in Fig. 10. The BWRVIP-14 95th percentile curve for a conductivity of $0.15 \mu\text{S}/\text{cm}$ lies slightly below the NUREG-0313 curve (see Figure 3-9, pg. 3-81 of BWRVIP-14). In Figure 10, it would lie just below the data for the irradiated 304 SS with a fluence of $0.3 \times 10^{21} \text{ n}/\text{cm}^2$. Most of the available data are for fluences of $10^{21} \text{ n}/\text{cm}^2$. In these case crack growth rates are about five times higher than the NUREG-0313 curve. Although the base metal data for a fluence of $0.3 \times 10^{21} \text{ n}/\text{cm}^2$ in Fig. 10 lies below the NUREG-0313 curve, the HAZ crack growth rates in Fig. 11 are a factor of five or more above the NUREG-0313 curve.

Although the data are limited, it would seem that it would be reasonable to assume that the distribution (i.e., both the median and the 95th percentile) for unirradiated stainless steel crack growth rates shifts a factor of five higher for a fluence of $5 \times 10^{20} \text{ n}/\text{cm}^2$. This would be conservative for lower fluences. The 95th percentile of unirradiated distribution (i.e., the BWRVIP-14 disposition curve) then lies 0.509 standard deviations above the median of the irradiated distribution. This makes it the 70th percentile of the irradiated distribution for a fluence of $5 \times 10^{20} \text{ n}/\text{cm}^2$.

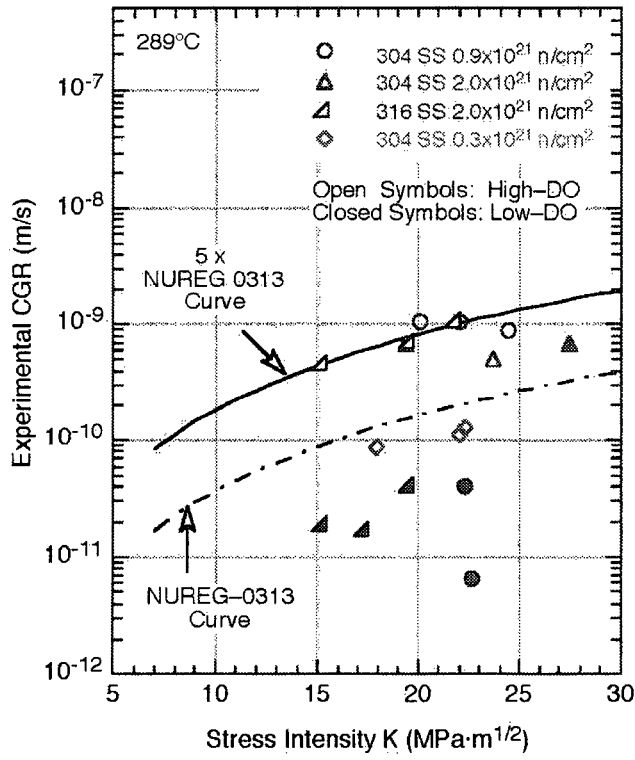


Figure 10.
ANL data on crack growth rates in base metal of irradiated stainless steels

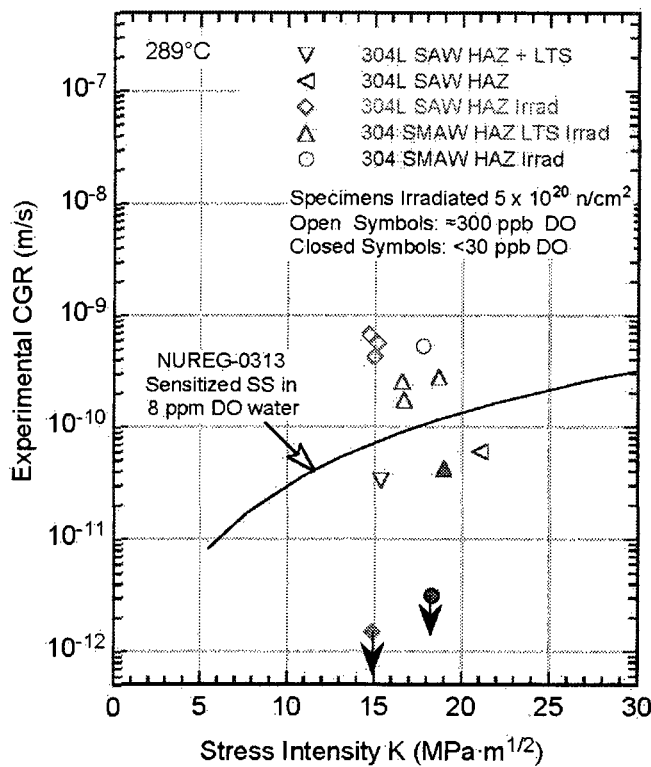


Figure 11.
ANL data on crack growth rates in HAZs
of irradiated weldments

References

1. W. J. Shack, Technical Evaluation Report on EPRI TR-105873, BWR Vessels and Internals Project, Evaluation of Crack Growth in BWR Stainless Steel RPV Internals, January 27, 1998.
2. W. J. Shack, O. K. Chopra, S. Majumdar, "Technical Evaluation Report on Project No. 704 — BWRVIP Response to NRC Safety Evaluation of BWRVIP-14," August 5, 1999.
3. W. Cheng and I. Finnie, "On the Prediction of Stress Intensity Factors for Axisymmetric Cracks in Thin-Walled Cylinders From Plane Strain Solutions," *Journal of Engineering Materials and Technology*, **106**, pp 227-231, 1985.
4. O. Chopra, E. Gruber, and W. J. Shack, "Crack Growth Rate of Stainless Steel Weld HAZ Irradiated in the Halden Reactor", Presented at ICG-EAC Yumebutai, Japan, April 18-23, 2004

O

BWRVIP RESPONSE TO NRC TECHNICAL EVALUATION REPORT DATED SEPTEMBER 12, 2005

Appendix O

BWRVIP Response to NRC Technical Evaluation Report dated September 12, 2005



2005-364 _____ BWR Vessel & Internals Project (BWRVIP)

September 12, 2005

Document Control Desk
U. S. Nuclear Regulatory Commission
11555 Rockville Pike
Rockville, MD 20852

Attention: Meena Khanna

Subject: PROJECT NO. 704 – BWRVIP Response to Draft Technical Evaluation Report on BWRVIP-14-A (Evaluation of Crack Growth in BWR Stainless Steel RPV Internals)

References: Letter from J.T. Beckham, Jr. (BWRVIP Chairman) to Document Control Desk (NRC), "BWR Vessel and Internals Project, Evaluation of Crack Growth in BWR Stainless Steel RPV Internals (BWRVIP-14). EPRI Report TR-105873, March 1996," dated March 18, 1996.

The BWRVIP provided the NRC with an informal copy of the draft report "BWRVIP-14-A: BWR Vessels and Internals Project, Evaluation of Crack Growth in BWR Stainless Steel RPV Internals" for review prior to publication. The NRC asked Dr. Bill Shack at Argonne National Laboratory (ANL) to review the report. Dr. Shack provided a summary of his comments to the BWRVIP during a BWRVIP-NRC staff meeting held in Washington on August 24-25, 2004. Enclosed are one copy of the draft ANL Technical Evaluation Report and five copies of the BWRVIP response to the report's major conclusions and recommendations.

Please note that the enclosed document contains EPRI proprietary information. Therefore, the request to withhold the BWRVIP-14 report from public disclosure transmitted to the NRC by the reference letter identified above, also applies to the enclosed document.

If you have any questions on this subject, please contact George Inch (Constellation Energy Group, BWRVIP Assessment Committee Chairman) by telephone at 315.349.2444.

Sincerely,

William A. Eaton
Entergy Operations
Chairman, BWR Vessel and Internals Project

Together . . . Shaping the Future of Electricity.

PALO ALTO OFFICE
3420 Hillview Avenue, Palo Alto, CA 94304-1395 USA • 650.855.2000 • Customer Service 800.313.3774 • www.epri.com

**BWRVIP Response to Draft Technical Evaluation Report on
BWRVIP-14-A, BWR Vessels and Internals Project, Evaluation of Crack Growth in BWR
Stainless Steel RPV Internals**

INTRODUCTION

The BWRVIP has reviewed the Draft Technical Evaluation Report (TER) prepared by Argonne National Laboratory (W. J. Shack and S. W. Tam) on the BWRVIP-14-A report. This document summarizes the major conclusions and recommendations of the TER and provides the BWRVIP responses to each item.

ITEM 1 - TER CONCLUSION REGARDING K-DISTRIBUTION IN SHELL-TO-RING WELDS

The TER states that the three approaches provided in the BWRVIP-14-A model are acceptable for materials with fluence $< 5E20$ n/cm² for H4/H5 shell-to-shell welds. The BWRVIP model for throughwall residual stresses and the corresponding K distribution is judged to be sufficiently conservative. Also, the residual stress distributions for other types of shell-to-ring welds (H1, H2, H3, H6a, H6b) in BWRVIP-14-A appear to be reasonable. However, BWRVIP-14-A assumes that the generic throughwall-K solution derived for shell-to-shell geometry is also applicable to shell-to-ring welds. Although the BWRVIP K-distribution is not conservative in all cases for shell-to-ring welds, they are conservative in most cases. ANL believes that confirmatory finite element calculations to determine the K-distributions in shell-to-ring welds would be helpful.

BWRVIP RESPONSE TO ITEM 1

The BWRVIP agrees with the conclusion that any of the three approaches described in BWRVIP-14-A report for the evaluation of cracking in the BWR shroud can be applied to the shell-to-shell welds (Welds H4 and H5). The BWRVIP however believes that the three approaches can also be applied to the shell-to-ring welds (Weld H2, H3, H6a and H6b) without the limitations proposed in the TER. The reasons for this conclusion are provided below.

The main issue raised in the TER with respect to the shell-to-ring welds is the fact that the Cheng-Finnie K solution which is more applicable to the cylindrical shell-to-shell welds was also used for the shell-to-ring welds. The complex geometry of the shell-to-ring welds does not lend itself to closed form solutions such as the Cheng-Finnie formulation for the K distribution. As such, the BWRVIP has performed additional evaluations to determine the K distributions for the shell-to-ring welds using finite element analysis (FEA) techniques.

Residual Stress Distributions for Shell-to-Ring Welds

The stress distributions for the shell-to-ring weld from Figures 4-8, 4-9 and 4-10 of BWRVIP-14-A are reproduced in Figures 1, 2 and 3. As can be seen from these figures, there is a wide variation in the distribution but the general trend is that the inside and outside portions are in tension while the middle portion is in compression. The wide variation in stress distribution poses a challenge in deriving a representative curve to use for evaluation purposes. Another complicating factor is that, as can be seen from Figures 1, 2 and 3, the stress distributions are non-symmetric and therefore the resulting K distributions will be different depending on whether a crack initiates from the inside diameter (ID) or the outside diameter (OD) of the shroud. The mean values for these stress distributions are also shown in Figures 1, 2 and 3 and their comparison to the BWRVIP-14-A generic stress distribution and the experimentally measured distributions are shown in Figures 4, and 5 for Welds H6a and H6b respectively. It can be seen that these mean curves have the same general trend as the experimental and BWRVIP-14-A generic residual stress curves. It should be noted in Figure 2 that the stress distribution for 67 ksi cases look distinctively different than the rest of the distributions shown in Figures 1, 2 and 3 in that they appear to be more of a through-wall bending stress distribution typically associated with small diameter thin wall piping. In addition, the 67 ksi yield strength is not very typical for Type 304 stainless steel material. As such, the mean curves for Welds H6a and H6b were calculated both with and without the 67 ksi cases included in the population. The comparison of all the average distributions for the three configurations and the overall average for all the distributions with BWRVIP-14-A generic residual stress distribution is shown in Figure 6. It is observed that the shape of the overall average curve matches the BWRVIP-14-A generic stress distribution fairly well even though the two curves are displaced with respect to each other. Hence, the BWRVIP-14-A generic residual stress distribution is believed to be an adequate and reasonable representation for the shell-to-ring welds.

The philosophy used in BWRVIP-14-A in determining the representative generic residual stress distribution to be used for evaluation of the shell-to-shell as well as the shell-to-ring welds followed that used by the NRC in NUREG-0313, Rev. 2 (Figure 4-1 of BWRVIP-14-A). It should be noted that in NUREG-0313, Rev. 2, the NRC did not choose the most bounding stress distribution but rather, a reasonable representation that of the data. The BWRVIP addressed the uncertainties in the generic stress distributions by adding two additional distributions (3.2 ksi membrane and 10 ksi surface residual stress conservatism).

K Distributions for the Shell-to-Ring Welds:

Several of the calculated stress distributions for Welds H2/H3, H6a and H6b including the mean distributions shown in Figures 1 through 6 were used to determine the K distributions for the shell-to-ring welds. Because of the complex geometry of the shell-to-ring welds, the K distributions were determined using FEA techniques. Two models were used for the evaluation. The first is a shell-to-shell model which served as a benchmark case. The second is a shell-to-ring model for determination of the K distribution for the shell-to-ring welds. The geometrical

configurations used to develop these models are shown in Figures 7 and 8. Both configurations were axi-symmetric models, with cracks initiating on the inside surface of the shroud wall. The axi-symmetric feature implies that the crack is a 360° circumferential flaw. These models are shown in Figures 9 and 10. The shell-to-shell model is based on the Weld H4 described in Figure H-2b of BWRVIP-14-A and the shell-to-ring configuration is based on Figure H-2d of BWRVIP-14-A.

The finite element models were developed using the ANSYS finite element software and selection of axi-symmetric PLANE82 element with mid-side nodes. The crack tip region is sufficiently detailed for the stress intensity factor calculation. In order to closely represent the singularity at the crack tip, the mid-side nodes of the crack front elements are re-located to the quarter point. The ends of the models are sufficiently far such that boundary effects on the cracked regions are negligible. For the shell-to-shell model (Figure 9), symmetric boundary conditions are applied at the flawed section, such that only one face of the crack needed to be included in the model. The far end of the model was unrestrained. For the shell-to-ring model (Figure 10), the lower far end of the model was fixed vertically and horizontally in order to simulate the restraining effects of the shroud support plate and the fixed base of the shroud. The upper far end of the model was unrestrained. Since there was no symmetry across the flawed section in this case, both faces of the crack are included in the model. To obtain the K distribution across the thickness for either model, the depth of the crack was varied from depth-to-thickness (a/t) ratio of 0.1 to 0.8.

The BWRVIP-14-A generic residual stress distribution was superimposed on the shell-to-shell model to determine the K distribution. The result of this evaluation is shown in Figure 11a. Also shown in this figure is the BWRVIP-14-A generic residual K distribution. As can be seen from this figure, The K distribution determined from the finite element analysis matched the BWRVIP-14-A generic distribution determined using the closed form solution of Cheng and Finnie. Another benchmark case was performed using one of the K distributions determined in the TER. This is shown in Figure 11b. This figure also shows that the FEA technique is consistent with the results of the closed form analytical results from the TER providing confidence in the FEA technique for determining the K distributions.

Having benchmarked the FEA techniques against the closed form solutions for the shell-to-shell welds, the shell-to-ring model was used to determine the K distributions for the BWRVIP-14-A generic stress distribution and its comparison to the Cheng-Finnie closed form solution. This K distribution comparison is shown in Figure 12. It can be seen that the closed form K distribution for a shell-to-shell weld (with R/t ratio of 60) bounds the FEA K distribution for the shell-to-ring welds. This demonstrates that the use of the Cheng-Finnie closed form solution to determine the K distribution for the shell-to-ring welds (as was done in BWRVIP-14-A) is reasonable.

The shell-to-ring model was also used to determine the K distributions for selected stress distributions for the shell-to-ring welds in Figure 1, 2 and 3. The results of these K

determinations are shown in Figures 13, 14 and 15 for Welds H2/H3, H6a and H6b respectively. Also shown in these figures is the K distribution assuming the BWRVIP-14-A generic (recommended) weld residual stress profile as well as the BWRVIP-14-A total K distribution (including the contributions from the surface residual stress and the 3.2 ksi membrane stress distributions). Comparisons of the BWRVIP-14-A K distributions to the K distributions for the average stress distributions for the three shell-to-ring configurations are shown in Figure 16. Figure 17 provides the comparison of the BWRVIP-14-A K distributions to the average K distribution for Weld H2/H3, H6a and H6b using the average stress distributions for all the distributions shown in Figures 1, 2 and 3.

As can be seen in Figure 13, for Welds H2/H3, the total BWRVIP-14-A K distribution essentially bounds all the calculated K distributions except for a small portion of TEPCO H3 (67 ksi) stress distribution. This curve however falls significantly below the BWRVIP curve for a/t values greater than 0.22 indicating that from a crack growth point of view, the BWRVIP curve is bounding. Equally as important, the BWRVIP curve bounds the average K distribution curve for cracks initiating from both the ID and the OD. The results of the K distributions for Weld H6a are shown in Figures 14. It can be seen that other than the distribution labeled "H6a Average OD to ID", the total BWRVIP-14-A distribution is a reasonable representation of the K distribution for this weld. This anomalous K distribution includes the total population of the stress distributions shown in Figure 2 including the two 67 ksi curves with very unusual stress distributions. It will be shown later in the crack growth discussion section that this K distribution is not representative of field experience. The K distributions for Weld H6b are shown in Figure 15. This figure indicates that even though one of the individual stress distributions resulted in a K distribution that was above the BWRVIP-14-A total distribution, the average curves are very comparable to if not below the BWRVIP K distribution. This is demonstrated very clearly in Figure 16 in which the average K distributions for all three shell-to-ring weld configurations are compared to the BWRVIP-14-A distributions. Finally, the overall average K distribution for all the three configurations is compared with the BWRVIP distributions in Figure 17. It can be seen from this figure that, the BWRVIP-14-A total K distribution represents a reasonable upper limit representation for these K distributions.

The above comparisons and discussions indicate that the BWRVIP-14-A total K distribution bounds most of the average stress distribution for the shell-to-ring welds and as such it is a reasonable representation not only for the shell-to-shell welds but also for the shell-to ring welds.

ITEM 2 - TER CONCLUSION REGARDING CRACK GROWTH EVALUATION IN RING TO SHELL WELDS

The TER states that the crack growth predicted by BWRVIP-14-A models will be non-conservative for a relatively small fraction of cases. It further states that if the total length of cracks in a given shell-to-ring weld that could be addressed by the generic results were limited to one half of the total circumference the consequences of underestimating crack growth would

be limited. The structural margins for gross failure of the shrouds would still be large. For longer cracks more specific analyses for shell-to-ring welds or a more conservative bounding crack growth rate of $5E-5$ in/h would be required.

BWRVIP RESPONSE TO ITEM 2

Crack Growth Evaluation of Ring to Shell Welds

Crack growth evaluations in the depth direction for the average K distributions and comparisons to the BWRVIP-14-A K distribution were performed using the crack growth model in BWRVIP-14-A. The evaluation was conservatively performed considering the K distributions that exceed the BWRVIP-14-A total K distribution in Figure 4-16. All other K distributions will be bounded by the BWRVIP-14-A total generic K predictions. The evaluation was performed for both normal water chemistry (NWC) with ECP of 200mV and conductivity of $0.15\mu\text{S}/\text{cm}$ as well as hydrogen water (HWC) conditions, with ECP of -230mV and conductivity of $0.15\mu\text{S}/\text{cm}$.

The crack growth results are shown in Figures 18, 19 and 20. Under NWC conditions shown in Figure 18, it can be seen that the crack growth rate for the average K distribution (green curve) of Weld H6a for a crack initiating from the OD is relatively fast. The analysis indicates that an initial 10% through-wall flaw will grow to 90% in about 24 months. This prediction is not consistent with field experience since such rapid crack growth rates have not been observed. To date, no through-wall flaws have been observed in the core shroud welds. This indicates that both the stress distribution and the resulting K distribution for this case are extremely conservative. The importance of reconciling the calculated K and crack growth predictions with field experience to determine the most reasonable distribution to use in safety assessment was recognized in the TER (page 5, first paragraph). All the other K distributions considered in the crack growth analysis as shown in Figure 18 produce crack growth rates which are comparable to the BWRVIP-14-A total K distribution prediction. Under HWC conditions as shown in Figure 19, even the worst average K distribution for Weld H6a indicated that an initial 10% through-wall flaw will take at least ten years to reach 90% of wall thickness. Finally, Figure 20 presents the comparison of the BWRVIP-14-A total K crack growth predictions with the overall average K distribution under both NWC and HWC conditions. As can be seen from this figure, the BWRVIP-14-A predictions are very comparable to the crack growth prediction of the average K distributions.

Field Measurements Versus BWRVIP-14-A Model

In BWRVIP-14-A, comparisons were made of the actual field crack growth measurements in the depth direction and the model predictions. This included both shell-to-shell welds as well as shell-to-ring welds. It was noted that the BWRVIP-14-A crack growth model and K distribution reasonably predicts field experience in both the shell-to-shell and shell-to-ring welds (Figure 2 of

Appendix K in BWRVIP-14-A). The comparison between the model predictions and the field measurements for the shell-to-ring welds show that in most cases the predictions are either conservative or are within the inspection uncertainty band. This is yet another confirmation of the reasonableness of the BWRVIP-14-A K distribution to represent both the shell-to-shell and shell-to-ring models.

Inspection Intervals for the BWR Shroud Welds

The inspection intervals for the shroud welds are typically between 6 to 10 years, as specified in BWRVIP-76. Considering the crack growth results for the overall average K distribution shown in Figure 20, this re-inspection interval is adequate to allow appropriate actions to be taken by plant owners to address cracking in the shroud. Hence, the combination of the analytical evaluations presented above and the inspection intervals ensure that cracking in all the shroud welds, including the shell-to-ring welds can be appropriately managed.

Monitoring of Future Inspection Results

In spite of the adequacy of the model in comparison to the field measurements in core shroud welds as discussed in the preceding sections and in BWRVIP-14-A, it is the intention of the BWRVIP to continue to monitor and collect future inspection data when they become available and compare the data with the BWRVIP-14-A model. The BWRVIP will be prepared to update the analytical model presented in BWRVIP-14-A if future field data indicates the need for such an action.

ITEM 3 - TER CONCLUSION REGARDING THE EFFECT OF FLUENCE ON CRACK GROWTH RATES IN WELD HAZ

For fluence levels up to $5E20$ n/cm², the BWRVIP-14-A 95th percentile disposition curve may bound the crack growth rate only about 70% of the time. ANL has observed a significant increase in crack growth rate in irradiated weld HAZ material at a fluence of $\sim 5E20$ n/cm².

BWRVIP RESPONSE TO ITEM 3

BWRVIP-14-A is applicable to fluences $< 5E20$ n/cm². For fluences in the range of $5E20$ n/cm² to $3E21$ n/cm² the approach described in BWRVIP-99 will be used.

CONCLUSION

From the evaluations presented above coupled with the field data on core shroud welds obtained to date, the BWRVIP believes that the model presented in BWRVIP-14-A is equally applicable to both the shell-to-shell and shell-to-ring welds and that there should be no further limitations imposed on the use of the BWRVIP-14-A model to the shell-to-ring welds. The BWRVIP will continue to evaluate future field data in comparison with the model predictions to determine the need to update the model in the future.

**Content Deleted –
EPRI Proprietary Information**

Figure 1. Calculated Axial Residual Stress Distributions for Welds H2/H3

**Content Deleted –
EPRI Proprietary Information**

Figure 2. Calculated Axial Residual Stress Distributions for Weld H6a

**Content Deleted –
EPRI Proprietary Information**

Figure 3. Calculated Axial Residual Stress Distributions for Weld H6b

**Content Deleted –
EPRI Proprietary Information**

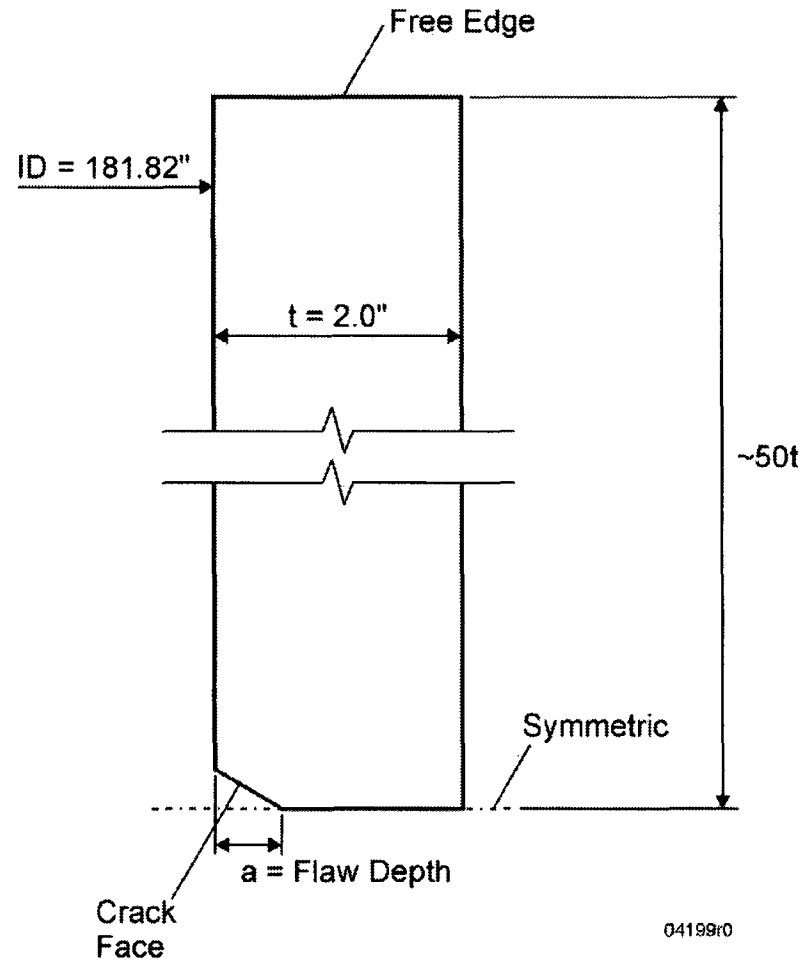
Figure 4. Welds H6a Average Residual Stress Distribution with Comparison to BWRVIP-14-A Generic Curve and Experimentally Measured Curve

**Content Deleted –
EPRI Proprietary Information**

Figure 5. Welds H6b Average Residual Stress Distribution with Comparison to BWRVIP-14-A Generic Curve and Experimentally Measured Curve

**Content Deleted –
EPRI Proprietary Information**

Figure 6. Average Residual Stress Distribution for Welds H2/H3, H6a and H6b and Comparison to BWRVIP-14-A Generic Curve



04199r0

Figure 7. Shell-to-Shell Weld Geometry

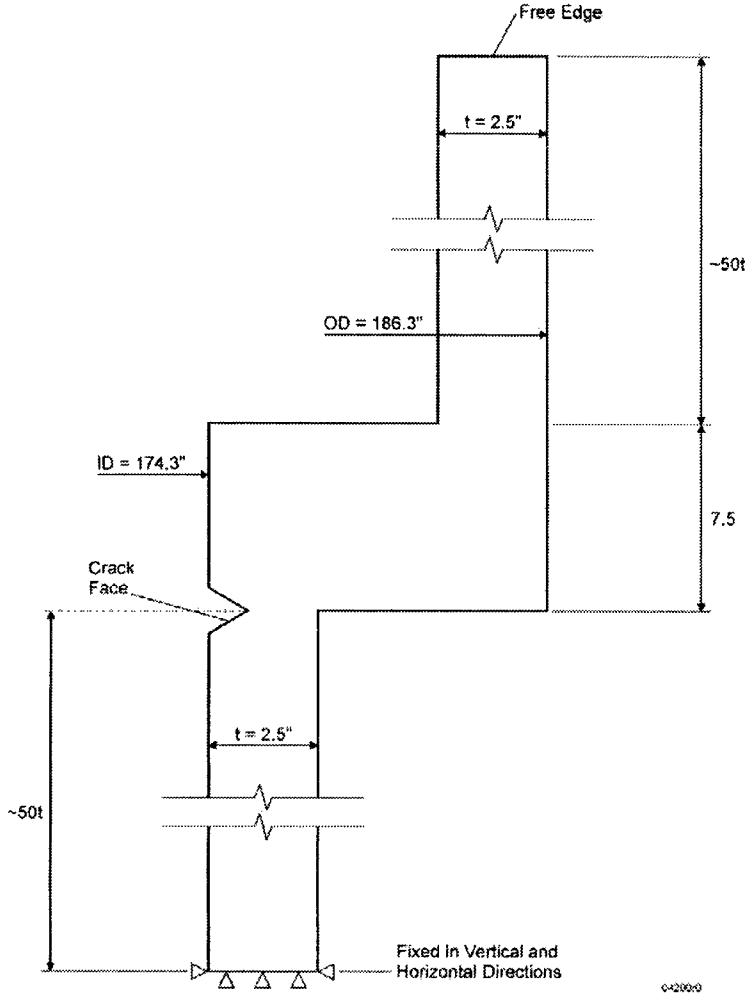


Figure 8. Shell-to-Ring Weld Geometry for H16a and H16b Welds

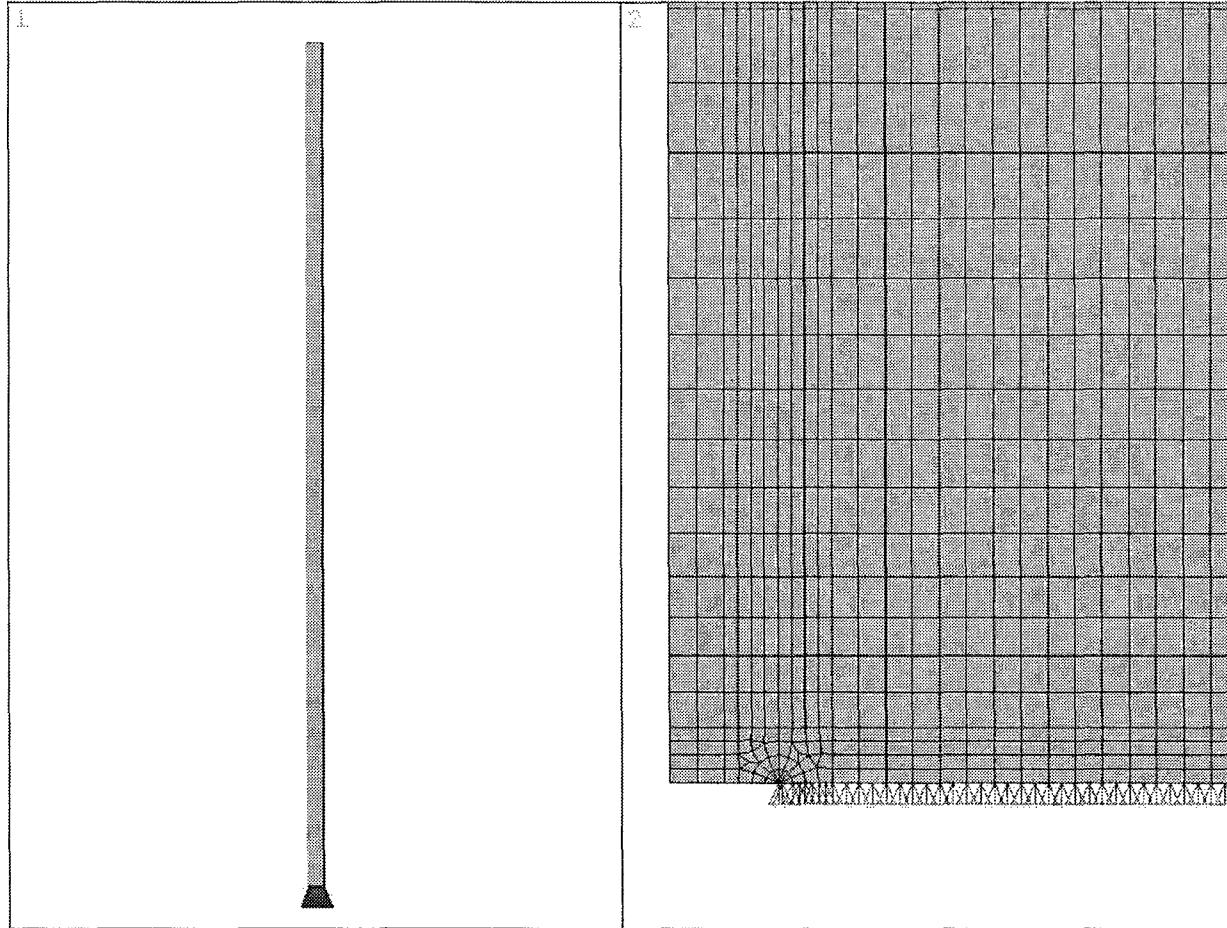


Figure 9. Shell-to-Shell Finite Element Model (Typical)
(Note: Right window shows detail at crack face)

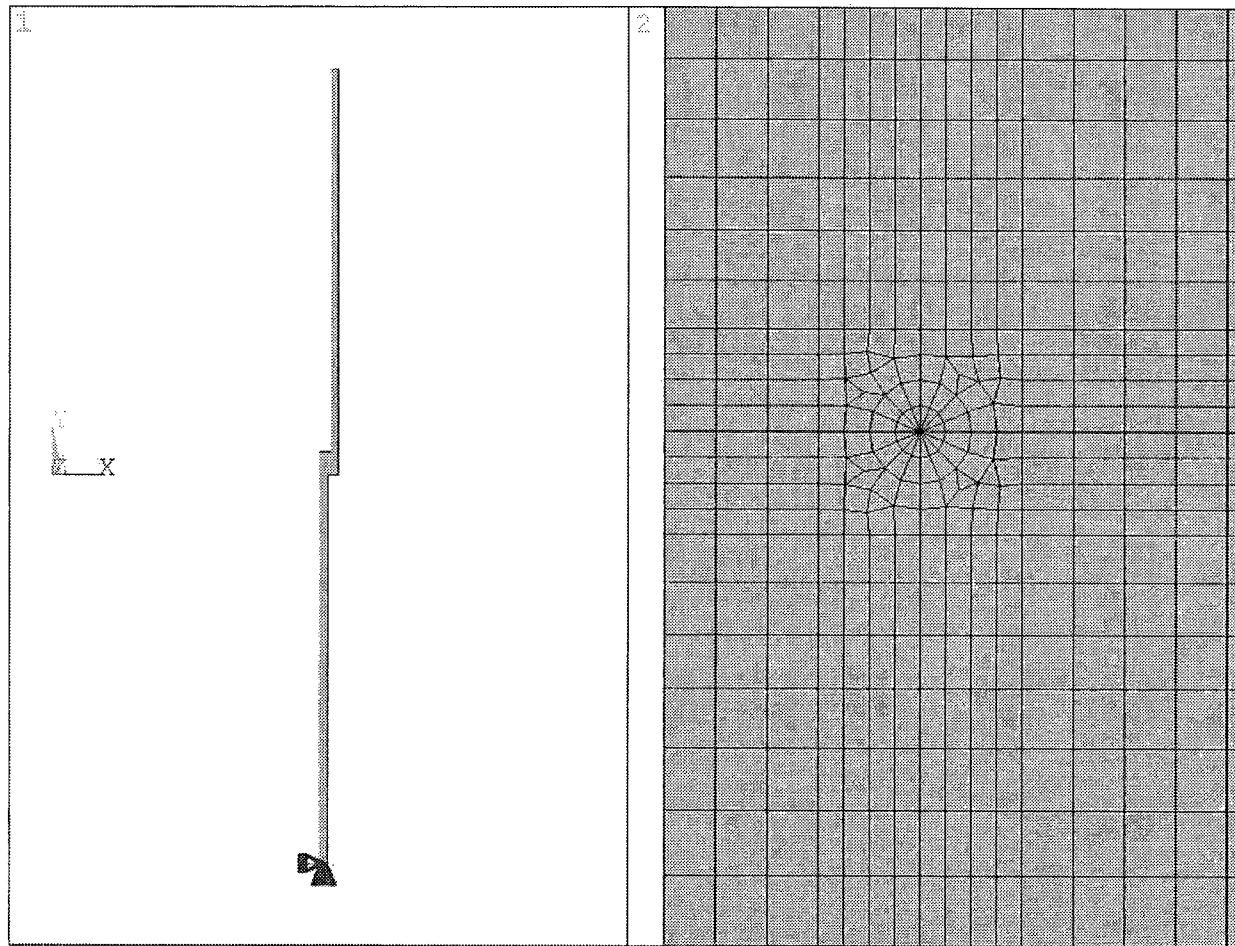


Figure 10. Shell-to-Ring Finite Element Model (Typical)
(Note: Right window shows detail at crack face)

**Content Deleted –
EPRI Proprietary Information**

Figure 11a. River Bend H4 Shell-to-Shell Weld K Distribution

**Content Deleted –
EPRI Proprietary Information**

Figure 11b: Shell-to-Shell Weld, River Bend H4 – 40 ksi Loading, TER vs. Finite Element Model

**Content Deleted –
EPRI Proprietary Information**

Figure 12: River Bend H6b Ring-to-Shell Weld K Distribution

**Content Deleted –
EPRI Proprietary Information**

Figure 13. Normalized K Distributions for Weld H2/H3

**Content Deleted –
EPRI Proprietary Information**

Figure 14. Normalized K Distribution for Weld H6a

**Content Deleted –
EPRI Proprietary Information**

Figure 15. Normalized K Distribution for Weld H6b

**Content Deleted –
EPRI Proprietary Information**

Figure 16. Normalized K Distribution for Average Stress Distribution for Welds H2/H3, H6a, and H6b in Comparison with BWRVIP-14-A K Distribution

**Content Deleted –
EPRI Proprietary Information**

Figure 17. Normalized K Distribution for Overall Average Stress Distribution for Shell-to Ring Welds in Comparison with BWRVIP-14-A K Distribution

**Content Deleted –
EPRI Proprietary Information**

Figure 18. Crack Growth Prediction Under NWC

**Content Deleted –
EPRI Proprietary Information**

Figure 19. Crack Growth Prediction Under HWC

**Content Deleted –
EPRI Proprietary Information**

Figure 20. Crack Growth Predictions for Overall Average K Distribution for Ring-to-Shell Welds and Comparison to BWRVIP-14-A K Distribution Prediction

P

NRC STAFF EVALUATION OF BWRVIP RESPONSE TO NRC SAFETY EVALUATION DATED AUGUST 22, 2007

Appendix P

NRC Staff Evaluation of BWRVIP Response to NRC Safety Evaluation Dated August 22, 2007



UNITED STATES
NUCLEAR REGULATORY COMMISSION
WASHINGTON, D.C. 20555-0001

August 22, 2007

Rick Libra, BWRVIP Chairman
DTE Energy
Fermi Nuclear Plant (M/S 280 OBA)
6400 N. Dixie Highway
Newport, MI 48166-9726

SUBJECT: STAFF EVALUATION OF BWRVIP RESPONSE TO NUCLEAR REGULATORY COMMISSION SAFETY EVALUATION OF "BWR VESSEL AND INTERNALS PROJECT, EVALUATION OF CRACK GROWTH IN BWR STAINLESS STEEL RPV INTERNALS (BWRVIP-14-A)" (TAC NO. MC2738)

Dear Mr. Libra:

The Nuclear Regulatory Commission (NRC) staff provided comments during a BWRVIP-NRC staff meeting at NRC headquarters on August 24-25, 2004, regarding the Electric Power Research Institute's (EPRI's) draft proprietary report, "BWR Vessel and Internals Project, Evaluation of Crack Growth in BWR Stainless Steel RPV Internals (BWRVIP-14-A)," dated November 2003. By letter dated September 12, 2005, the Boiling Water Reactor Vessel and Internals Project (BWRVIP) submitted their response to the NRC staff's comments by providing additional information addressing each of the issues identified by the NRC staff during the meeting on August 24-25, 2004.

There were three issues that the NRC staff requested that the BWRVIP address. The first issue was the need for confirmatory finite-element analysis (FEA) to determine the stress intensity (K)-distributions in the core shroud ring-to-shell welds since the BWRVIP-14-A report assumes that the generic through-wall K-distribution derived for the core shroud shell-to-shell (H4 and H5) weld geometry is also applicable to the core shroud ring-to-shell (H1, H2, H3, H6a and H6b) welds. By letter dated September 12, 2005, the BWRVIP provided additional evaluations to determine the K-distributions for the core shroud ring-to-shell welds using FEA techniques. The FEA techniques were benchmarked against the Cheng-Finnie analytical solutions for the core shroud shell-to-shell welds and show excellent agreement. Therefore, the additional finite element analyses provided in the BWRVIP response to the NRC comments on the draft BWRVIP-14-A report provide a necessary basis of comparing the BWRVIP generic K-distributions to the core shroud ring-to-shell weld K-distributions. These FEA results should be incorporated into the revised version of BWRVIP-14-A.

The second issue was in regards to requiring a more conservative bounding crack growth rate or the need to perform a more specific analysis for the core shroud ring-to-shell welds. For

some weld geometries and some material conditions the generic BWRVIP-14-A K-distributions are not conservative in all cases for the core shroud ring-to-shell welds. Similarly, the BWRVIP-14-A 95th percentile crack growth rate curve is expected to bound most of the crack growth rates. The K-distribution and the crack growth rates are uncorrelated variables. This suggests that the crack growth predicted by the BWRVIP-14-A guidelines will be non-conservative for a relatively small fraction of cases. If the total length of cracks in a given weld that could be addressed by these generic BWRVIP-14-A crack growth models were arbitrarily limited to a maximum of one-half of the total circumference, the consequences of underestimating the crack growth would be limited. With the low applied loads that are present on shrouds, crack opening areas will be small. The structural margins for gross failure of the core shrouds would still be large. For longer cracks, more specific analysis for core shroud ring-to-shell welds or a more conservative bounding crack growth rate of 5×10^{-5} in/h would be required.

Based on the combination of the K-distribution developed by the BWRVIP for H6a welds and the BWRVIP-14-A crack growth rate model (denoted as "H6a Avg OD to ID NWC" in Figure 1), an outside diameter (OD) to inside diameter (ID) crack in the H6a weld takes approximately 22 months to grow from 10 percent to 80 percent through-wall. The combination of the BWRVIP-14-A generic K-distribution and the BWRVIP-14-A crack growth rate model (denoted as the "VIP-14A Total (NWC)" crack growth curve) predicts that it will take approximately 214 months to grow from 10 percent to 80 percent through-wall under normal water chemistry. It should be noted that the generic K-distribution (used to calculate the "VIP-14A Total (NWC)" crack growth curve) includes operational loads and contributions intended to represent the effect of local stresses. The other projected crack growth curves shown in Figure 1 (i.e., "H6a Avg OD to ID NWC") based on other, specified K-distributions do not include any contribution from operating stresses. Including these operating stresses would further increase the difference between the growth predicted by the BWRVIP-14-A generic K-distribution and the H6a (core shroud ring-to-shell weld) K-distribution.

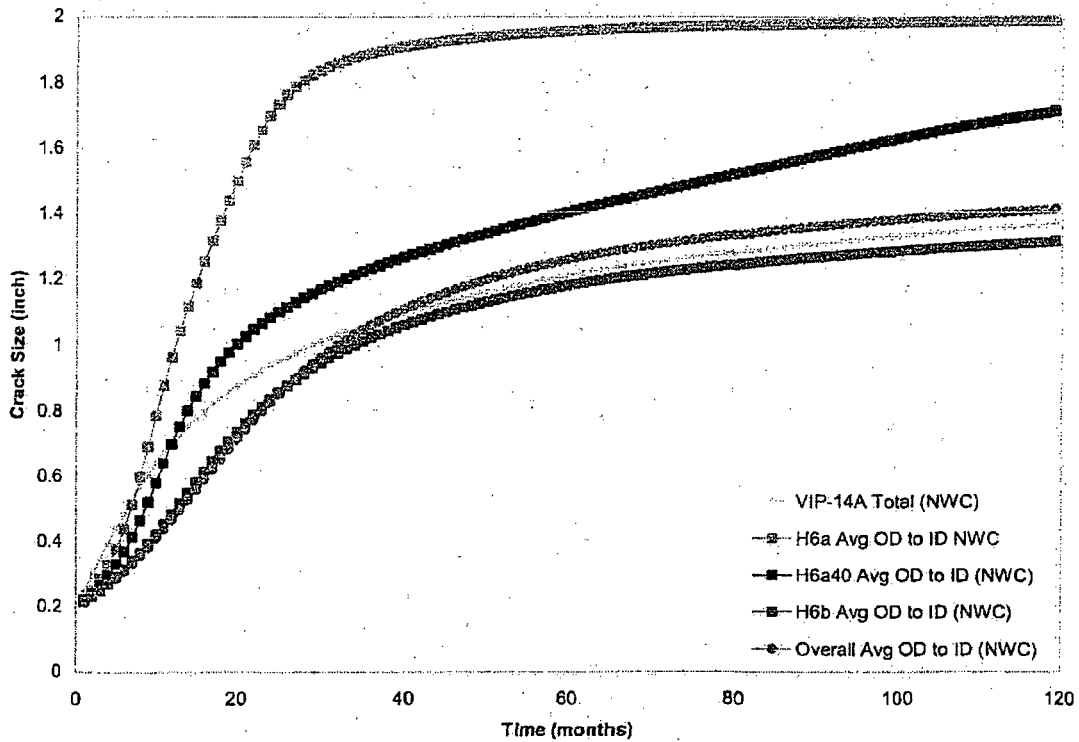


Figure 1. Predicted Crack Growth in Core Shroud Ring-to-Shell Welds

To date, no through-wall cracking has been found in core shroud welds despite the extensive cracking that has been observed. There are seven measurements on H2 and H3 welds. The "VIP-14A Total (NWC)" crack growth curve bounds the measured crack extension in all but one case. In that case the measured extension was 0.3 inches, the predicted extension 0.17 inches. The BWRVIP response states that the results for the H6a K-distribution contradicts this field experience, that such K-distributions are unlikely to actually occur, and that the generic BWRVIP-14-A K-distribution together with the BWRVIP-14-A crack growth rate correlation provides an adequate description of through-wall crack growth in ring-to-shell welds.

Although it is clear that field experience does show that K-distributions such as that postulated for the H6a weld are unlikely to occur in practice, it is difficult to quantify just how unlikely they are. A semi-quantitative argument to justify the low likelihood can be developed. According to information supplied by the BWRVIP, cracking has occurred in at least 26 core shroud welds.

* Personal communication, Bob Carter (EPRI) to Meena Khanna (USNRC), May 16, 2006.

Let the probability of that a crack in a weld has grown through-wall be $F(t)$ where t is the time since the crack initiated. The probability that the crack has not grown through-wall is $1 - F(t)$. The probability, P , that no crack has grown through-wall in any of the 26 core shroud welds that have cracked is:

$$P = \prod_{i=1}^{26} (1 - F(t_i))$$

where t_i is the time since initiation available for crack growth for each crack. This should include only time during which no mitigating measure such as hydrogen water chemistry (HWC) was applied. These times are not actually known. It is assumed that 10 years (120 months) is a conservative estimate of this time. This case simplifies to

$$P = (1 - F)^{26}$$

where F is the probability of through-wall growth after 120 months. The question is how large can F be before P is so low that it contradicts the field observation that no cracking has occurred. If we take $P = 0.05$, a typical statistical threshold for likeliness, then the field observations imply that F must be less than 0.11.

To compute F , the distribution of stress intensity factors is assumed to be characterized in terms of the distribution of times required to grow a flaw from $0.1h$ to $0.8h$ (where h is the wall thickness) for a given crack growth rate, which is taken as the BWRVIP "95th percentile" growth rate. This distribution is assumed to be log-normal with the time corresponding to the BWRVIP-14-A generic K-distribution as the median, and the time corresponding to the H6a K-distribution as a high percentile. This percentile value is chosen to make the likelihood of through-wall growth consistent with field experience. The crack growth rate is also assumed to be distributed normally with a 95th percentile value similar to the BWRVIP-14-A crack growth rate model and the 5th percentile value an order of magnitude lower.

Monte Carlo calculations were performed by taking a sample from the failure time distribution and a sample from the crack growth rate distribution, and using the crack growth rate value to scale the time sample (which was computed using the BWRVIP crack growth rate 95th percentile correlation). The Monte Carlo samples can then be rank ordered to estimate the probability of failure, i.e., growth to $0.8h$, by a given time. Calculations are shown in Figure 2 for cases where the time for growth to $0.8h$ corresponding to the H6a stress intensity distribution is taken as the 95th, 99th, and 99.9th percentile value of the distribution. For the 95th percentile case, the probability that the crack has grown to $0.8h$ through-wall is 0.17 and the probability that no cracking this deep would have occurred in any of the 26 cases is 0.007.

This is too low to be statistically plausible. For the 99th percentile case, the probability that the crack has grown to 0.8h through-wall is 0.11 and the probability that no cracking this deep has occurred is 0.05. While low, this is considered statistically possible and the conclusion is that the H6a K-distribution represents the 99th or higher percentile of the K-distributions observed in service. The value of 214 months for the BWRVIP-14-A generic K-distribution and 95th percentile crack growth rate corresponds to the 25th percentile of the F99 distribution. Thus it would give conservative answers greater than 75 percent of the time. The crack depth would exceed 0.8h less than 11 percent of the time.

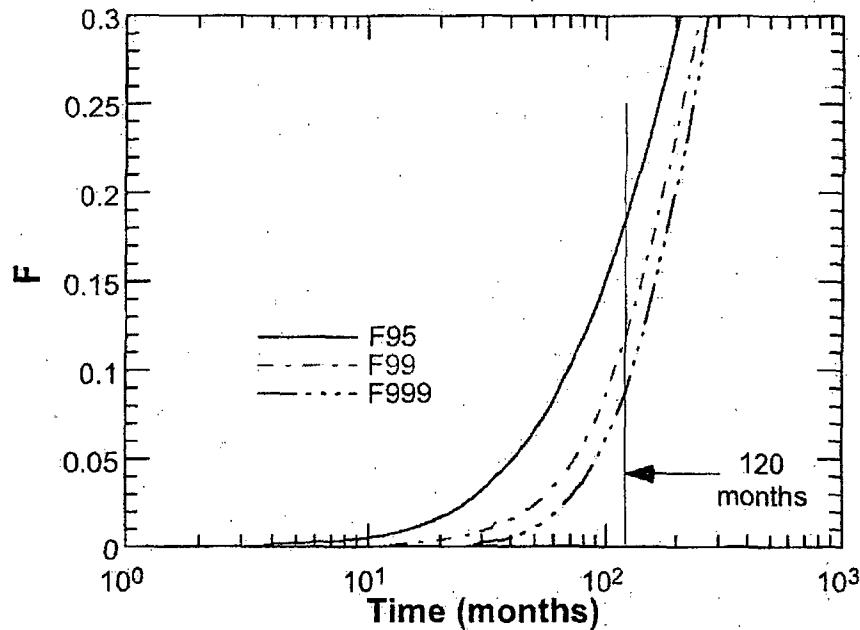


Figure 2. Times for Growth to 0.8h for Three Different Distributions of Stress Intensity Factor.

These results support the assertion in the BWRVIP letter dated September 12, 2005, that the combination of the BWRVIP-14-A generic K-distribution and the BWRVIP 95th percentile crack growth rate curve will provide reasonably conservative estimates of through-wall growth of cracks even though they may not be bounding in all cases.

The operating experience reported in BWRVIP-14-A should be updated to better reflect the number or instances of core shroud cracking that have occurred without through-wall growth. The extensive field experience on cracking is critical to the demonstration of the adequacy of the BWRVIP-14-A K-dependent approach for crack growth.

The third issue was in regards to the effects of neutron fluence on crack growth rates in the weld heat affected zones. For neutron fluence values up to 5×10^{20} n/cm² ($E > 1$ MeV), the BWRVIP-14-A 95th percentile crack growth rate curve may bound the crack growth rate only about 70 percent of the time. The NRC has observed a significant increase in crack growth rate in irradiated weld heat affected zone material at a neutron fluence value of approximately 5×10^{20} n/cm² ($E > 1$ MeV).

The BWRVIP proposes to use the BWRVIP-14-A "95th percentile" crack growth rate curve for unirradiated materials up to a neutron fluence value of 5×10^{20} n/cm² ($E > 1$ MeV) and to use a correlation presented in the BWRVIP-99 report, "Crack Growth Rates in Irradiated Stainless Steel in BWR Internal Components," for higher neutron fluence values. This results in a large jump in postulated crack growth rates at a neutron fluence value of 5×10^{20} n/cm² ($E > 1$ MeV). In reality, the transition is continuous, and the proposed crack growth rate correlation will be somewhat non-conservative for neutron fluence values less than but near 5×10^{20} n/cm² ($E > 1$ MeV) and quite conservative for the portions of the core shroud with neutron fluence values greater than 5×10^{20} n/cm² ($E > 1$ MeV). The potential non-conservatism is relatively small. The BWRVIP-14-A "95th percentile" crack growth rate curve may be expected to bound 70 percent of the crack growth rates for neutron fluence values somewhat below 5×10^{20} n/cm² ($E > 1$ MeV) instead of the 95 percent expected for unirradiated materials.

In its letter dated September 12, 2005, the BWRVIP provided additional information on the neutron fluence values associated with core shrouds. The neutron fluence varies significantly around the core shroud and through the thickness for the various ring-to-shell (horizontal) welds. In general the peak neutron fluence locations occur where the core is closest to the core shroud at the 45, 135, 225 and 315 degree locations (+/- 5 degrees). Thus only a limited region of the core shroud circumference and thickness will experience the peak neutron fluence.

This variability strongly mitigates the effect of any potential non-conservatism in the BWRVIP-14-A report at neutron fluence values just below the threshold value of 5×10^{20} n/cm² ($E > 1$ MeV). The portions of the core shroud for which the crack growth rate might be non-conservative is limited in extent both azimuthally and through-thickness.

Together with the conservatism inherent in the K-distribution in most cases, this level of conservatism in the crack growth rate model should assure conservative predictions of through-wall crack growth in almost all cases.

Therefore, the proposal to use the unirradiated crack growth rate curve for neutron fluence values less than 5×10^{20} n/cm² ($E > 1$ MeV) and the BWRVIP-99 crack growth rate correlation for neutron fluence values greater than 5×10^{20} n/cm² ($E > 1$ MeV) is considered acceptable.

The NRC staff has reviewed the BWRVIP's responses provided in your letter dated September 12, 2005, and finds that the BWRVIP has adequately addressed the issues raised during the August 24-25, 2004, meeting. The NRC staff requests that the BWRVIP incorporate the staff's recommendations, as stated above, as well as the responses to the NRC staff's issues in your letter dated September 12, 2005, into the -A version of the BWRVIP-14 report. The NRC staff also requests that the BWRVIP submit to the NRC the -A version of the BWRVIP-14 report within 180 days of receipt of this letter. Please contact John Honcharik of my staff at (301) 415-1157, if you have any further questions regarding this subject.

Sincerely,



Matthew A. Mitchell, Chief
Vessels & Internals Integrity Branch
Division of Component Integrity
Office of Nuclear Reactor Regulation

Project No. 704

cc: BWRVIP Service List

cc:

Randy Stark, EPRI BWRVIP Integration Manager
Raj Pathania, EPRI BWRVIP Mitigation Manager
Ken Wolfe, EPRI BWRVIP Repair Manager
Larry Steinert, EPRI BWRVIP
Electric Power Research Institute
3420 Hillview Ave.
Palo Alto, CA 94303

Paul J. Davison
BWRVIP Executive Oversight Committee
PSEG Nuclear, LLC
Salem/Hope Creek Nuclear Station
11 Yubas Ave.
Burlington, NJ 08016

Bob Geier, Technical Chairman
BWRVIP Assessment Committee
Exelon Corporation
Cornerstone II at Cantera
4300 Winfield Rd.
Warrenville, IL 60555

Denver Atwood, Technical Chairman
BWRVIP Repair Focus Group
Southern Nuclear Operating Co.
Post Office Box 1295
40 Inverness Center Parkway
(M/S B031)
Birmingham, AL 35242-4809

Jeff Goldstein, Technical Chairman
BWRVIP Mitigation Committee
Entergy Nuclear NE
440 Hamilton Ave. (M/S K-WPO-11c)
White Plains, NY 10601

Charles J. Wirtz, Chairman
BWRVIP Inspection Focus Group
FirstEnergy Corp.
Perry Nuclear Power Plant
(M/S A250)
10 Center Road
Perry, OH 44081

Amir Shahkarami, Executive Chairman
BWRVIP Integration Committee
Exelon Corporation
Cornerstone II at Cantera
4300 Winfield Rd.
Warrenville, IL 60555-4012

Robert Carter, EPRI BWRVIP Assessment
Manager
Jeff Landrum, EPRI BWRVIP Inspection Manager
EPRI NDE Center
P.O. Box 217097
1300 W. T. Harris Blvd.
Charlotte, NC 28221

Richard Anderson, Executive Chairman
BWRVIP Assessment Committee
Vice President, Nuclear
FirstEnergy Service Co.
Perry Nuclear Power Plant (M/S A-PY-290)
10 Center Road
Perry, OH 44081

Scott Oxenford, Executive Chairman
BWRVIP Mitigation Committee
Vice President, Technical Services
Energy Northwest
P.O. Box 968
Richland, WA 99352-0968

Dennis Madison
BWRVIP Executive Oversight Committee
Site Vice President
Southern Nuclear Operating Co.
Edwin I. Hatch Nuclear Plant
US Hwy 1 N
Baxley, GA 31515-2010

Q

PLANTS WITH SHROUD CRACKING

Appendix Q

Plants With Shroud Cracking

**Content Deleted –
EPRI Proprietary Information**

**Content Deleted –
EPRI Proprietary Information**

R

RECORD OF REVISIONS

BWRVIP-14-A	<p>Information from the following documents was used in preparing the changes included in this revision of the report. These documents are also listed as References 21 through 32 in Section 8.0.</p> <ol style="list-style-type: none">1. <i>BWR Vessels and Internals Project, Evaluation of Crack Growth in BWR Stainless Steel RPV Internals (BWRVIP-14)</i>. March 1996. EPRI Report TR-105873.2. Letter from C. E. Carpenter (NRC) to J. T. Beckham Jr. (BWRVIP Chairman), "Proprietary Request for Additional Information – Review of BWR Vessel and Internals Project Proprietary Report, <i>BWR Vessel and Internals Project, Evaluation of Crack Growth in BWR Stainless Steel RPV Internals (BWRVIP-14)</i>," December 9, 1996. (BWRVIP Correspondence File Number 96-746)3. Letter from V. Wagoner (BWRVIP) to C. E. Carpenter (NRC), "BWRVIP Response to NRC Request for Additional Information on BWRVIP-14," July 28, 1997. (BWRVIP Correspondence File Number 97-651)4. Letter from G. C. Lucas (NRC) to C. Terry (BWRVIP Chairman), "Safety Evaluation of the BWR Vessel and Internals Project BWRVIP-14 Report (TAC No. M94975)" and enclosure, June 8, 1998. (BWRVIP Correspondence File Number 98-260)5. W. J. Shack (Argonne National Laboratory) "Technical Evaluation Report on EPRI TR-105873, BWR Vessels and Internals Project, Evaluation of Crack Growth in BWR Stainless Steel RPV Internals," January 27, 1998. (BWRVIP Correspondence File Number 98-260)6. Letter from C. Terry (BWRVIP Chairman) to C. E. Carpenter (NRC), "BWRVIP Response to NRC Safety Evaluation of BWRVIP-14," November 24, 1998. (BWRVIP Correspondence File Number 98-458)7. Letter from J. Strosnider (NRC) to C. Terry (BWRVIP Chairman), "Final Safety Evaluation of the BWR Vessel and Internals Project BWRVIP-14 Report (TAC No. M94975)," December 3, 1999 (with enclosure TER on Project 704). (BWRVIP Correspondence File Number 99-496)8. W. J. Shack, O. K. Chopra, S. Majumdar, (Argonne National Laboratory), "Technical Evaluation Report on Project No. 704 - BWRVIP Response to NRC Safety Evaluation of BWRVIP-14," August 5, 1999. (BWRVIP Correspondence File Number 99-496)9. "Summary of February 17, 2000 BWRVIP/NRC Meeting," February 29, 2000. (BWRVIP Correspondence File Number 2000-049)10. Letter from C. Terry (BWRVIP Chairman) to C. E. Carpenter (NRC), BWRVIP Document 200-198, "Project No. 704 – BWRVIP Response to NRC Final Safety Evaluation of BWRVIP-14," July 11, 2000. (BWRVIP Correspondence File Number 2000-193)
-------------	--

Record of Revisions

	<p>11. Letter from J. R. Strosnider (NRC) to C. Terry (BWRVIP Chairman), "BWRVIP Response to NRC Final Safety Evaluation of BWRVIP-14 (TAC No. M94975)," May 13, 2001. (BWRVIP Correspondence File Number 2001-163)</p> <p>12. Letter from W. H. Bateman (NRC) to C. Terry (BWRVIP Chairman), "Clarification to NRC Letter Regarding BWRVIP Response to BWRVIP-14 Final Safety Evaluation (TAC No. M94975)," July 20, 2001. (BWRVIP Correspondence File Number 2001-243A)</p> <p>13. W. J. Shack and S. W. Tam (Argonne National Laboratory), "Technical Evaluation Report on BWRVIP-14-A, BWR Vessels and Internals Project, Evaluation of Crack Growth in BWR Stainless Steel RPV Internal," Draft, July 30, 2004.</p> <p>14. Letter from W. A. Eaton (BWRVIP Chairman) to M. Khana (NRC), "PROJECT NO. 704 – BWRVIP Response to Draft Technical Evaluation Report on BWRVIP-14-A (Evaluation of Crack Growth in BWR Stainless Steel RPV Internals)," September 12, 2005, (BWRVIP Correspondence File Number 2005-364)</p> <p>15. Letter from M. A. Mitchell (NRC) to R. Libra (BWRVIP Chairman), "Staff Evaluation of BWRVIP Response to Nuclear Regulatory Commission Safety Evaluation of "BWR Vessel and Internals project, Evaluation of Crack Growth in BWR Stainless Steel RPV Internals," (TAC NO. MC2738)," August 22, 2007, (BWRVIP Correspondence File Number 2007-261)</p> <p>Details of the revisions can be found in Table R-1.</p>
--	---

Table R-1
Revision Details

Required Revision	Source of Requirement for Revision	Description of Revision Implementation
Revise text in Sections 1.1 and 3.5 to document the operating experience to better reflect the number of instances of core shroud cracking that have occurred without through-wall growth.	NRC Staff Evaluation of BWRVIP Response to NRC SE (2007-261)	Sections 1.1 and 3.5 revised to provide Appendix Q which contains instances of crack shroud cracking that have occurred in the US without through-wall growth.
Revise text in Section 1.2 to indicate that the crack growth model is for the depth direction and also emphasize the fluence limitation of the model.	Editorial	Section 1.2 revised to indicate that the crack growth model is in the "through-wall" depth direction. The limitation of the model for fluence $\leq 5 \times 10^{20}$ n/cm ² (E > 1.0 MeV) was emphasized
Revise text in Section 2.0 to indicate the source of the second database.	Editorial	Section 2.0 revised to indicate that the second database was based on laboratory work as well as crack arrest verification systems (CAVS) data developed by GE.
Revise text in Section 3.3 to provide the best fit correlation model as well the 95 th percentile model	Editorial	Equations 2-2 and 2-3 provided to provide the best fit and the 95 th percentile models respectively.
Revise text in Section 3.5 to reflect updated Figure 3-9.	Editorial	Section 3.5 revised to reflect changes made to Figure 3-9. Figure 3-9 updated to reflect revised K distribution in Section 5. Additional plant data was added to Figure 3-9 for completeness. The source of the data in Figure3-9 was tied to Section 6.3.
Revise text in Section 4.1 to indicate maximum axial operating stress in the shroud.	BWRVIP Response to Initial SE (98-458) (page 8)	Section 4.1 revised to indicate that maximum operating membrane stress in the core shroud is on the order of 1.6 ksi. As a result of this change, Tables 4-1 and 4-2 were also modified accordingly by reporting only the membrane stresses.
Revise Section 4.6 to incorporate the FEA results to provide justification that the BWRVIP generic residual stress distribution is applicable to both the shell-to-shell and shell-to-ring welds.	NRC Staff Evaluation of BWRVIP Response to NRC SE (2007-261)	Section 4.6 revised to incorporate Appendix O which contains the FEA results providing justification that the BWRVIP residual stress distribution is applicable to both the shell-to-shell and shell-to-ring welds.

**Table R-1
Revision Details (Continued)**

Required Revision	Source of Requirement for Revision	Description of Revision Implementation
Insert Section 4.7 to address localized stresses developed in the weld during fabrication.	BWRVIP Response to Initial SE (98-458) (page 6) BWRVIP Response to TER Item 3.2 (99-443)	Section 4.7 inserted in report to address localized stresses per BWRVIP Document 98-458 as follows. 1. Addition of a very conservative membrane stress of 3.2 ksi to account for operating and local stresses on the shroud. 2. A surface residual stress distribution to account for local surface effects resulting from weld repairs and other local phenomena. As a result of the new text in Section 4.7, Table 4-3 was modified and Figures 4-12, 4-13 and 4-14 were added.
Revise text in Section 5.1 deleting reference to Bamford and Buchalet stress intensity factor (K) formulation per response to Item 2 of RAI Response.	RAI Response (97-651)	Section 5.1 revised deleting reference to Bamford and Buchalet stress intensity factor (K) formulation, since an alternate fracture mechanics model was proposed as discussed below in Section 5.2.
Revise Section 5.1 to indicate that the Cheng and Finnie K solution was used also for the applied stresses.	Editorial	Section 5.1 modified to indicate that the Cheng and Finnie K solution was used also for the applied stresses.
Revise text in Section 5.2 to present new stress intensity factor (K) formulation per response to Item 2 of RAI Response.	RAI Response (97-651)	Section 5.2 revised to show new stress intensity factor (K) formulation by Cheng and Finnie and presented in Appendix B of RAI response.
Revise Section 5.2 to incorporate the FEA results to provide justification that the BWRVIP generic K distribution is applicable to both the shell-to-shell and shell-to-ring welds.	NRC Staff Evaluation of BWRVIP Response to NRC SE (2007-261)	Section 4.7 revised to incorporate Appendix O which contains the FEA results providing justification that the BWRVIP K distribution is applicable to both the shell-to-shell and shell-to-ring welds.
Revise text in Section 5.3 to be consistent with newly inserted Section 4.7 and newly revised Section 5.2.	RAI Response (97-651)	Section 5.2 revised such that the discussion of localized stresses and their effect on K distribution is consistent with newly inserted Section 4.7 and newly revised Section 5.2.

Table R-1
Revision Details (Continued)

Required Revision	Source of Requirement for Revision	Description of Revision Implementation
Revise text in Section 6.1 incorporating BWRVIP response to Final SE which was accepted by USNRC on May 13, 2001.	BWRVIP Response to NRC Final SE (2000-198)	Section 6.1 revised incorporating BWRVIP Response to Final SE by incorporating three evaluation approaches. 1. Stress Intensity Factor (K) Independent Approach. 2. Stress Intensity Factor (K) Dependent Approach. 3. Stress Intensity Factor (K) and Environment (ECP and Conductivity) Dependent Approach.
Revise text in Section 6.1.1, 6.1.2 and 6.1.3 to indicate that the maximum conductivity level with the three evaluation approaches is 0.3 $\mu\text{S}/\text{cm}$.	Editorial	Sections 6.1.1, 6.1.2 and 6.1.3 modified to indicate that the three evaluation approaches are applicable up to 0.3 $\mu\text{S}/\text{cm}$ corresponding to Action Level 1 limit defined in the 2004 BWR Water Chemistry Guidelines (BWRVIP-130).
Revise text in Section 6.1 to indicate that fluence level of 5×10^{20} n/cm ² (E > 1 MeV) requires plant specific analysis	BWRVIP Response to Initial SE, Page 2, Item 5 (98-458)	Text in Section 6.1 revised to indicate that K-independent crack growth rates are only applicable to components with fluences less than 5×10^{20} n/cm ² (E > 1 MeV) since the database is presently based only on unirradiated materials.
Revise the Analysis in Chapter 6 (Section 6.2) to include the effects of circumferential crack growth	RAI Response, Item 5 (97-651)	This revision was not incorporated because as explained below, Section 6.2 was revised to include a new plant specific example.
Revise text in Section 6.2 to reflect new plant specific example provided in Initial SE response.	BWRVIP Response to Initial SE (98-458)	Revise Section 6.2 to indicate new plant specific example provided in Initial SE response, considering the revised K distribution presented in Section 5.2 for the various stresses.
Insert Section 6.3 to compare analytical crack growth prediction with field data	BWRVIP Response to NRC Final SE (2000-198)	Section 6.3 was inserted to provide comparison between analytical crack growth predictions with field data and to demonstrate that the analytical approach reasonably accounts for the effects of localized stresses resulting from weld repairs.
Revised text in Appendix H, page H-25 per response to Item 2 of RAI Response.	RAI Response (97-651)	Text on page H-25 of Appendix H modified per proposed revision in Appendix A of RAI Response.

**Table R-1
Revision Details (Continued)**

Required Revision	Source of Requirement for Revision	Description of Revision Implementation
Revise Section 7.0 to be consistent with all changes made in revised document.	Editorial	Revise Section 7.0 (Summary and Conclusion) consistent with all the changes made in the revised document.
Revise Section 8.0 to be consistent with new References added to revised report.	Editorial	Revise Section 8.0 (References) consistent with new References added to the report.
Revise Appendices to include new Appendices J, K, L, M, N, O, P, Q and R.	Editorial	Appendix J replaced, New Appendices K, L and M added.
Revise Executive Summary to reflect changes made to the report.	Editorial	Revised Executive Summary to reflect changes made to report.
Restrict applicability of CGR evaluations at high conductivities.	BWRVIP review	Section 6 revised to limit the use of 5E-05 in/hr as well as the use of Equations 6-5 and 6-6 to conductivities less than or equal to 0.3 micro-Siemens/cm.
Clarify that crack growth rates for HWC are also applicable when Noble Metal Chemical Application is used.	BWRVIP review	Text revised in Sections 1 and 6.
End of Revisions		

The Electric Power Research Institute (EPRI), with major locations in Palo Alto, California; Charlotte, North Carolina; and Knoxville, Tennessee, was established in 1973 as an independent, nonprofit center for public interest energy and environmental research. EPRI brings together members, participants, the Institute's scientists and engineers, and other leading experts to work collaboratively on solutions to the challenges of electric power. These solutions span nearly every area of electricity generation, delivery, and use, including health, safety, and environment. EPRI's members represent over 90% of the electricity generated in the United States. International participation represents nearly 15% of EPRI's total research, development, and demonstration program.

Together...Shaping the Future of Electricity

Program:

Nuclear Power

© 2007 Electric Power Research Institute (EPRI), Inc. All rights reserved. Electric Power Research Institute, EPRI, and TOGETHER...SHAPING THE FUTURE OF ELECTRICITY are registered service marks of the Electric Power Research Institute, Inc.

 Printed on recycled paper in the United States of America

1016569NP

Electric Power Research Institute

3420 Hillview Avenue, Palo Alto, California 94304-1338 • PO Box 10412, Palo Alto, California 94303-0813 USA
800.313.3774 • 650.855.2121 • askepri@epri.com • www.epri.com